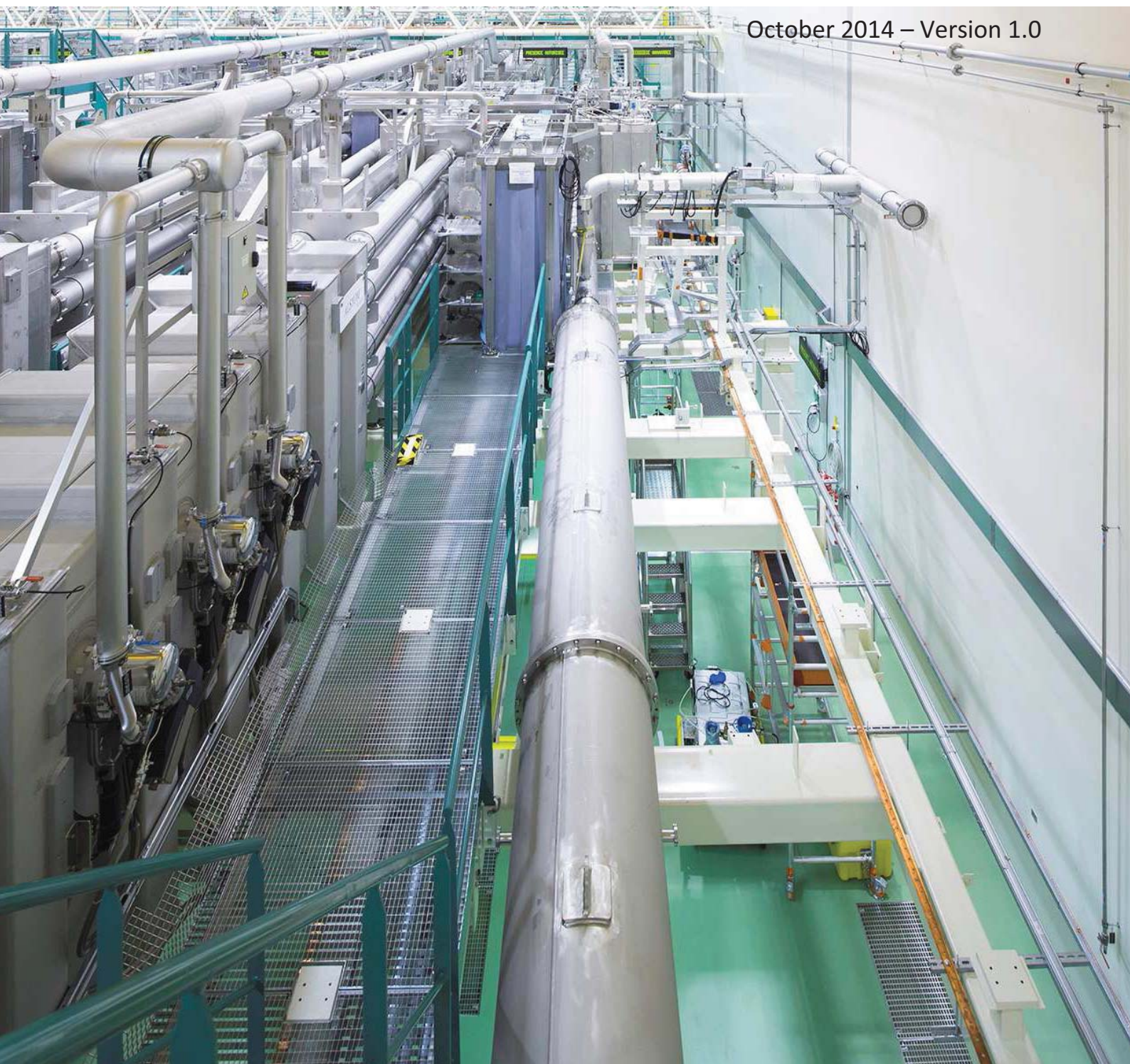


# LMJ – PETAL Scientific Case

## For academic access program

October 2014 – Version 1.0



# CONTENTS

<b>LMJ-PETAL SCIENTIFIC CASE.....</b>	<b>5</b>
Introduction.....	5
<b>MATERIALS AND HIGH ENERGY DENSITY PHYSICS .....</b>	<b>7</b>
Introduction.....	7
1. Planetary Interiors inside and outside our solar system .....	8
1.1 Erosion of the heavy elements cores of giant planets and icy giants .....	9
1.2 Modeling of icy giants, of cores of gas giant planets, and of “super-Earths” .....	10
1.3 Metallization of hydrogen at high pressure .....	11
1.4 Phase separation of the hydrogen-helium mixture .....	12
2. Physical – Chemistry of materials at ultra-high pressure.....	13
2.1 Status and opportunities .....	13
2.2 How to progress .....	14
2.3 The place of the LMJ-PETAL facility.....	15
3. Pathways to reach extreme states .....	15
4. Diagnostics.....	18
4.1 Introduction and state-to-the-art.....	18
4.2 Challenges and opportunities with LMJ-PETAL .....	19
4.3 Practical issues.....	20
5. Simulations .....	21
5.1 Brief Status .....	21
5.2 The open questions, challenges and impact .....	21
5.3 Research directions and opportunities with LMJ-PETAL.....	22
Practical conclusions .....	23
Sigles.....	25
References .....	26
<b>LABORATORY ASTROPHYSICS ON LMJ-PETAL .....</b>	<b>29</b>
Introduction.....	29
1. Atomic and Nuclear Physics.....	30
1.1 The state of the art .....	30
1.2 The LMJ-PETAL programme.....	32
1.3 Short term Experiments .....	34
1.4 Longer terms.....	36
2. Radiation Magneto Hydrodynamics .....	37
2.1 The big challenges .....	37
2.2 The state of the art .....	38
2.3 The long-term program .....	41
2.4 Science on a shorter time-line.....	43
2.5 The needed steps to go .....	43
3. High Energy Astrophysics and Interstellar Medium .....	44
3.1 Short-term goals.....	44
3.2 Mid-term (5-10 years) goals .....	47
3.2 Long-term goals (>10 years) .....	48
4. Diagnostics for laboratory Astrophysics .....	50



4.1 Petal diagnostics.....	50
4.2 LMJ diagnostics .....	50
4.3 Magnetic field diagnostics.....	50
5. Recommendations .....	51
References.....	53
<b>DEMONSTRATING DIRECT DRIVE INERTIAL FUSION USING THE LMJ-PETAL LASER SYSTEM.....</b>	<b>55</b>
Introduction .....	55
1. Review of the experimental studies of alternative ICF schemes .....	56
1.1 Shock ignition experiments.....	57
1.2 Experiments related to the fast ignition scheme .....	62
2. Theoretical and numerical developments: the actual status and the developments required to achieve the objectives.....	65
2.1 Challenges of the ICF research .....	65
2.2 State of the art .....	66
2.3 Long-term programme in computational ICF.....	67
2.4 Near term scientific program .....	68
3. Experimental goals .....	71
3.1 Shock ignition as the basis of consolidation of ICF research in Europe .....	71
3.2 Parameter domain for the experimental research .....	71
3.3 Physical issues of the shock ignition scheme .....	71
3.4 Target development and manufacturing .....	75
3.5 Target geometry.....	75
3.6 Diagnostics .....	76
4. Preparatory plans for LMJ-PETAL: work at intermediate scale facilities and numerical modelling development .....	78
4.1 General purposes of the LMJ-PETAL academic IFE program .....	78
4.2 Preparatory shock-ignition studies at small and intermediate scale facilities.....	79
4.3 Preparatory fast-ignition studies at small and intermediate scale facilities.....	81
4.4 Preparatory Polar Direct Drive studies at small and intermediate scale facilities.....	82
5. Proposals for the first phase of LMJ-PETAL experiments.....	83
5.1 Strong shock excitation for the conditions relevant to the shock ignition scheme.....	83
5.2 Laser plasma interaction in a long scale length plasma .....	83
5.3 Optimization of the ion acceleration for the ion fast ignition scheme .....	84
References.....	85
<b>HIGH ENERGY PHYSICS.....</b>	<b>87</b>
Introduction .....	87
1. The big challenges of the topic .....	87
2. The state of the art.....	88
2.1 Plasma based electron acceleration .....	88
2.2. Plasma-based proton and ion accelerators.....	89
2.3 Plasma based relativistic electron-positron pair creation .....	90
2.4 Investigate the nonlinear and dispersive properties of the quantum vacuum in strong laser fields.....	90
3. The long-term program .....	91
3.1 Laser-plasma electron acceleration .....	91

3.2 Cascaded Compression Conversion (C3) .....	91
3.3 Plasma based relativistic electron-positron pair creation.....	92
3.4 Laser-plasma ion acceleration to GeV .....	92
3.5 Control of the characteristics of laser-accelerated relativistic ion beams .....	93
3.6 Application to the study of relativistic collisionless shocks.....	94
3.7 Alternative acceleration schemes .....	94
3.8 Radiation processes.....	94
4. Science on a shorter time-line .....	95
4.1 Laser-plasma electron acceleration to 100 GeV.....	95
4.2 Laser-plasma ion acceleration to progress towards GeV energies and to study collisionless shocks .....	98
4.3 Electron positron pair creation.....	99
4.4 Plasma-based high power optics (the C3 technique) .....	100
4.5 Strong field QED .....	101
5. The needed steps to go .....	102
5.1 Simulating electron acceleration to TeV and the focusing of laser pulses to extreme intensities .....	102
5.2 Theoretical and numerical steps required to achieve ion acceleration to GeV .....	102
5.3 Diagnostic development for electron acceleration to 100 GeV .....	103
5.4 Diagnostics for ion acceleration and positrons generation.....	103
5.5 Target preparation for electron acceleration to 100 GeV .....	103
5.6 Target preparation for ion acceleration .....	104
Conclusion .....	105
Sigles .....	106
References .....	107

## **Annexe: LMJ-PETAL User guide**

# LMJ-PETAL SCIENTIFIC CASE

## Introduction

This document has been commissioned by ILP (Institut Lasers et Plasmas) in order to provide the scientific background foreseen for the “Academic Access” of the LMJ-PETAL facility as agreed and decided by CEA and Region Aquitaine.

LMJ is the largest laser facility being built in Europe: 176 beams will be installed, delivering up to 1.3 MJ-400 TW on target. The first light is expected end of 2014 with 1 bundle of 8 beams (1 beam delivers up to 7.5 kJ). In the coming year CEA will commission new bundles on LMJ. Progress in the commissioning will be posted regularly on the LMJ web site as the LMJ builds up. Otherwise, the PETAL laser is now being installed in the LMJ laser bay; it will deliver up to 3.6 kJ and around  $10^{20}$  W/cm<sup>2</sup> on target with pulses ranging from 0.5 to 10 ps. Coupling PETAL to LMJ target chamber and commissioning LMJ-PETAL will start in 2016 using the diagnostics provided by the PETAL+ project.

Coupling a long and short pulses-large energy multi beams facility with a high power-short duration auxiliary laser, will offer new possibilities of research not available until now. A percentage between 20 and 30% of LMJ shots will be provided for use to academic civilian research. In this context ILP has identified four priority research themes and four international scientific working groups have been established to prepare the following guide lines to research program on these topics. The outcome of this work has preliminarily been presented at the scientific community and discussed in the LMJ COST workshop held in Bordeaux in March 2014.

The four topics are the following:

Material and High Energy Density Physics. In high intensity laser-plasma interaction, the plasma ablation process induces by reaction a compression wave into the target, bringing the matter to almost unexplored conditions [low temperature < 20 000 K - high pressure > TPa]. The LMJ laser facility will allow experiments dealing with planetology and physical-chemistry of materials at ultra-high pressures, the PETAL laser driving x-ray diagnostics required for matter characterization.

Laboratory Astrophysics. LMJ appears as the most powerful facility in Europe to provide experimental conditions appropriate for astrophysical phenomena studies. Besides, PETAL will be used to create hard X-ray or charged particles sources to probe the matter. The proposal is organized in three topics: Atomic and Nuclear Physics (radiation processes and reaction rates); Radiation Magneto Hydrodynamics (relevant accretion-ejection processes); High Energy Astrophysics and Interstellar Medium (particularly collisionless shocks and MHD turbulence).

Inertial Confinement Fusion by Direct Drive for Energy Production. A determinant stage to settle the basic schemes for an Inertial Fusion for Energy (IFE) power plant is to experimentally validate the alternative ignition schemes which circumvent the major obstacles of the conventional approach. Among them, shock ignition appears achievable with the present-day laser technology and proper to an industrial implementing. The study of this process can be planned with the LMJ facility.

High Energy physics. This topic is more precisely devoted to the processes PETAL will give access to, on account of its performances. They are: acceleration of electrons to ultra-relativistic energies,

generation of relativistic ion beams, electron-positron pair creation. The proposal includes investigating the issues of a new approach to generate high power lasers: the Cascade Compression Conversion.

These four themes differ with regard to the energy needed, the diagnostics available or the numerical simulations required.

- As an example, it will be possible to enter upon Material and High Energy Density Physics and Laboratory Astrophysics even at the first stage of LMJ-PETAL, the short-term programme of these researches being easily able to evolve with the increase in intensity.
- The Inertial Confinement Fusion is of course one of the main motivation for the development of huge laser systems like LMJ and also for PETAL which will allow backlighting of compression experiments. The LMJ-PETAL facility can provide the platform to demonstrate shock ignition by polar direct drive in the next decade. However, it is clear that an IFE programme requires the development of a clear scientific and technological roadmap, which goes beyond the present document in the direction of a more programmatic and structured research program.
- The topic High Energy Physics, which relies mainly on PETAL, presents a feature somewhat more prospective.

we observe that all these topics have many cross-links with various domains of physics (planetology, high energy physics, magnetic confinement fusion) mainly on account of a transverse subject: the behavior of matter under extreme conditions, involving equations of state (EOS), radiative transfer (opacities, emissivities) and transport coefficients. Numerical simulations of the intended experiences require to improve numerical models and dispose of very accurate basic data bases.

Even if the experimental goals of each chapter are different, several transversal issues are easily identified: development and implementation of new diagnostics, target development and manufacturing, development and use of numerical codes open to the academic community for the design of experimental proposals and data interpretation. The growth of the LMJ-PETAL scientific case will thus offer an uncommon opportunity to strengthen by collaborative exchanges the bridges between the European plasma laboratories, and even open new possibilities for future applications, such as laser-driven proton therapy.

The four themes quoted above are described in the following chapters. Each of them presents a description of the topic, its big challenges, how a laser facility such as LMJ-PETAL can contribute, the state of the art, a long term program (ten-fifteen years), a shorter time-line experimental program (~five years starting from 2017) and the correlative steps required to achieve the objective. We think that the present document as well as the “Academic Access” of LMJ-PETAL which will take place starting in 2017 (with the first call for proposal in 2014) will be a first step towards the formation of a stronger scientific community in Europe working on the establishment of a programmatic approach of these topics.

# MATERIALS AND HIGH ENERGY DENSITY PHYSICS

**Contributors:** Alessandra Benuzzi-Mounaix, Fabien Dorchie, Tristan Guillot, François Guyot, Paul Loubeyre, Stéphane Mazevet, Thibaut de Rességuier

## Introduction

The irradiation of a sample by a high intensity laser pulse ablates a plasma cloud, which expands toward the laser source and drives by reaction a compression wave into the sample. If another laser pulse is used to generate X-rays from a backlighter, they can be used to probe the evolution of the sample structure during shock or ramp compression.

While synchrotron and free electron laser X-ray facilities are prospecting to acquire 100 J class lasers, and high power kJ class lasers are getting equipped with short pulses, LMJ-PETAL, coupling long and short pulses, will offer a unique opportunity to reach and study matter at greater pressures than in these facilities, allowing to investigate completely new materials and phenomena. The figure below shows a plot in temperature-density space indicating regions encompassed by different physical processes and conditions. Regions that will be accessible in the LMJ first stage as it begins operations and in the full LMJ are indicated in the figure and 1Mbar contour is shown.

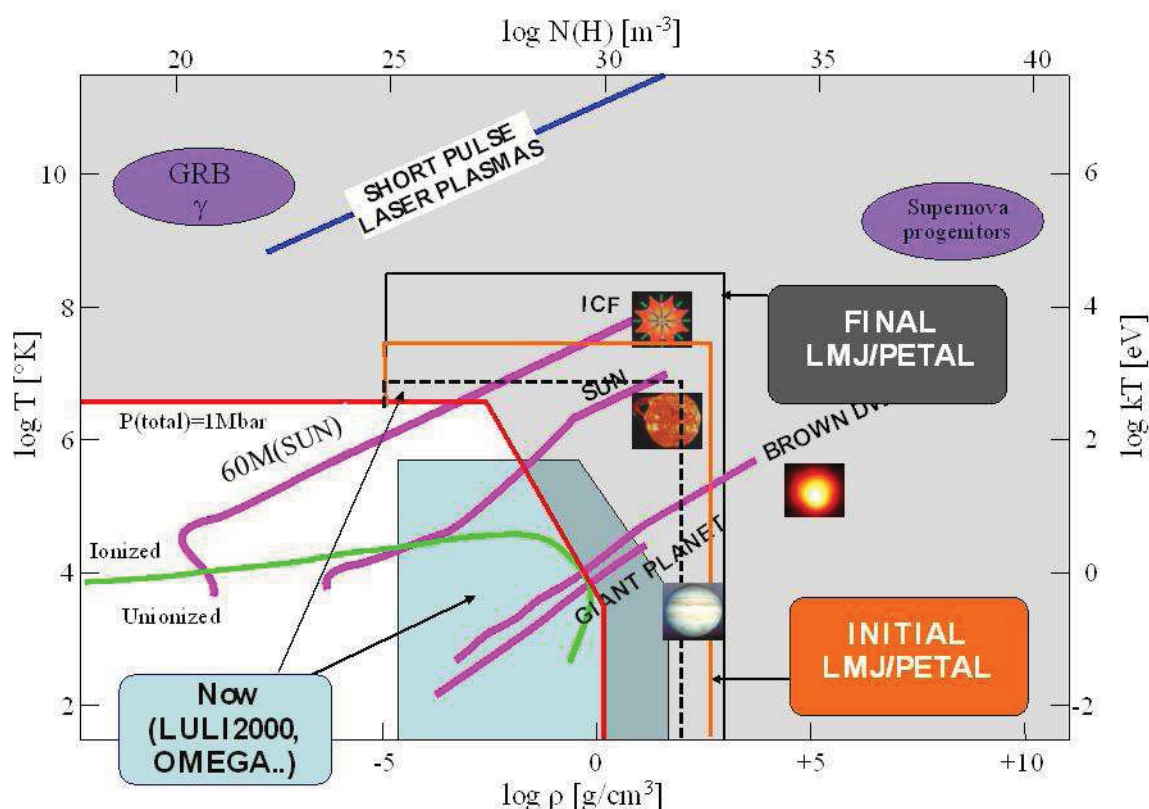


**Figure 1:** Phase diagram showing the region accessible with LMJ facility

The materials structures at these densities and temperatures along compression path are poorly known and will reveal entirely new phenomena and new phases. The reactive chemistry of elements with core electrons participating into bonding will open new fields in material science. At high temperatures, direct investigations of stellar interior conditions by a combination of nanosecond pulses to create the conditions and short pulses to probe the matter should open new dialogs with stellar astrophysics. A challenge of special interest that can be met by our scientific community is the high density low temperature regime ( $\log T < 4$ , pressure exceeding 10 Mbar = 1 terapascal (TPa)). This is so far almost unexplored by solid state physics and materials science and is beyond reach for plasma physics. At the border of presently accessible pressure-temperature conditions, a new paradigm is emerging: **extreme pressures seem to turn simplicity into complexity**. For example, simple metals that are expected to end up in the simple body cubic centered (bcc) structure at high pressures and temperatures adopt open and complex structures at TPa pressures, complexifying considerably the phase diagrams. Superionic phases are emerging in some molecular systems, which is key to the modeling of transport properties of icy giant planets. Pressure-induced chemical complexity (e.g. immiscibilities) is of prime importance **in solid state physics, materials science and planetology**. The LMJ-PETAL setup will open up a unique possibility, using the LMJ ("pump") to reach this pressure-temperature regime and using PETAL ("probe") to produce short pulses of X-rays to characterize this matter. Due to the limited access and high cost of a single shot on such a facility, the LMJ-PETAL shots should be dedicated to reach the few TPa range in close coordination with the studies of materials that will in parallel be investigated up to the TPa range in front of synchrotron, XFEL and KJ laser facilities. This complementarity should motivate numerous scientists involved in extreme conditions at synchrotron and XFEL to get interested in this pressure extension of their normal investigation domain.

*N.B: acronyms, references and authors are listed at the end of section.*

## 1. Planetary Interiors inside and outside our solar system

We now know more than 1600 exoplanets in orbit around stars as close as a few to several hundred light years away. These planets, whose masses range from that of our Earth and below up to more than Jupiter's mass (and extending to the brown dwarf range) can in some cases be characterized with a variety of methods: their mass can be measured with radial velocimetry, their size can be determined when they transit in front of their star. In the most favorable cases, their atmospheric thermal structure and even their dynamics can be determined, and one can detect spectral signatures from chemical species present in their atmospheres and/or the presence of clouds/hazes. These data are often of limited accuracy, but they give access to a very rich statistical information to understand globally these new worlds and planet formation mechanisms. Beyond this global information, certain "exotic" planets provide keys to help solving problems which are much wider (the archetype being 51 Peg b the first giant planet detected around a solar-type star which showed the importance of migration in protoplanetary disks - see [16]). Lastly, the characterization of planets which are very hot (because close to their parent star) enables one to detect elements or compounds



such as water, alkaline elements and even silicates which are hidden from electromagnetic radiation in the solar system giant planets because of their condensation at depth (e.g. [9]).

In parallel, studies on the planets of our solar system are crucial to get much more detailed and precise information which can be compared and linked to the more global knowledge acquired on exoplanets. This is in particular the case of Jupiter and Saturn, for which new data on their internal structure, magnetic field and composition are to be obtained starting in 2016 thanks to the space missions Juno and Cassini-Huygens. Furthermore, free oscillations of these two planets have been detected at last, directly in the case of Jupiter [6] and indirectly through resonances of its rings in the case of Saturn [11], which should on a longer timescale lead to the possibility to measure directly density jumps due to phase transitions or to changes in chemical composition in the deep interiors [14].

Laboratory experiments to compress matter to ultra-high pressure and its interpretation through theoretical studies and numerical models are crucial to correctly interpret these astrophysical measurements in terms of internal structure, evolution and planetary formation. Indeed, the equations of state and phase diagrams, beyond 1 TPa, of primary constituents of giant planets, such as  $H_2$ , He,  $H_2O$ , silicates, iron are at the basis of all the models of internal structure and evolution of those planets. The behavior of mixtures of these primary constituents, their equations of state and their possible separation are also crucial to understand planetary evolution and internal structure due to the action of gravity and the possible formation of layers of differing composition (e.g. [8, 15, 22, 31, 33, 36, 37]). Thanks to the very high laser energy available, equations of states and complete phase diagrams will be recorded along the compression path (typically up to 4 TPa 10 000K, see “pathways to reach extreme states” below) thus providing important data on  $H_2$ -He mixtures, ices, silicates, and metallic iron-based alloys at conditions of large super Earths and icy giants. The obtained data will be key to interpret the new observations acquired on Jupiter and Saturn (in particular extremely accurate gravity fields yielding constraints on the interior density profile) and on exoplanets (in particular chemical compositions).

Some of the experiments for planetology which could be realized at the LMJ-PETAL using the synergies between LMJ and PETAL are presented hereafter.

### **1.1 Erosion of the heavy elements cores of giant planets and icy giants**

The problem of the erosion of the cores of the giant planets is linked to the interpretation of the abundances measured in these planets. For example, we do not yet know whether such an erosion is responsible for the enrichment in heavy elements observed in solar system giant planets, an enrichment over the solar values which is progressively higher from Jupiter to Neptune (see e.g. [10]). This external heavy element signature has also potentially very significant effects on the thermal evolution of these planets [8] and on their internal structure with the possibility of semi-convective layers in the envelope [15].

The progresses of numerical simulations have implied the possibility to directly test the solubility of various elements in metallic hydrogen, particularly water [38], rocks [38] and iron [36]. These calculations predict that these elements should be soluble in most astrophysical conditions, implying a possible progressive erosion of planetary cores limited by energetic and hydrodynamical

considerations. A test in the laboratory of these predictions would be desirable. Equations of state of ices, silicates and iron metal, in particular up to several TPa and moderate temperatures relevant to giant planets interiors, are the necessary ingredients for building a consistent thermodynamic model of their solubility in H<sub>2</sub>-He mixtures.

## **1.2 Modeling of icy giants, of cores of gas giant planets, and of “super-Earths”**

One of the research areas most quickly evolving concerns the study of planets of sizes intermediate between terrestrial and giant planets, such as Uranus and Neptune. We now have detected numerous such exoplanets and their occurrence rate appears to be at least five times higher than giant planets with the mass of Saturn and above [24, 13]. These planets can be studied more easily than terrestrial planets because of their relatively large sizes (about 4 times that of the Earth), and the fact that they are more frequent than giant planets implies that they can be found around stars which are on average closer to us and therefore brighter.

These planets are more complex than gas giants such as Jupiter because of the large diversity of possible compositions and because of our poor knowledge of the behavior of their constituents at high pressures. Uranus and Neptune are named "ice giants" because their internal structure is in majority compatible with a mixture of water, methane and ammonia which were condensed in the form of ices in the protosolar disk (e.g. [28]). These ices must have been accreted inside these planets but they are of course under a different fluid or superionic phase in the interiors, and we do not know whether they are assembled with other compounds (iron, rocks, H<sub>2</sub>-He), and in which proportions. Models with several layers have been calculated (e.g. [25]), but we do not know how close they apply to the real planets due to the absence of real constraints on the phase separation of the different species. Are rocks fully solubilized in water at these pressures and temperatures? What about iron, and the effect of other species (e.g. NH<sub>3</sub>)?

Equations of state of silicates and iron-based alloys and of their assemblages are needed to model their solubilities in ices at the relevant planetary conditions. These considerations apply to the possible heavy element cores of gas giant planets. In that case, equations of state of iron-based alloys, silicates and ices are needed to model the mutual solubilities of all these compounds in the TPa pressure range, as well as their solubilities in H<sub>2</sub>-He mixtures.

As far as terrestrial type planets (i.e. having a density close to that of the Earth) are concerned, equations of state and phase diagrams of iron-based alloys, of silicates and of their assemblages, and also of carbon compounds, will be needed up to several TPa-10000 K in order to test density models of these planets as well as to investigate their mutual reactivities and solubilities (e.g. modeling the reactivities at the core-mantle boundaries of these objects)

The possibility to directly characterize these exoplanets (thanks in particular to space missions in preparation such as JWST, CHEOPS, TESS, all due to be launched around 2018) will require to know accurately the various phase diagrams. The laboratory measurement of the behavior of various assemblages (water with -rocks, iron, molecular hydrogen, methane, ammonia...etc.) will thus be extremely valuable. It will contribute to much better constraint planetary models by providing an integrated view of the equations of state of planetary materials such as (1) H<sub>2</sub>O, CH<sub>4</sub>, NH<sub>3</sub>; (2) solids and melts in the Mg-Si-O system (i.e. “silicates” or “rocks”); (3) solids and melts in the Fe-Ni-Si-O-S

system (i.e. metallic alloys) up to very high pressures (several TPa) and not so elevated temperatures (typically less than 20000 K or 2eV).

As far as PETAL is concerned, generation of X-ray pulses might not appear appropriate for studying elements as light as  $H_2$  or  $H_2$ -He mixtures but transverse X-ray radiography and X-ray Thomson scattering could provide important original data in this yet unexplored pressure-temperature regime. Two important examples are given below.

### **1.3 Metallization of hydrogen at high pressure**

Recent ab initio calculations of the compression of hydrogen to high pressures [22] have shown the presence of a first order phase transition in fluid hydrogen, but at lower temperatures than previously expected. The critical point of this liquid-liquid transition as predicted by models is around 2000K for a pressure around 1 to 1.2 Mbar (100 to 120 GPa), much below the adiabat expected for any giant planet. However, laboratory experiments in the pressure and temperature domain relevant for giant planets (around 5000 to 10000K and 1 to 5 Mbar) show that the transition to a conducting state of hydrogen occurs at these temperatures and pressures, i.e. at much higher temperatures than predicted by theory [19]. It is obvious that a full exploration of this parameter domain by dynamical measurements in the several TPa range would bring very important constraints to better understand this region and subsequently planetary interiors. This is important to interpret gravity and magnetic field measurements by Juno since Jupiter's magnetic field is largely controlled by this region (e.g. [33]).

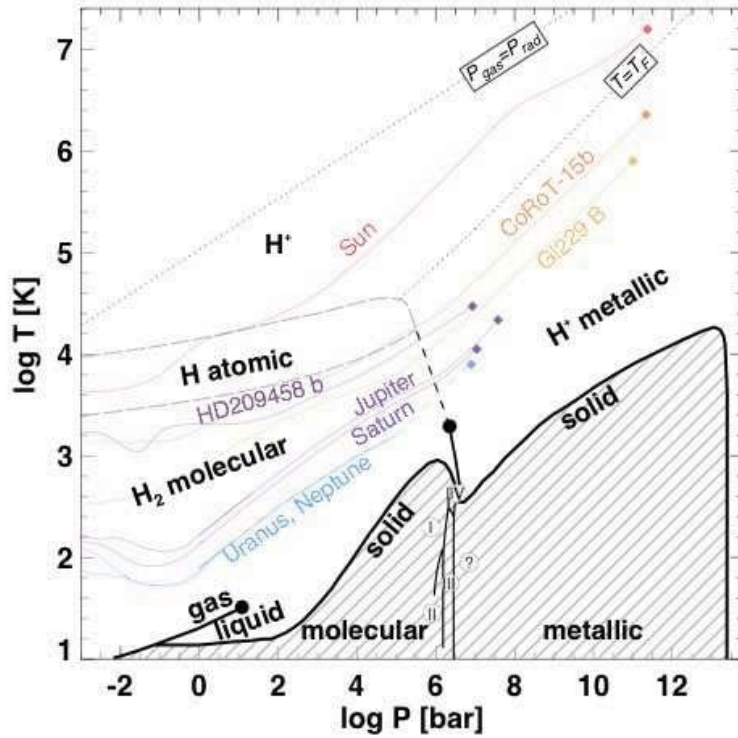


**Figure 2:** Phase diagram for hydrogen in the pressure-temperature plane, with pressure in bars ( $1\text{bar} = 10^5\text{ Pa} = 10^6\text{ dyn cm}^{-2}$ ). The thick lines indicate the first order (discontinuous) phase transitions, the black circles the critical points. Colored lines show profiles for a selection of noteworthy substellar objects: giant planets from Uranus to Jupiter, the hot Jupiter HD 209458 b, the brown dwarfs Gl 229 B, CoRoT-15 b and our Sun (from [10]).

#### 1.4 Phase separation of the hydrogen-helium mixture

We have known since the early 80s that Saturn's atmosphere is helium poor, and it has been verified by in-situ measurements by the Galileo probe in 1995 that it is also the case for Jupiter (see [9] and references therein). This is interpreted as due to the phase separation of helium in metallic hydrogen at pressures of around a Mbar ([34], see also [4]), which has been confirmed by the low abundance of neon in the atmosphere, this gas being easily soluble and therefore carried down into helium droplets [29, 37]. Although the idea dates back to work in the late 1960's and it has been implemented (at least qualitatively) into interior models since then, we still lack a proper phase diagram. Important progresses have been made in this domain thanks to ab-initio numerical simulations of the hydrogen-helium mixture [18, 21, 32] but relatively significant differences ( $\sim 700\text{ K}$ ) remain which limit the interpretation of abundance measurements in Jupiter and Saturn. Measurements with the LMJ that would take advantage of the larger sample sizes could potentially lead to great improvements of our knowledge of the behavior of the hydrogen-helium mixture up to several TPa pressures. The determination of a precise phase diagram would not only greatly narrow down the ensemble of possible solutions for internal structure models (e.g. [12]) with a direct application to the interpretation of the Juno and Cassini-Huygens measurements, but it would also be crucial to better understand the thermal evolution of these planets.



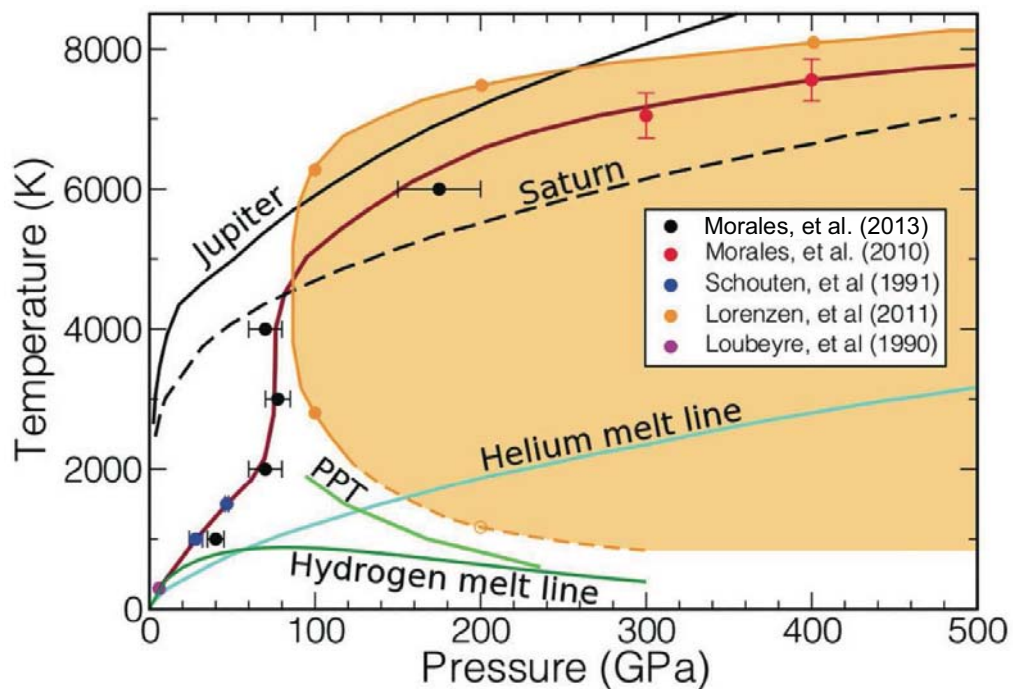


**Figure 3:** Phase diagram of the hydrogen-helium mixture for a helium mole concentration of 8%. The orange region shows where the two elements are expected to separate from each other according to the calculations of Lorenzen et al. [18]. The red curve correspond to the critical temperature for that separation according to Morales et al. [21]. Numerical results by Schouten et al. [30] and experimental determinations by Loubeyre et al. [20] are also shown. The back curves show the isentropes of Jupiter (plain) and Saturn (dashed) respectively. (From Morales et al. [21])

## 2. Physical – Chemistry of materials at ultra-high pressure

### 2.1 Status and opportunities

Over the past 20 years, remarkable progress has been achieved in the measurement of the phase diagram of the elements up to the Mbar range. That has been made possible with the extensive use of the 3<sup>rd</sup> generation synchrotron facilities by the high pressure community. The traditional view of highly compressed matter and materials is that the valence electrons are pushed into continuum to form a near-free electron gas surrounding ions which should pack in more simple structures. Hence, the systematic transformation of insulator to metal under pressure. That has certainly been successful in understanding material properties up to the Mbar since the compressional energy given to system in this pressure range is roughly the energy scale of bonding and valence electrons. However, some recent observations give evidence that materials at higher pressures will behave quite differently. Sodium, an archetypical ambient pressure free electron metal, adopts the most

complex structure ever observed in an elemental solid, with 500 atoms in the unit cell near 1 Mbar, and becomes a transparent insulator with an open ionic structure near 2 Mbar [23]. That observation has spurred various computational searches of the phase diagrams of the elements in the TPa range using density functional theory. Indeed, extreme pressure seems to turn simplicity into complexity. Aluminum, for example, is expected to adopt more open structures at TPa pressures as the valence electrons move away from the ions in the formation of electride structures [26]. Several stable phases of nitrogen at multi-TPa pressures are predicted including a metallic salt structure consisting of partially charged  $N^{+\delta}_2$  pairs and  $N^{-\delta}_5$  tetrahedra, which is stable in the 2 TPa range [34]. Finally, solid hydrogen in the few Mbar range is predicted to adopt a complex phase diagram with 1D, 2D and mixed phases [Geneste et al. to be published].

Systematic exploration of the phase diagram of the elements up to the TPa range is a new frontier in condensed matter physics with potential applications to the synthesis of very novel materials and great usefulness in characterizing the properties of the constituents of the interior of exo-planets (see paragraph 1).

The compressional energy given to a system is about 1 eV at 1 Mbar ( $\sim 0.1$  TPa) and 1 Kev at  $\sim 10$  TPa. 1 eV being the order of the bonding energy in molecules, changes in chemical bonding have been observed. Solid  $N_2$  transforms into a polymer at about 1 Mbar, with the transformation of triply bonded molecules into an extended singly bonded solid [3]. Poly-N is a High Energy Density Material and if recoverable at ambient pressure, it would revolutionize the spatial propulsion. Water transforms into an ionic solid [1]. Certainly going to the Mbar is inimical to the chemical bond but by going in the TPa range new chemical bonding might re-emerge, this time due to the core electrons. That is a very speculative proposal at present that awaits for proof of principle example. These new chemical forces will certainly drive the auto-organization of matter under such extreme pressure with again valuable relevance for planetary interiors.

## 2.2 How to progress

“Materials at TPa pressures” is thus the new frontier for extreme condensed matter. The good strategy to achieve measurements in this pressure range with a fine enough microscopic characterization is being discussed by the static and dynamic compression communities. Recent achievements assure the foundations of various projects. In static, it has been shown recently that 0.6 TPa pressure is becoming accessible with the diamond anvil cell using a geometry based on the design of the double-stage anvils [2]. Hence, the fine exploration of the properties of matter under TPa could continue in front of synchrotron facilities. In dynamic, by using few 10's of J lasers, small enough to fit in a synchrotron or in a x-ray free electron laser (XFEL) experimental hutch, matter could be dynamically compressed by a shock in the TPa pressure range, on few 100  $\mu m$  diameter though. Even if it is very promising, the reliability of such experiments remains to demonstrate. Dynamical community is moving in front of these facilities that can give a fine x-ray characterization of the microscopic properties of the sample. The X-ray absorption is the most adapted diagnostics by enabling the measurements of the electronic and structural properties of the sample in the solid and fluid phases. But spectacular advances have been achieved on few KJ to MJ large laser facilities. The laser energy is used to compress matter to extreme pressure and various paths of compression can

be followed from quasi-isentrope to Hugoniot. Ramp compression of diamond has been achieved up to 5 TPa on NIF facility using 600 kJ [Smith et al. to be published]. Some laser beams can also be used to provide the x-ray diagnostics. Recently, compressed Fe to 0.56 TPa has been finely characterized by Extended x-ray absorption fine structure (EXAFS) spectroscopy, with similar fineness than on a synchrotron facility, in front of the OMEGA facility [7]. X-ray diffraction has also been achieved to 0.9 TPa on Molybdenum.

## **2.3 The place of the LMJ-PETAL facility**

As discussed above, there are very complementary approaches to progress in the exploration of the phase diagram of the elements in the TPa range. They are complementary and all necessary. In fact, there is now some porosity between the static and dynamic communities. Some groups are involved in both approaches in front of various facilities. However, it should be clear that the few TPa range coupled to moderate to low temperatures will only be achievable on MJ laser facilities. The LMJ laser will provide energy and pulse shape to generate the controlled dynamic compression of matter. The PETAL laser is driving of the x-ray diagnostics that will be developed to characterize microscopically matter under such extreme pressure

## **3. Pathways to reach extreme states**

Traditionally shocks are used to compress matter dynamically to high pressures but heat considerably also the sample. For pressures exceeding 0.2 TPa, this heating is too strong to reach states relevant for planetary cores and for investigating pressure-induced complexity in materials. This temperature elevation is due to the strong entropy increase in the shock process. For this reason, in the last recent years, an alternative method of laser-driven compression has been developed. This technique is referred as “ramped” or “shockless” or “quasi-isentropic compression” and it is based on irradiating a sample with a temporally increasing laser pulse. To reach several TPa states using this method, laser pulse length of more than 20 ns and tens of kJ of laser energy are necessary.

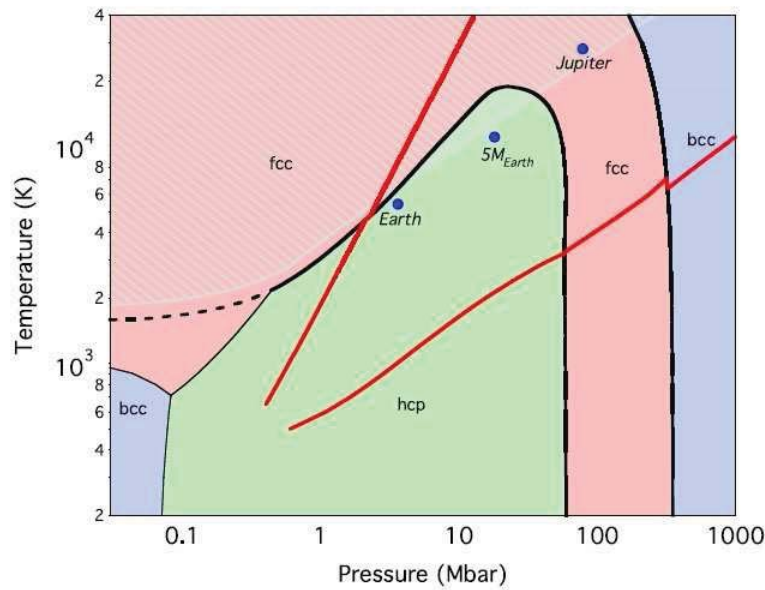


**Figure 4:** Iron Phase diagram (Stixrude 2012): Hugoniot, isentrope, earth and super earth states are shown

In recent experiments at LIL, pressures up to 8 Mbar (0.8 TPa) and temperatures lower than 10,000 K (relevant to giant planets and super earths) have been obtained by applying this ramp technique and equations of state have been measured. LMJ-PETAL facility offers an unique possibility to go beyond these conditions and to simultaneously probe the microscopic structure thanks to X-ray diagnostics. To get reliable and useable data, it is fundamental to study also the kinetics of phase transitions depending on load rate of the compression. Indeed, we need to understand how the phase diagram can be investigated using dynamic compressions, taking into account kinetic hindrances such as overshoots in pressure and temperature necessary to accomplish the phase change.

Another motivation for the creation of extreme states of matter with different compression rates is understanding the nature and time-dependence of material deformation under dynamic loading conditions. Different compression rates will be obtained by changing the laser ramp. This is an important goal in condensed matter physics. As the interatomic spacing decreases, overlapping electronic band structure and increased levels of stress can fundamentally alter the transport, chemical, and mechanical characteristics of the material. The LMJ-PETAL will allow to create novel states of matter and materials at very high compressions requiring an understanding of the physical principles that underpin exactly how such states are reached, including the roles of metastability. An example is investigating the overheating. A crucial point is to investigate the superheating of a solid that occurs when the long-range order of the crystalline structure is maintained up to certain temperature above the equilibrium melting temperature.



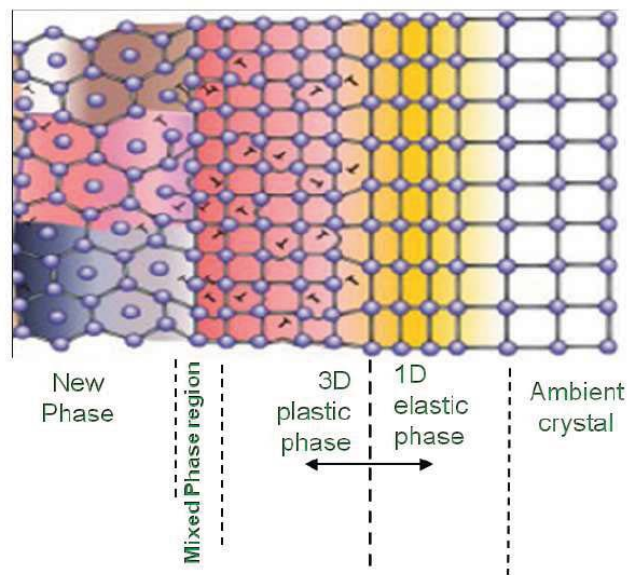


**Figure 5:** A schematic representation of how a material evolves under extreme compression

The response of materials to compression is not merely encompassed by asking how a solid can behave like a liquid. The complexity of the potential response is such that the opposite question, i.e. how liquids can behave like solids, is also one that arises at ultrahigh strain rates, as material response becomes highly time dependent. The physics of the time dependence of phase transitions and inelastic deformation ensures that compression time (or rate) itself will be one of the areas of parameters space that needs to be explored, as well as compression, deformation, and temperature. Understanding these processes will lead to accessing not only new stable, but also metastable states.

Our knowledge of the electrical and thermal properties, as well as optical properties, is also poorly developed for extreme states, and one of the greatest challenges will be to develop experimental techniques that allow us to probe these parameters. The extreme states generated by LMJ beams will be transient and in conjunction with development of loading paths, the use of highly time-resolved diagnostics will be of paramount importance. The measurements of phase and structural changes will be achieved thanks to X-ray diagnostics like X-ray diffraction or XANES/EXAFS (see below, paragraph “diagnostics”).

## 4. Diagnostics

### 4.1 Introduction and state-to-the-art

Some challenges remain regarding diagnostics. First, **we need to control and characterize the thermodynamic conditions achieved**: temperature, pressure and/or density, spatial homogeneity, temporal evolution ... Second, **we need to get reliable data in order to understand the physics** that governs matter in these extreme conditions. **Macroscopic properties** are very useful to describe large systems such as planet interiors or other astrophysical objects: equation of state – EOS – (or more exactly relation between temperature, density and pressure), transport coefficients (optical, thermal and electrical conductivities), and radiation properties (opacities, emissivity). **The specific complexity of this physics occurs at the microscopic scale**: atomic and electron structure, that imposes to use large-scale calculations (quantum description of electrons on a system with large number of atoms). Such calculations need to be supported and tested by reliable experimental data, and at the microscopic scale, which is more natural and relevant.

**Optical diagnostics** were the first to be used to diagnose high energy density (HED) matter. Among them, **VISAR and SOP** are still the most used in a large range of experiments. The VISAR (Velocity Interferometer System for Any Reflector) uses a nanosecond laser beam (different but synchronized to the high energy one used to achieve HED), to probe the rear side of a shock-compressed target (1D compression from the front side) and to get shock/fluid or rear surface velocity.

SOP (Streaked Optical Pyrometry) consists in measuring the self-emission from the rear side of the target. Assuming gray body type radiation and using VISAR reflectivity measurements, the temperature can be inferred, with a good efficiency, as long as the temperature exceeds  $\sim 0.5$  eV.

These visible diagnostics are used systematically in shock compression and in isentropic compression experiments and allow us to obtain useful equation of state data. Therefore, **they provide essential control of the temperature / density conditions achieved but they don't provide measurements on structure**.

Recent years have seen a significant development of **new diagnostics based on the use of X-ray pulses** generated by the interaction of a synchronized laser pulse (nanosecond or picosecond) on a backlight target. They can prospectively provide unprecedented data from the inside of the target, extending studies in a wide range of materials, and **giving access to the physics at the atomic scale**. Most of the time, these techniques have been exploited by using X-ray sources generated from a picosecond beam synchronized with the high-energy ns beam(s). More unusually, more than ten beams (nanosecond) at Omega have been focused on a plastic sphere to produce bright broadband X-ray source for EXAFS experiment [39].

In the last years, some experiments have been performed using X-ray Free Electron Laser as a bright ( $\sim 10^{12}$  photons per pulse), tunable (range  $\sim 1 - 10$  keV), collimated and extremely short X-ray probe ( $< 100$  femtosecond). At this time, two systems offer beam time access for experiments (LCLS in USA and SACLA in Japan). They are based on electron accelerators. Some are coupled with high-energy lasers, but with energy  $\sim 10$  J, limiting the studies in a moderate pressure regime. Note that the

HIBEF project aims at coupling kiloJoule class optical laser with the European XFEL under construction at Hamburg.

Four X-ray diagnostics that have been explored are listed below, based on the effective interesting results that have been yet demonstrated, and on their expected suitability when operated with single-shot high energy laser facilities such as LMJ-PETAL.

1. The X-ray diffraction and/or diffuse scattering probe the long-range order and/or correlations between atoms. It requires a quasi-monochromatic X-ray emission and 2D spatial detection (angularly resolved X-ray scattered signal).
2. The transverse X-ray radiography using quasi-monochromatic X-ray emission to allow probing the pressurization ramp and possibly obtain a time resolved macroscopic measurement of density (if coupled to a time-resolved 1D or 2D detector).
3. The X-ray Thomson elastic and/or inelastic scattering, using quasi-monochromatic X-ray emission, provides information about correlation between ions and/or electrons and gives access to the plasmas parameters (electronic density, temperature and ionization). The principle is to spectrally resolve the X-rays scattered by the medium under study. It requires high-resolution X-ray spectrometers ( $\sim 1\text{eV}$ ) set-up at different angles from the X-ray probing axis.
4. The X-ray absorption fine spectroscopy including XANES (X-ray Absorption Near-Edge Spectroscopy) and EXAFS (Extended X-ray Absorption Fine Structure) probes the electron structure and the short-range atomic order. It requires a broadband X-ray spectrum (up to  $\sim 200\text{ eV}$ ) and two high-resolution X-ray spectrometers ( $\sim 1\text{ eV}$ ): one to register the transmitted spectrum while the other one monitors the incident spectrum.

Besides these basic descriptions, the X-ray diagnostic choice is strongly driven by the physics and particularly by the element under consideration. XANES and EXAFS are related to X-ray measurements near absorption edge. Compounds containing light elements only, such as  $\text{CH}_4$ ,  $\text{H}_2\text{O}$  or  $\text{NH}_3$ , would require working with X-rays with so low energies that the absorption would be saturated even for the thinnest samples compatible with laser compression. X-ray scattering (including diffraction) would be the best choice method of study. In contrast, silicates and iron alloys could be probed both by elastic X-ray scattering and by X-ray absorption fine spectroscopy.

## **4.2 Challenges and opportunities with LMJ-PETAL**

Offering such amount of energy, LMJ-PETAL will clearly open new frontiers in the HED physics, significantly extending the phase diagram towards high pressures (using LMJ), and drastically improving the possible X-ray probes (using PETAL). The first point is clearly associated with the energy that can be invested in the HED production. The second point depends partly on the energy in the laser used to produce the X-ray probe. Many experiments have demonstrated the proof-of-principle of each diagnostic, but in some cases, the X-ray statistics was not high enough to give clean and quantitative measurements. A last, but not least, important challenge is to integrate a large set of diagnostics together (on the same shot), since a lot of physics can be extracted from the combination of optical and X-ray diagnostics.

As LMJ-PETAL will be a complex and expensive system, delivering a limited number of shots, it is not relevant to think about exploring new prospective diagnostics. Integrating the existing and robust diagnostics is already a big challenge, even if taking advantage from knowledge and expertise acquired on smaller scale laser systems (kiloJoule).

VISARs and SOP should not be overlooked anyway, since they will provide the control of the target thermodynamic parameters, and also exploitable physical data. VISAR requires a probe laser beam synchronized with the main laser pulses. This pulse must be long enough in time to probe all the sample compression, in particular in quasi-isentropic scheme (up to 40 ns). Time-resolution is currently provided by electronic signals used to trigger the streak optical cameras ( $\sim 10$  ps). A full time evolution is given by these streaks in a single shot.

Concerning X-rays, different strategies can be considered. One can use some nanosecond laser pulses to produce a bright and nanosecond X-ray source. Then time resolved diagnostics are implemented in order to follow the full temporal evolution of the target. That option is energy consuming since time resolved diagnostic alters the X-ray photon number statistics. The other option consists in producing a bright and short X-ray pulse from the interaction of PETAL with a backlight target. That assumes a “perfect” synchronization ( $\sim 10$  ps) between PETAL and LMJ, and a good predictability of the target temporal evolution (given by optical diagnostics), in order to catch the matter in the desired thermodynamic conditions.

#### **4.3 Practical issues**

There is no universal X-ray source for the different considered types of X-ray diagnostics. X-ray diffraction, radiography and/or scattering require quasi-monochromatic source. X-ray absorption needs broadband emission (over  $\sim 200$  eV). That indicates that preliminary work will have to be performed on X-ray source development, even by extrapolating results from smaller scale facilities.

Similarly, specific detection is required for each diagnostic. The detectors are based on the same general devices: imaging detectors and/or X-ray spectrometers. But the spectral range and resolution ( $\sim 1$  eV resolution required for x-ray spectrometer) will have to be defined for each experiment. Another issue concerns the geometry between the main target (HED sample), the X-ray backlight and the detection. For absorption spectroscopy and radiography, one has to measure the X-ray probe along the axis from backlight to HED sample. For X-ray scattering and diffraction, the detection should be at a large angle from this axis.

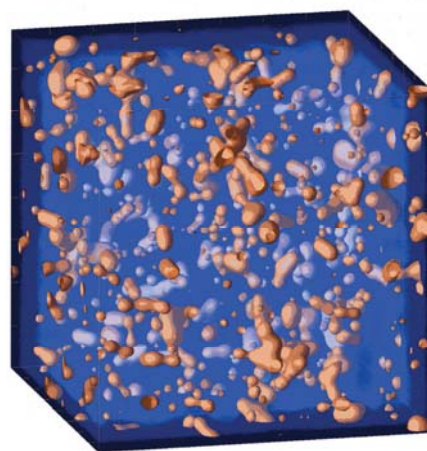
The main conclusion is that despite the wide scientific potential of LMJ-PETAL, each experiment needs specific design and preparation. At least, in the first years, the versatility will not be high enough to perform all of them. It is necessary to select some of these, taking into account the constraints of the facility: available diagnostic, geometry, and so on.



## 5. Simulations

### 5.1 Brief Status

After fifteen years of use, molecular dynamics simulations based on density functional theory have provided a solid theoretical framework to calculate the properties of matter at the extreme densities and temperatures relevant to the high energy density domain. As the method contains no adjustable parameters, it has been used rather systematically to describe a large variety of simple compounds in the regime relevant to planetary interiors and the high energy density domain. While initially applicable to a restricted density-temperature range, the significant increase in computational power available worldwide makes it now possible to simulate entire phase diagrams for simple elements starting from densities close to a fraction of solid density.



There is no limit in the densities that can be simulated at present. Regarding temperatures, current computational facilities limit simulations to about 10 eV around normal conditions to a few keV at the most extreme densities. Combined with Path Integral Monte Carlo simulations that are amenable in the missing temperature domain, complete phase diagrams are now available for the basic elements and compounds needed to model planetary interiors such as H, He, H-He, Fe, SiO<sub>2</sub>, H<sub>2</sub>O. Various comparisons at the level of the equation of states along the principal and multiple shock Hugoniot indicate that the method is rather robust to produce equations of states with no significant discrepancies identified for these simple elements so far. Despite this remarkable success, several questions and challenges remain.

### 5.2 The open questions, challenges and impact

From a simulation standpoint, the main challenges that need to be tackled in the coming years for addressing all the situations encountered in the high energy density regime concern the particle and time barrier, the high temperature limit, the behavior of DFT functionals at extreme conditions and the validation of the transport properties. To encompass these limitations would allow a direct comparison between the theoretical predictions and the experimental data at the same time and length scales and for various complex materials. This would also enable ones to investigate transient phenomena such as the kinetics of phase transitions in both equilibrium and non-equilibrium situations and elucidate chemistry in the extreme.

Under the paradigm of “complexity at the extreme” that appears amenable for the size of the experimental and theoretical communities that can be potentially involved at the national or European level, these challenges may translate into two priorities:

**1. Validating the behavior of DFT functionals** at high pressures and high temperature and whether Thomas Fermi approximation is the proper limit:

- Contrary to common wisdoms, it appears that under DFT simulations, several elements behave as electrolytes instead of displaying a free electron gas behavior at extreme densities and moderate temperature.
- Whether finite temperature DFT combined with temperature independent functionals is a sufficient assumption remains to be validated in the extreme.
- Is the chemistry induced by core electrons and occurring as the valence electrons constitute a metallic background properly predicted by DFT functionals.

**2. Phase diagrams in the extreme:** ab initio simulations predict that extreme density conditions bring about unique phenomena such as ionic phases for molecular systems, immiscibility for binary system, zero temperature melting.

To understand and master these issues would validate the properties currently predicted for planetary interiors and for which no experimental data are available. To reach these goals also requires going beyond the number of particles that can be currently simulated by an order of magnitude to model complex molecular systems, iron alloys, and silicates that display these unique phenomena at extreme conditions. This also requires to elaborate innovative simulation methods to elucidate these complex phase diagrams and phenomena, as well as the calculation of relevant quantities that can be used as relevant diagnostics that can validate the ab initio predictions.

### 5.3 Research directions and opportunities with LMJ-PETAL

The coupling between LMJ and PETAL opens up the opportunity to reach the high density low temperature conditions relevant to planetary science combined with X-ray diagnostics. This will not only allow ones to investigate phase diagrams way outside the principal Hugoniot region but also to bring information beyond the usual macroscopic quantities such as shock velocity or reflectivity using X-ray diagnostics.

From a simulation standpoint, the X-ray diagnostics currently available, elastic scattering/diffraction, and XANES spectroscopy described in the previous section bring about different sets of information. Elastic scattering/diffraction measurements bring information on the atomic correlations in respectively the liquid and solid condensed phases. XANES spectroscopy also carries information on the local atomic order but further brings information directly on the electronic structure as the cross section is proportional to the partial density of states of the element whose absorption edge is

investigated. Two classes of experiments can be envisioned in this new installation two address the two challenges identified above:

1. **LMJ-PETAL used with XANES diagnostic** to validate the behavior of functionals at large in extreme conditions. This also partially validates the predictions regarding properties such as optical absorption and electrical conductivity.
2. **LMJ-PETAL used with elastic scattering/diffraction diagnostics** to identify new solid phases, ionic phases, immiscibility regions, and to measure high pressure melting curves.

## Practical conclusions

In the worldwide active research about materials under extreme conditions, the LMJ-PETAL facility will have a special place in providing pressure conditions of several terapascals ( $1 \text{ TPa} = 10^{12} \text{ Pa} = 10 \text{ Mbar}$ ), associated to temperatures remaining below 20000 K, and while providing the x-ray diagnostics mandatory to investigate matter under these conditions. This pressure and temperature domain is necessary for exploring emergence of pressure-induced complexity in condensed matter and for understanding (exo)planetary interiors. Only a MJ class laser such as LMJ, coupled to a time resolved short pulse of X-rays provided by PETAL can meet this scientific challenge.

It is likely that even the first stage of LMJ-PETAL will allow to reach several TPa and moderate temperatures by combinations of shocks and quasi-isentropic compressions using an LMJ focal spot exceeding 1 mm for minimizing 2-dimensional effects. Regarding target design, indirect drive should also be considered in order to mitigate preheating by the generated plasma corona and to increase the spatial uniformity of the compression. Using this configuration, multiple steps target geometry could be used to get on the same shot fluid and sound velocity data.

The main diagnostic requirements for realizing these experiments are thus:

- 2 VISARs and 1 Streaked Optical Camera for control of pressure and temperature conditions and for reflectivity measurements
- A good characterization of the PETAL x-ray source, especially in terms of photons numbers and spectral distribution, which requires PETAL only shots
- Broadband distribution (e.g. 200 eV, energy fixed by the backlighter) is needed for X-ray absorption spectroscopy. Quasi-monochromatic beams (energy fixed by the backlighter) are needed for x-ray diffraction, scattering, radiography.
- Detectors (incident beam, transmitted beam for x-ray absorption, Imaging Plates, CCD's,... for diffraction, scattering, radiography,...) could be discussed in part by capitalizing on the knowledge acquired by synchrotron and XFEL communities.

The last fundamental requirement will be the target fabrication support. A crucial point is the precision, reliability and reproducibility of the measurements. This depends strongly on target quality and characterization. An important effort on both financial and human resource side of new assembling techniques development must be done.

The high scientific profile of experiments done at LMJ-PETAL will be achieved through the uniqueness of the several TPa-moderate temperature conditions reached. LMJ-PETAL will probably not be the place for developing new untested risky diagnostics. The same considerations apply to targets on which specific careful design and realization work (direct drive or indirect drive) should be done. Pre-modeling of experiments using hydrocodes should of course be done at the best level.

In the coming years, a great deal of research on materials under extreme conditions will be developed in front of synchrotrons, XFEL's, and 10J to 1 kJ class lasers. The challenge is that the extension of these research projects to even more extreme conditions will bring together all these communities who will find interest to extend their discoveries of new materials in the range of several TPa and temperatures below 20000 K, which can be reached and studied only with a huge scientific instrument such as LMJ-PETAL.



## Sigles

CHEOPS	Characterizing ExoPlanet Satellite
EXAFS	Extended x-ray absorption fine structure
HED	High Energy Density
JWST	James Webb Space Telescope
LCLS	Linac Coherent Light Source
SACLA	Spring 8Angstrom Compact free electron LAser
SOP	Streaked Optical Pyrometry
TESS	Transiting Exoplanet Survey Satellite
VISAR	Velocity Interferometer System for Any Reflector
XANES	X-ray Absorption Near-Edge Spectroscopy
XFEL	X-ray Free Electron Laser

## References

- 1 Cavazzoni C. et al. Superionic and metallic states of water and ammonia in giant planet conditions. *Science* 283, 44 (1999).
- 2 Dubrovinsky L. et al. Implementation of micro-ball nanodiamond anvils for high pressure studies above 6 Mbar. *Nature Com.* 3, 1163 (2012).
- 3 Eremets M. et al. Single bonded cubic form of nitrogen. *Nature Mater.* 3, 558 (2004).
- 4 Fortney, J. J., Nettelmann, N., 2010. The Interior Structure, Composition, and Evolution of Giant Planets. *Space Sci. Rev.* 152, 423–447.
- 5 Gaulme, P., Schmider, F.-X., Gay, J., Guillot, T., Jacob, C., 2011. Detection of Jovian seismic waves: a new probe of its interior structure. *A&A* 531, A104.
- 6 Gaulme et al. (2013)
- 7 Geneste G. et al. Phase diagram of metallic hydrogen: a rich polymorphism from 1D to 3D structures. To be published.
- 8 Guillot, T., Stevenson, D. J., Hubbard, W. B., Saumon, D., 2004. The interior of Jupiter. *Jupiter. The Planet, Satellites and Magnetosphere*, pp. 35–57.
- 9 Guillot, T., 2005. THE INTERIORS OF GIANT PLANETS: Models and Outstanding Questions. *Annual Review of Earth and Planetary Sciences* 33, 493–530.
- 10 Guillot, T., Gautier D. 2014. Giant Planets. *Treatise in Geophysics* 2nd Edition, G. Schubert & T. Spohn eds. In press.
- 11 Hedman, M. M., Nicholson, P. D., 2013. Kronoseismology: Using Density Waves in Saturn's C Ring to Probe the Planet's Interior. *AJ* 146, 12.
- 12 R. Helled & T. Guillot – Interior Models of Saturn: Including the Uncertainties in Shape and Rotation – *The Astrophysical Journal*, 2013 – [iopscience.iop.org](http://iopscience.iop.org)
- 13 Howard, A., et al. 2012. Planet Occurrence within 0.25 AU of Solar-type Stars from Kepler. *ApJS*, 201, 15.
- 14 Jackiewicz, J., Nettelmann, N., Marley, M., Fortney, J., 2012. Forward and inverse modeling for jovian seismology. *Icarus* 220, 844–854.
- 15 Leconte, J., Chabrier, G., 2012. A new vision of giant planet interiors: Impact of double diffusive convection. *A&A* 540, A20.
- 16 Lin, D.N.C., Bodenheimer, P. and Richardson, D.C. 1996. Orbital migration of the planetary companion of 51 Pegasi to its present location. *Nature* 380, 606-607.
- 17 Lorenzen, W., Holst, B. and Redmer, R. 2009. Demixing of Hydrogen and Helium at Megabar Pressures. *Physical Review Letters*, 102, 115701
- 18 Lorenzen, W., Holst, B., Redmer, R., 2011. Metallization in hydrogen-helium mixtures. *Phys. Rev. B* 84 (23), 235109.
- 19 Loubeyre, P., Brygoo, S., Eggert, J., Celliers, P. M., Spaulding, D. K., Rygg, J. R., Boehly, T. R., Collins, G. W., Jeanloz, R., 2012. Extended data set for the equation of state of warm dense hydrogen isotopes. *Phys. Rev. B* 86 (14), 144115.
- 20 Loubeyre, P., Letoullec, R., Pinceaux, J. P., 1991. A new determination of the binary phase diagram of H<sub>2</sub>-He mixtures at 296 K. *Journal of Physics Condensed Matter* 3, 3183–3192.

- 21 Morales, M. A., Hamel, S., Caspersen, K., Schwegler, E., 2013. Hydrogen-helium demixing from first principles: From diamond anvil cells to planetary interiors. *Phys. Rev. B* 87 (17), 174105.
- 22 Morales, M. A., Pierleoni, C., Ceperley, D. M., 2010. Equation of state of metallic hydrogen from coupled electron-ion Monte Carlo simulations. *Phys. Rev. E* 81 (2), 021202.
- 23 Ma Y. et al. Transparent dense sodium. *Nature* 458, 182 (2009).
- 24 Mayor, M. et al. 2011. The HARPS search for southern extra-solar planets XXXIV. Occurrence, mass distribution and orbital properties of super-Earths and Neptune-mass planets. *ArXiv* 1109.2497
- 25 Nettelmann, N., Helled, R., Fortney, J. J., Redmer, R., 2013. New indication for a dichotomy in the interior structure of Uranus and Neptune from the application of modified shape and rotation data. *Plan. Space Sci.* 77, 143–151.
- 26 Pickard C. and Needs R.J. Aluminium at terapascal pressures. *Nature Mater.* 4, 624 (2010).
- 27 Pin Y. et al. 2013. Solid Iron Compressed Up to 560 GPa. *Phys. Rev. Lett.* 111, 65501.
- 28 Podolak, M., Hubbard, W. B., Stevenson, D. J., 1991. Model of Uranus' interior and magnetic field. *Uranus*, UofA Press, pp. 29–61.
- 29 Roulston, M. S., Stevenson, D. J., 1995. Prediction of neon depletion in Jupiter's atmosphere. In: *EOS*. Vol. 76. p. 343.
- 30 Schouten, J. A., de Kijper, A., Michels, J. P. J., 1991. Critical line of He-H<sub>2</sub> up to 2500 K and the influence of attraction on fluid-fluid separation. *Phys. Rev. B* 44, 6630–6634.
- 31 Smith et al. R. Ramp compression of diamond to 5 TPa. to be published.
- 32 Soubiran, F., Mazevet, S., Winisdoerffer, C., Chabrier, G. Optical signature of hydrogen-helium demixing at extreme density-temperature conditions. *Phys. Rev. B*, 87, 165114
- 33 Stanley, S., Glatzmaier, G. A., 2010. Dynamo Models for Planets Other Than Earth. *Space Sci. Rev.* 152, 617–649.
- 34 Stevenson, D. J., Salpeter, E. E., 1977. The dynamics and helium distribution in hydrogen-helium fluid planets. *ApJ* 35, 239–261.
- 35 Sun J. et al. 2013. Sable All-Nitrogen Metallic Salt at Terapascal Pressures, *Phys. Rev. Lett.* 11, 175502.
- 36 Wahl, S. M., Wilson, H. F., Militzer, B., 2013. Solubility of Iron in Metallic Hydrogen and Stability of Dense Cores in Giant Planets. *ApJ* 773, 95.
- 37 Wilson, H. F., Militzer, B., 2010. Sequestration of Noble Gases in Giant Planet Interiors. *Physical Review Letters* 104 (12), 121101.
- 38 Wilson, H. F., Militzer, B., 2012. Solubility of Water Ice in Metallic Hydrogen: Consequences for Core Erosion in Gas Giant Planets. *ApJ* 745, 54.
- 39 Yaakobi B. et al., *Phys. Plasmas* 15 (2008) 062703



# LABORATORY ASTROPHYSICS ON LMJ-PETAL

**Contributors:** R. Bingham, Ch. Blancard, A. Casner, J.P. Chièze, A. Ciardi, P. Drake, J.E. Ducret, E. Falize, G. Gregori, J. Harris, M. Koenig, R.C. Mancini, G. Pelletier, A. Ravasio, S. Rose, S. Turck-Chièze, V. Wakelam.

## Introduction

The means of astronomical observations have been developed considerably over the last decade, often bringing a new vision of our universe that is on its formation, evolution or internal transformations. The data obtained from these observations are more and more accurate thereby allowing models and simulations codes that are necessary for our understanding. However, it remains, in many cases, challenges for astrophysical objects or situations that spatial measurements cannot fully meet. Physicists have therefore developed a "local" way to satisfy dedicated studies of these challenges: Laboratory Astrophysics. This is a discipline that has emerged over the past two decades with the development of the high- energy and high pulse power facilities: lasers, Z- Pinch. Examples of physical processes that can be addressed experimentally include strong shocks, hydrodynamic instabilities, ejection processes, accretion processes, complex opacities, magnetic field generation or particle acceleration. All these processes are involved in a wide range of astrophysical phenomena such as supernovae, young stars jets, planet formation, evolution and structure of stars, etc. In France and in Europe in general, several teams participate actively to progress in laboratory astrophysics using several laser facilities operating in EU (LULI2000, VULCAN, ORION). However none of these latter can provide enough energy to access full scaled conditions for astrophysics situations. Indeed, laboratory astrophysics consists in recreating in the laboratory the conditions existing throughout the universe, reproducing complex objects... To this end, three categories of experiments have been distinguished [1]: identical (exact conditions of objects are created), similar (astrophysical situation can be scaled exactly into the laboratory) or resemble (only part of processes involved are relevant). The laboratory astrophysics working group is therefore divided into these 3 sub-topics trying to cover most of the issues that can be studied in this field using the full range of pulsed power facilities in EU.

Over 90 % of the visible baryonic matter in the universe is in the form of plasma. The effects and the transport properties of radiation in various astrophysical environments, together with a deep understanding of the interplay between hydrodynamics and radiation, remain a central issue in astrophysics. In stellar interiors, plasmas cover a very wide thermodynamical domain, that only high energy and high power lasers enable to explore. They pave the way for the experimental determination of fundamental physical data, such as the radiative properties - the *opacities* - of hot plasmas in stellar envelopes and interiors, or, relevant for stellar evolution and Big Bang nucleosynthesis, the direct determination of nuclear *reaction rates* among low Z elements, retrieving genuinely complex plasma screening effects. Moreover, one advantage of the unsteady nature of the laser experiments is their ability to simulate a large panel of violent phenomena occurring in the universe, e.g. associated with supernova explosions, star formation, accretion and ejection of matter from young stars or compact objects, or, else, radiation dominated photoionized plasmas, near



strong XUV sources. LMJ and PETAL will be able to produce and diagnose high velocity shocks, moving at a several hundreds kilometres per second, evolving well in the so-called *radiative shock* regime, affected by various *dynamical and thermal instabilities*, pertinent for studies of supernovae remnants and accretion/ejection processes. Moreover, important domains pertinent for high energy astrophysics will be experimentally addressed, thanks to the ability of PETAL to produce copious proton beams, in the 10-100 MeV energy range. Among them, the physics of *collisionless shocks* will be experimentally explored for the first time, together with Weibel instability, cosmic ray acceleration by shocks and diffusion, kinetic dynamo from turbulence. In this respect, due to large experimental scales and high temperatures, LMJ will enable scaled experiments with magnetic Reynolds numbers significantly larger than presently achieved.

The LMJ-PETAL facility will provide new capabilities to this field both by generating macroscopic volumes of matter under astrophysical conditions (LMJ) and by probing it through the *production of secondary sources* of protons, X rays and gamma rays (PETAL). PETAL will offer direct measurements, with high spatial and temporal resolution, of the density and the velocity field in the plasma, as well as the measurement, using proton beams, of intense magnetic fields.

## 1. Atomic and Nuclear Physics

The description of astrophysical objects requires a good understanding of the underlying microscopic physics, which includes radiation processes and reaction rates. This topic addresses two kinds of processes to study on the LMJ + PETAL facility, along the next decade: the transport and interaction of photons with matter and the production of elements through reaction rates, delivering a substantial energy. We consider here specific plasma physics that is only known theoretically and that could be checked in the laboratory. They concern the interior of stars, the ejection of matter from supernovae and the X-ray observations of specific lines of elements coming from X-ray binaries or Seyfert galaxies. All of them benefit already of a first generation of precise satellite observations. The interest of such fundamental physics experiments is reinforced by their dual use: their results have also direct consequences for societal applications related to fusion, similarity of thermodynamical conditions and related problems.

### 1.1 The state of the art

#### 1.1.1 Opacities

The description of stellar interiors requires detailed microscopic physical inputs that compete with macroscopic physics through the non-linear stellar structure equations, resolved presently in 1D and partly in 3D codes. The strong development of seismic investigations of stars, presently with SoHO, COROT, KEPLER (pursued in the next decade by PLATO around 2024), has pushed more precise delivery of fundamental physics and has revealed discrepancies that cast some doubt on the validity of the atomic and plasma physics used in these codes. Depending on the performances of the facilities, some specific problems can be solved. Waiting the use of LMJ class lasers (from about 50 kJ

to 2MJ), smaller installations like OMEGA, OMEGA-EP and LULI 2000, or Z pinch at Sandia, have been already extremely useful to solve problems on photon absorption by matter from aluminium to nickel.

LULI2000 achieved temperatures of 10-30 eV, at low densities, typically a few  $10^{-3}$  g/cm<sup>3</sup> and has measured for the first time chromium, iron and nickel absorption opacities in equivalent astrophysical conditions, extending the US approach of the nineties (Figure 1). Z pinch has been used to check iron plasmas, which have been heated at Sandia at a temperature of  $150 \pm 6$  eV with an electron density of  $(6.9 \pm 1.7) \times 10^{21}$  cm<sup>-3</sup>, providing invaluable benchmark data for the validation of opacity calculations [2,3].

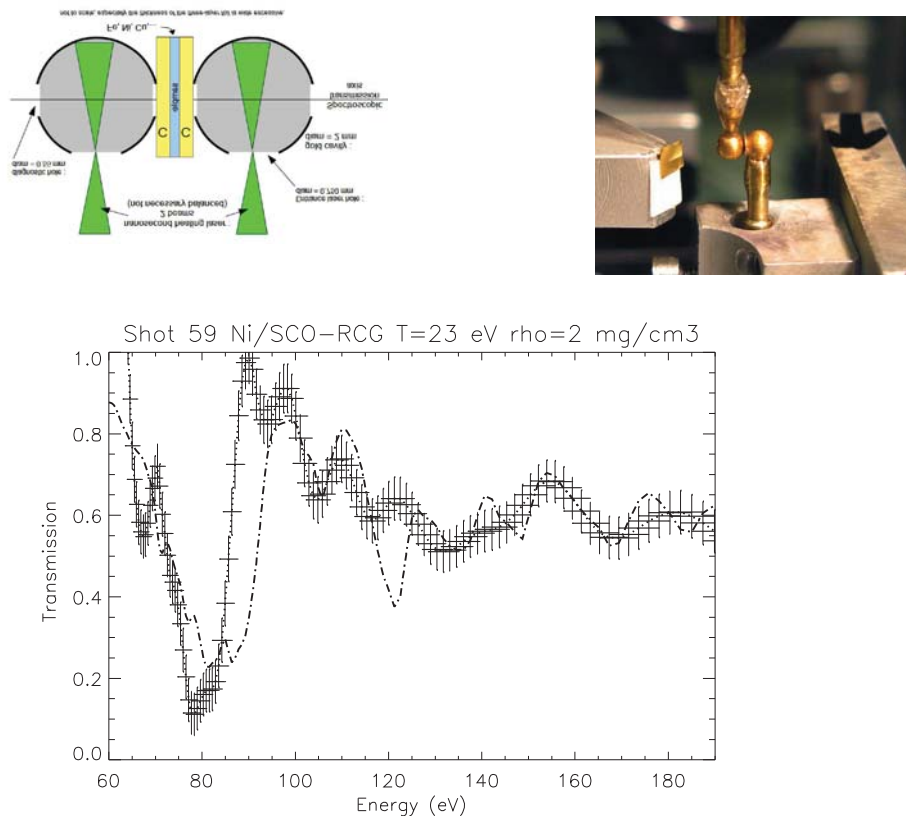


**Figure 1:** In the LULI 2000, the foil is placed inside two cavities in order to guarantee a limited differential density and temperature in the foil (less than 10%). The first experiment on Nickel measured at  $23 \pm 1.5$  eV and  $2 \pm 0.5$  mg/cm<sup>3</sup> is compared to SCO-RCG calculation at the resolution of the experiment. [4].

In all these conditions, the plasma is constituted by a large number of elements, most of them are partially ionized trace elements, but their detailed calculations of photo absorption are extremely time consuming and their contribution important; therefore, the knowledge of the validity of the different approximations is very useful, and the completeness of the calculations appear crucial [5]. The relative importance to treat all the transitions and to consider the interaction of configurations gain in parallel of new code developments and performances. In parallel to the experimental development of this activity a strong comparison with new codes of opacity is performed and new partial tables are prepared to interpret the most recent seismic results [4,6,7,8].

Emissivity measurements at higher temperatures and densities have been performed [4] on the Orion facility. These results are also compared to codes and will be useful for Astrophysics provided that plasma departure from Local Thermal Equilibrium (LTE) is demonstrated to be sufficiently low.

### **1.1.2 Nuclear rates**

The study of nuclear reactions within plasmas is a developing field of research. It's aiming at determining reaction rates of nuclear fusion reactions within plasmas [10,11], studying nuclear reaction mechanisms [12,13] or probing the structure of the hot spot at the end of the target implosion [14]. The determination of the reactions rates has the goal to quantify the importance of plasma screening effects on the nuclear fusion probability of closely approaching ions, which have to go through the Coulomb barrier in order to react, in a kinetic energy regime very low with respect to this barrier, hence the potential important role of electron screening. However, the studies performed using the interaction of femtosecond (fs) lasers with atomic clusters are limited to rather low plasma densities since what is measured is the fusion probability of ions accelerated by the Coulomb explosion subsequent to the absorption of the fs laser pulse on the clusters with the residual gas of the cluster source. Moreover, the LULI experiment [12] involves a major part of high-energy protons (above 1 MeV) interacting with boron nuclei.

### **1.1.3 Photo Ionization**

During the past decade, several experiments have been performed with the goal of creating well-characterized photoionized plasmas in the laboratory, using the pulsed-power Z facility at Sandia National Laboratories and the high-power GEKKO XII laser at Osaka University [15]. However, photoionized plasma equilibrium (PIE) relevant to astrophysics in the laboratory requires long-duration X-ray drives since laboratory photoionized plasmas have relaxation times of order 10ns [16,17] with, In addition, ionisation parameter ranging from  $20 \text{ erg cm s}^{-1}$  to 300 or 1000  $\text{erg cm s}^{-1}$ .

## **1.2 The LMJ-PETAL programme**

We describe hereafter the directions of investigations, where the LMJ associated to PETAL will be particularly useful for astrophysical science. Depending on the experiments, PETAL could be used as a strong complementary heater, or as a ps probe of the plasma to avoid a limited evolution of the thermodynamical conditions. Our expertise has been acquired on smaller installations in X and XUV domains and is continued in parallel on ORION facility and LULI2000.

### **1.2.1 Checking LTE opacity calculations for internal solar-like stars**

The thermodynamical conditions of Sun and solar-like radiative interiors have never been reached in the laboratory [18], but some approaching experiments on the Z pinch machine have been performed. T varies from 200 eV to 1.3 keV, density from  $0.2 \text{ g/cm}^3$  to  $150 \text{ g/cm}^3$  for a mixture from H to Ni [19]. The plasma is dominated by completely ionized hydrogen and helium, which deliver most of the free electrons to the other elements, so the transport of energy by photons is complex

since it needs to describe free-free, bound-free and bound-bound processes. The description of the solar radiative zone also requires a simultaneous treatment of the magnetic field, hydrodynamical horizontal shear and microscopic physics that describes the migration of elements and the radiative acceleration. In addition, plasma effects (ionization by pressure...) and coulomb effects must be considered for each element, differently ionized.

***The achievement of experimental conditions relevant to solar-like interiors physics have been expected for a long time. These much needed conditions match the performances of the LMJ-PETAL laser system.*** The updated solar photospheric composition leads to discrepancies between standard solar models and both helioseismic and neutrino observations [20]. A smooth increase of the mixture opacity from 2% to 5% in the central regions, to 12% to 15% at the base of the solar convection zone could restore the agreement between solar models and helioseismology inferences. Such an increase is larger than the level of agreement between OP and OPAL Rosseland opacities used by the astrophysical community. ***Therefore, investigation of the different aspects of the radiative transport in these conditions is a milestone of LMJ +PETAL.***

### **1.2.2 Nuclear reaction rates and screening by fusion of two light elements**

Stars evolve through successive fusion reactions in their interior. So, since the seventies, many measurements of fusion cross sections have been performed with particle accelerators. However, this information is not directly usable for stellar conditions: generally the energy region of interest is not reached, as the cross section is too low. Moreover, the laboratory experiment is polluted by laboratory screening, which is different from the stellar screening effect due to the free electrons: an increase of up to 40% of the value is derived from laboratory experiment. Finally the ions environment is not totally well understood. Some tentative first experiments have been performed on NIF [10] and on LULI2000 [12]. Using LMJ or PETAL to produce the stellar plasma represents a unique way to really address the problem of the measurement of the reaction rate that includes naturally the different processes at work during the fusion.

### **1.2.3-Checking photoionized plasmas for quasars or black holes**

Laboratory experiments on photoionized plasmas relevant to astrophysics are relatively new as compared to the large volume of work on plasmas whose atomic kinetics is driven by a distribution of particles, or where particle collisions play a leading role. Unlike collisional plasmas, in photoionized plasmas, photoexcitation and photoionization dominate the atomic kinetics. The dearth of laboratory photoionized plasma data is due to inadequate X ray radiation source: intense and broadband sources of X-rays are difficult to produce in the laboratory. Yet, laboratory data are critical in order to benchmark laboratory and astrophysical spectral modelling codes, developed on the basis of best-theory efforts that are currently used to interpret Chandra and XMM-Newton observations, and prepare the ATHENA+ perspective [16].

### 1.3 Short term Experiments

Astrophysicists have been waiting for long to perform experimental checks of LTE opacity calculations at high density (0.2 times solid density up to several hundred  $\text{g.cm}^{-3}$ ) and high temperature (several hundred eV to several keV) that take into account all the important photoabsorption and photodiffusion processes and all the specific plasma effects. However, performing such experiments require the complete modification of the previously used techniques since one needs to obtain simultaneously high density and temperature. This is difficult to get in cavities with limited gradients. We look for LTE conditions that will be achieved with LMJ equipped with the picosecond PETAL beam, at least used as a backlighting probe. Such programme justifies short term and long-term programmes that will evolve with the foreseen increase of energy and beam number of LMJ.

Our working community now disposes of new codes that perform high quality calculations for elements from Hydrogen to Nickel like OPAS [21] SCO-RCG [22] or ATOMIC in US [23] that need detailed validation (see Figure 2 for the complexity of the different behavior of all the elements in the Sun). They are useful to check and interpret the present discrepancy on the sound speed between solar standard model and seismology that is largely influenced by the treatment of the radiative transport and microscopic diffusion that takes into account the radiative acceleration of the individual element through their photon absorption [19, 24]. This microscopic diffusion competes with the turbulent layer at the base of the convective zone.

Therefore, it is fundamental to verify the individual spectral absorption on a large energy range (500 eV to 5-10 keV) for at least three different elements: O or C, Si, Fe and mixtures similar to astrophysical conditions including iron. This is the justification of a long-term, multi annual, training programme aiming at the reproduction of the central region of the Sun at LTE.

The calculations can fail in correctly describing line broadening calculations and line shapes modelling. It can be also assumed that the basic calculations partly fail in the ionic partition functions, with consequences on the number of bound states. One can also question the effect of dense media, the impact of the environment on the number of bound states, etc.



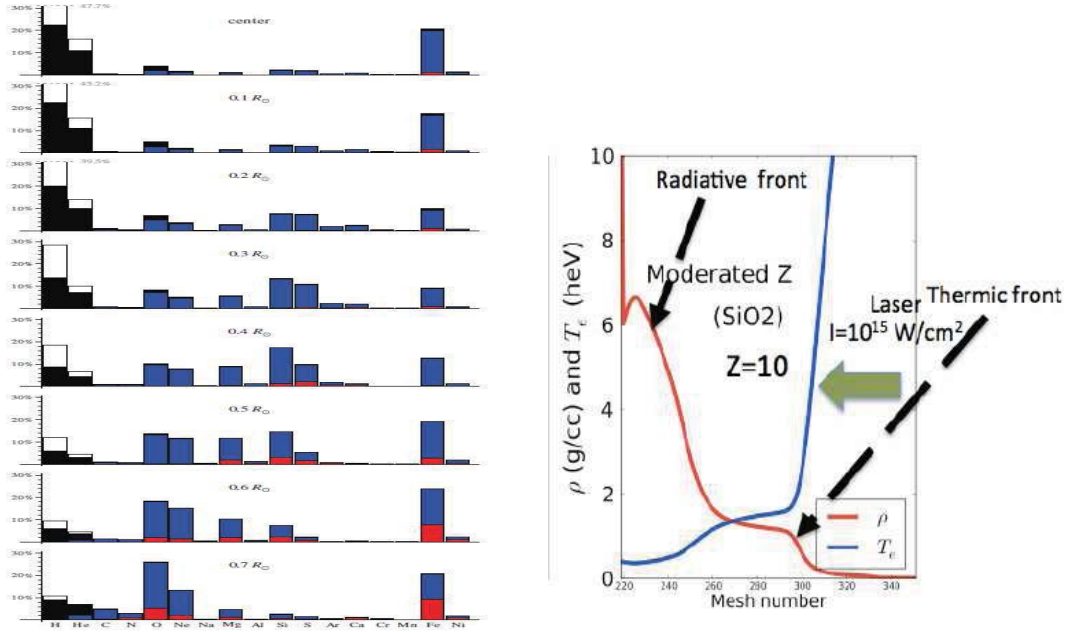


**Figure 2:** Relative contributions of each element (max=30%) to the OPAS Rosseland mean opacity of the mixture. Scattering (white), free-free (black), bound-free (blue), and bound-bound (red) contributions are indicated. The principle of the DFA [25] is under study for astrophysical objectives and will be adapted to the LMJ performances.

At the base of the solar convection zone, iron is a major metallic contributor to the opacity of the mixture with oxygen. Iron L-shell opacities have been measured, at Sandia, for plasmas where the iron charge state distribution is rather close to the one expected at the solar radiation convection boundary and not the number of free electrons. Hence, it has been shown that the theoretical transmissions deduced from extensive detailed line-by-line opacity calculations were in excellent agreement with the Fe transmission data. Attempts to increase both temperatures (T) and electronic densities (Ne), and reach those expected at the solar convection zone boundary ( $T \sim 200$  eV and  $N_e \sim 10^{23} \text{ cm}^{-3}$ ), are underway, but, up to now, they are unconvincing.

Silicon is also an significant contributor to the opacity of the solar plasma mixture between 0.3 and 0.5 solar radii. In this region, temperatures and electron densities are typically between [340 eV - 600 eV] and [ $6.9 \cdot 10^{23} \text{ cm}^{-3}$  -  $6.4 \cdot 10^{24} \text{ cm}^{-3}$ ], for which range opacity calculations predict that the atomic structure and the radiative properties of highly ionized silicon ions are strongly affected by density effects. Theoretical results depend on how density effects are modelled. In order to settle between these calculations, ORION-type buried layer (or reduced mass targets) experiments are very interesting. K-shell high-resolution emission spectroscopy could be performed. Because temperatures are moderate and because silicon is a low-Z element, the LTE conditions could be more easily achieved.

Two different approaches are presently studied for LMJ-PETAL for a global check of the thermodynamical regions of the Sun up to the nuclear core, where the plasma effects have to be verified. We consider the ORION approach that consists in cylindrical explosion of the target by short pulse opacity experiments [4] and the Double Front Ablation (DFA) approach developed at CELIA [25] already used in Japan. The second one has the advantage of producing a very stable temperature and density plateau able to perform measurements close to LTE in foams, but may be in a lower temperature range. Checking all the details of the calculations justifies a high resolution X-ray

spectrometer. So the program schedule will be adapted to the available diagnostics in order to begin as soon as possible the first investigation of this fundamental ingredient of stellar physics. This ingredient is essential not only for astrophysics but also for the simulation of experiments on LMJ and PETAL.

The PETAL short-pulse laser beam could be used to heat the sample in order to obtain an over-dense medium, and LMJ ns laser beams could be used to shock it [26]. One remaining problem concerns the independent T and Ne diagnostics. At 0.5 solar radius, Si and Fe exhibit close bound-bound contributions to the total opacity. It would be interesting to measure both K-shell emission of Si and L-shell emission of Fe for hot dense mixtures of such elements. In order to experimentally test mixing models (EoS, microfields...), it could be interesting to vary the Fe/Si ratio. In the central region where plasma and relativistic effects, as well as electron degeneracy, are present, bound-free processes on iron plays a significant role, so it would be extremely useful to validate its ionic distribution in a representative mixture environment.

## 1.4 Longer terms

The opacity measurements will probably cover short and longer terms, but the other fields will be introduced as the LMJ installation improves in performance.

The main interest of performing nuclear physics experiments with the LMJ-PETAL facility is the unique combination of thermodynamical plasma conditions it will offer. High densities, such as those, which will be reached at LMJ-PETAL, will provide Coulomb screening conditions for the nuclear fusion reactions in the intermediate screening regime [27]. Such experiments require, in order to be quantitative, a very homogeneous laser irradiation of the target in order to reach as spherical as possible a hot spot during the stagnation phase and well-defined temperatures and densities. Therefore, they will be feasible once the laser facility will be well in hand of the operators & researchers. Moreover, they will necessitate the development of nuclear diagnostic tools to measure absolute production rates, energy spectra and particle identification. These diagnostics will be also needed by other fields of research of laser plasmas and should be developed in common with these other scientific programs.

The combination of LMJ and Petal lasers offers an excellent opportunity to investigate Photo Ionized Experiments (PIE) in the laboratory. First, long duration x-ray drives can be achieved by staggering several LMJ beams, each of 10 ns to 20 ns duration, to drive a configuration of multiple *halfraum* cavities. Since the X-ray flux produced by each individual halfraum will approximately follow the time-history of the laser pulse, by stacking up a sequence of laser pulses with suitable time delays, each one irradiating a different halfraum, an X-ray drive with duration in the tens of ns can be achieved. In this connection, a recent proof-of-principle experiment using the long-duration beams of OMEGA-EP has produced encouraging results and suggests the feasibility of this concept [28]. With the larger energy per beam and number of beams available at LMJ, this experimental design can produce X-ray drives characterized by radiation temperatures of several hundreds of eV lasting for tens of ns. We note in passing that the development of long-duration X-ray drives would also enable new and unique science relevant to other areas of laboratory astrophysics, such as shock physics and hydrodynamic instabilities.

A thorough characterization of PIE in the laboratory would require a simultaneous measurement of the opacity (i.e. transmission) and self-emission spectrum of the photoionized plasma. Such a simultaneous measurement in photoionized plasmas is still a standing challenge. Previous experiments have measured one or the other but not both in the same experiment [17,29,30,31]. The opacity would be extracted from the transmission of backlight photons of a laser-produced plasma driven with the high-intensity PETAL laser. The possibility of using a separate laser for this measurement would afford the flexibility of studying the opacity of the plasma at different times thus checking whether or not the plasma has reached the expected steady state. The simultaneous self-emission measurement would require a line-of-sight quasi-orthogonal to that of the transmission measurement and a high-sensitivity spectrometer, since the self-emission of laboratory photoionized plasmas tends to be of relatively low intensity.

## **2. Radiation Magneto Hydrodynamics**

### **2.1 The big challenges**

The extraction of energy from mass accreting onto compact sources (black holes, white dwarfs, young stars, etc) is at the core of some of the most powerful and interesting astrophysical phenomena. One example is the ejection of mass in the form of winds and collimated jets which play a fundamental role in the life-cycle of many of these objects, and are found to extend over parsec-scale in the case of non-relativistic atomic and molecular jets from newly forming stars, to mega-parsec scales for relativistic jets from massive black holes in active galaxies. These highly complex flows inject energy and momentum far afield into their environment, generating strong shocks and radiation. Among the different phenomena, flow instabilities and radiative shock waves are some of the most interesting. The strong interaction of gas and radiation flows has always been an essential component of astrophysical studies. Instabilities also occur in many areas of laboratory and astrophysics, are the Rayleigh-Taylor and Richtmyer-Meshkov instabilities, which arise when the interface between a light and heavy fluid is accelerated under suitable conditions. In particular understanding of ablative Rayleigh-Taylor Instability (RTI) is crucial in Inertial Confinement Fusion (ICF) and Astrophysics.

Radiation fluid dynamics is, however, an extremely complex subject mixing both classical and quantum physics into a set of highly non-linear, coupled, multi-dimensional, integro-partial differential equations. Beginning with work on stellar structure and evolution in the early and mid 20<sup>th</sup> century, astrophysicists have become proficient at learning to reduce complex radiation fluid dynamical systems to a range of limits where some analytic and semi-analytic solutions can be obtained. Such limits often include assumptions of simplified geometries, simplified closure relations between radiation and matter, simplified treatments of radiation transfer or, most importantly, ignoring time-derivatives and searching for steady state flows. Even with the development of advanced computing techniques (such as Adaptive Mesh Refinement), radiation transfer often poses

the most challenging aspects of those codes. Time-scale, length-scale and frequency binning requirements can push realistic radiation-fluid dynamic simulations to the edge of what is feasible in terms of time and memory requirements. The difficulty of solving radiation fluid dynamical systems is particularly vexing as such system lies at the heart of one of the most pressing frontier problems in astrophysics: Cosmology.

In this context, LMJ will provide an important opportunity to produce in laboratory extreme radiation hydrodynamic regimes relevant to the physics of supernovae explosion, accretion and ejection processes, and ionization fronts.

## 2.2 The state of the art

### 2.2.1 Accretion-Ejection

Accretion processes are among the most important phenomena in high-energy astrophysics. They are the main source of radiation in several binary systems, and are widely believed to provide the power supply in several astrophysical objects. Understanding the complex physical mechanisms which allow releasing the gravitational energy in the form of radiation, is fundamental to interpret astronomical observations. Among the different X-ray binary systems, the cataclysmic variable stars provide a unique insight on accretion processes in extreme astrophysical regimes. Cataclysmic variables are close binary systems containing a white dwarf which accretes matter from a late type Roche-lobe filling secondary star (see Figure 3a). Because other sources of luminosity are relatively unimportant, there provide the best opportunity to study accretion processes in isolation. For several years, many researches have focused on the high-energy environment near the photosphere of the compact objects. In these systems, the magnetic field is strong enough to prevent the formation of the accretion disk and to channel the accreted plasmas up to the compact object magnetic poles (see Figure 3a), leading to the formation of accretion column [39].

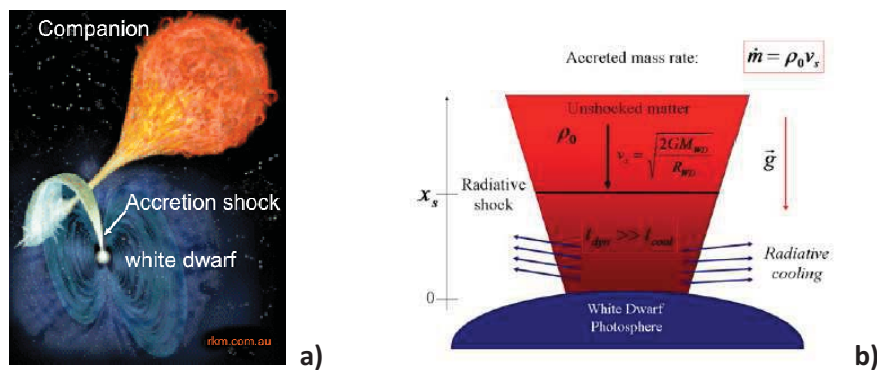


**Figure 3:** a) AM Herculis star b) accretion zone near the white dwarf photosphere [52]

Understanding the physics of the emitted X-ray region is fundamental since it is at the base of the determination of the white dwarfs properties. In these specific astrophysical objects, the impact of

the supersonic free-fall accreting matter with the white dwarf's photosphere leads to the formation of a radiative reverse shock which heats the infalling plasma up to 10-50 keV (see Figure 3b). Then the post-shocked matter cools by different radiative processes that lead to the formation of a highly-stratified structure in temperature and density. The structure of this high-energy environment is very complex and a multi-scale physics occurs, implying difficulties to theoretically and numerically model them. Moreover, the size scales associated with these zones are on the order of the white dwarf radius or smaller, which complicates their direct observations and the determination of the physics of the impact zone. Thanks to recent works on the scalability of radiation hydrodynamics flows [41,42], we proved that exact scaling laws exist for different accretion column regimes and specifically for the radiation-dominated cases, i.e. in the case where the magnetic field only channels the flows. These phenomena can be reproduced at diagnosable scales in laboratory with powerful lasers. Thus, the experimental challenge is to generate plasma conditions allowing reproducing similar conditions of astrophysical conditions.

It has been proved that exact scaled models of the accretion shocks in magnetic cataclysmic variables can be produced on Mega-joule facilities [42,43] (see Figure 4). In order to test and validate the target designs different experiments have been performed on various intermediate laser facilities (LULI2000, GEKKO XII, ORION and Omega) where the possibility to diagnose and study the dynamics of reverse shock has been shown. These experiments have been the keystone of the preparation of future experiments on LMJ-PETAL.

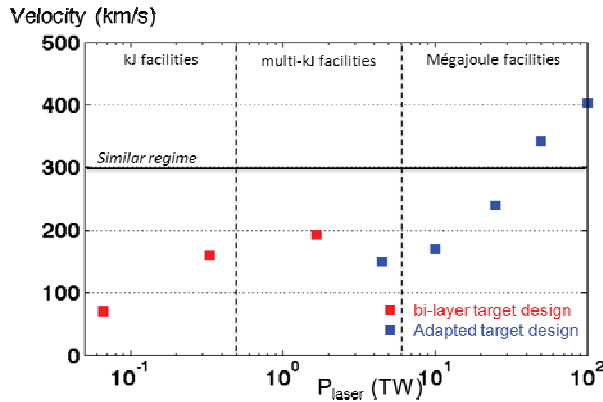


**Figure 4:** Velocity in function of laser power. The similar regime is obtained for the LMJ with an energy of 400 kJ in direct drive.

Closely related to mass accretion, the ejection of jets also plays an important role in many astrophysical object [50]. Jets from young stellar sources, for example, are responsible for allowing accretion to proceed by removing angular momentum from the accretion disk, and may also affect the physical properties of protoplanetary disks. At the same time, outflows can limit the protostellar mass by clearing early on in the star formation process the infalling parental envelope, and are sufficiently powerful to sustain the turbulence in their local environment. Jet propagation through the interstellar medium drive radiative bow shocks and sweeps up molecular material into gigantic (several solar masses) molecular outflow [51]. In this interaction jets are also potentially susceptible



to instabilities, such as the shear Kelvin-Helmholtz and Rayleigh-Taylor instabilities. However while in young stellar jets, the characteristic time for cooling by radiative losses is much smaller than the characteristic hydrodynamic time-scales, laser experiments of jets propagation have so far been mostly limited to non-radiative jets. Flows in such regime are known to differ substantially from radiative, high Mach number flows such as those of young stellar jets, both in terms of the propagation dynamics and stability.

### 2.2.2 Instabilities

Understanding of ablative Rayleigh-Taylor Instability (RTI) is crucial in Inertial Confinement Fusion (ICF) and Astrophysics. In ICF, a spherical shell is imploded to achieve high fuel density and temperature, adequate to sustain thermonuclear burn. The implosion performance can be significantly degraded by RTI in both acceleration and deceleration phases of implosions. In fact, results of the National Ignition Campaign have identified mixing as the primary contributor of degraded neutronics performance in cryogenic implosions. In astrophysics, thermonuclear supernovae of type Ia (SNe Ia) take a pivotal role in the derivation of cosmological parameters and for distance determination of high-redshift galaxies. However, many details regarding why are SNe Ia “standard candles” and their burn dynamics remain unanswered. The deflagration to detonation transition (DDT, or delayed detonation) is one mechanism suggested to govern the explosion of thermonuclear SNe Ia and is currently not yet understood. Only ignition may permit studying nuclear burn wave physics in the laboratory. However, based on the analogy between flames front and ablation front [46], highly nonlinear RTI measurements at ablation front can provide important insights into the initial deflagration stage. Turbulence is shown to accelerate significantly the transport of released energy to the stellar surface leading to complete disruption of the white dwarf. The transition could be generated by the formation of shocks in the steep density gradients of white dwarfs envelopes due to an amplification of sound waves generated by the RT induced turbulent deflagration [45] (Figure. 5 left).

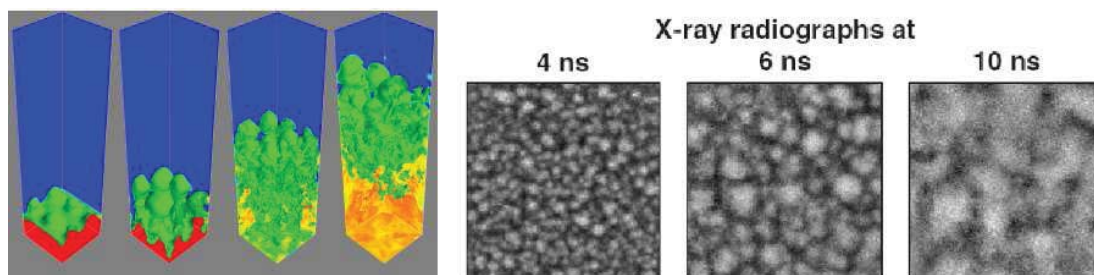


**Figure 5:** (left) Simulations of a RT driven flame in 3D. Starting from a bimodal perturbation large scale structures develop first, follow by a turbulent cascade toward the small scales, in contrary to the 2D case [45]. (right) Evolution of 3D, broadband modulations due to ablative RT instability measured in direct-drive experiments [47].

### 2.2.3 Ionization fronts

The study of the early evolution of the Universe as a whole has become, in popular parlance, a precision science with detailed comparisons between theory and observations now possible at a range of scales. Fluctuations in the Cosmic Microwave Background (CMB) have provided fundamental insights into the cosmological plasma system in the Universe's first few hundred thousand years. Studies of the Large Scale Structure of galaxy clusters and superclusters have provided information about evolution on far longer timescales. The critical missing link however is the physics of the so-called Dark Ages. This is the period when the first stars and proto-supermassive black holes were forming in the sea of neutral hydrogen left over from the era of "recombination" when the CMB was released. Understanding the Dark Ages is essential to cosmology for within it are answers needed to understanding everything from the chemical evolution of the Universe to the evolution of galaxies.

Understanding the Dark Ages however requires understanding the end of the Dark Ages, which is, essentially, a radiation-fluid dynamics problem. Astrophysicists care about the Dark Ages because that is when stars and black holes first form. But as soon as they form they also begin producing large fluxes of ionizing radiation (UV and X-rays). This radiation quickly creates ionization bubbles in the surrounding neutral gas. The interaction of the ionization bubbles is what eventually leads to the transition from a fully neutral and opaque cosmic plasma to the fully ionized and transparent medium we see today. *Thus the complex and time-dependent nature of interacting ionization fronts represents an essential problem that must be solved if astrophysicists are to understand the Universe's evolution through, and transition out of, the Dark Ages.* We note that a number of new multi-billion dollar astronomical facilities are coming on line over the next decade that have been optimized to include studies of the Dark Ages. Thus, data constraining problems like the ionization front interactions of stars and young quasars will be available soon.

## 2.3 The long-term program

Extending the current work in this area of laboratory astrophysics [39] to more astrophysics-relevant regimes forms the rationale of the long term programme in radiation hydrodynamics.

### 2.3.1 Accretion-Ejection

Experiments on LMJ will allow for the first time to study the evolution radiative plasma jets into highly nonlinear stages and over long timescales (> microseconds). These studies will provide insights into the development of turbulence, and the mixing with the ambient medium, the effects of radiation on the jets dynamics, stability and the formation of internal structures in the jet. In addition, by imposing magnetic field of a fraction of a MG with an external coil, it will be possible to study the effects of a magnetic field on these phenomena for the first time.

LMJ has unique capabilities to produce very high-Mach number flows, which leads to the formation of astrophysics-relevant accretion shocks. These experiments will be an important complement to current astronomical observations. Using PETAL, the post-shocked region can be diagnosed in detail, and will be crucial to disentangle the effect of radiative losses on the shock structure. Such data are fundamental for astronomers to make progress in understanding observations [44]. The energy

available at LMJ will allow large amounts of material to be heated and put into motion allowing the development of the instabilities in both the linear and non-linear regimes to be investigated, where, in the latter regime, non-LTE and radiation physics will be expected to play an important role in the dynamics. LMJ will allow us to explore new regimes of blast waves and to study their dynamics at late time after the hydrodynamic (Sedov phase) - radiative transition [38]. The study of blast waves, the development of various instabilities (cooling, Rayleigh-Taylor or Vishniac instabilities) and turbulence, will give for the first time profound insights into fundamental questions concerning supernova remnant dynamics. Naturally, the exact nature of the instabilities will depend on the non-LTE equation of state of the materials and by the mechanisms of energy transfer across the interface – for example by radiation.

### **2.3.2 Instabilities**

While linear growth of single-mode perturbations has been extensively studied, advanced nonlinear stage of the RTI with broadband perturbations was only recently addressed. Figure 5 (right image) shows an example of 3D, broadband modulations in nonlinear regime measured in DD experiments [47]. As a target accelerates, the size of the RT features increases while larger bubbles overtake smaller bubbles. Bubble competition and bubble merger was shown to take place in these experiments with two "generations of bubbles" produced by nonlinear RT instability. The dependence of RT growth and growth constant on initial conditions could not be studied, due to limited acceleration.

LMJ-PETAL provides a unique platform to study the physics of nonlinear turbulent mixing flows in HED plasmas because it can accelerate targets over much larger distances and longer time periods than previously achieved before. Experimental schemes have already been designed for NIF [48] and could be scaled down according to the available laser energy in the first years of LMJ-PETAL. Moreover the PETAL beam could be used to probe self-generated B-field created by RTI [49] with side-on proton radiography.

### **2.3.3 Dynamics of ionization fronts**

Ionization fronts are an area where novel work will become possible using LMJ (see § 1: Atomic and Nuclear Physics related to Astrophysics). These ionization fronts develop in star-forming regions, where ionizing radiation from young stars propagates through the region, encountering dense molecular clouds and also other ionization fronts. The simplest ionization front, known as an "R-type", progressively ionizes gas that is initially neutral. Its speed is linearly proportional to the flux of photons. As the photon flux away with distance from the radiating star, the speed of the front eventually drops below the sound speed of the heated matter behind it. At this point, a shock wave moves ahead of the ionization front and the front is now referred to as a "D-type" front. For more complex conditions, one can identify theoretically several regimes for both types of front, in which the front is subsonic or supersonic with respect to the matter ahead of or behind the front, and in which the medium is compressed or expanding on one side or the other. In order to study the complex interactions of multiple ionization fronts, one needs to be able to drive shock waves and/or ionizing radiation through a complex target from multiple directions, while also irradiating other

targets to provide x-ray sources for diagnostic purposes. Doing this in a realistic and relevant three-dimensional geometry requires a laser with the capabilities of LMJ.

## **2.4 Science on a shorter time-line**

A pressing need for the academic community would be to facilitate the access to an open, validated code (with sources available) for the preparation and the interpretation of laser plasma experiments. Note that the CHIC code (presently accessible at CELIA, France) has been developed for this purpose and could be a good option for 2D simulations. On the short time-line, one can also use dedicated codes (e.g. FLASH and CRASH) whose development have been supported by DOE to provide to the US (and now international) academic community the ability to simulate complex experiments. However the link between laser experiments and astrophysical applications should be also developed using 2D or 3D laser code for laser experiments and existing astrophysical codes developed by the academic community

## **2.5 The needed steps to go**

Radiation MHD experiments are very complex and demanding. A significant effort is needed to carry out the theoretical and modelling work, the development of diagnostics and the interpretation of the results. To achieve these objectives, dedicated supports from the different EU institutions and probably EU programs will be needed to bridge the gap between the astrophysics and high energy density plasma physics communities. European and international workshops, meetings, invitation of experts, will help to define needs, numerical techniques and to benchmark existing codes on dedicated problems.

On the theoretical aspects, for the preparation and interpretation of the experiments, the community needs:

- A three-dimensional, radiation magnetohydrodynamic code capable of modelling the laser plasma interaction. Such code should include a state-of-the-art radiation module with chemical kinetics and non-equilibrium thermodynamics, and should be able to deal with ohmic dissipation, the self-generation of magnetic fields, and anisotropic transport coefficients. This code (and its sources) should be an open academic code available to the whole European community.
- State-of-the-art post-processing tools for direct comparison of the simulations with the experiments.
- High quality atomic data: EOS and opacities, to be integrated with the code mentioned above, and for post-processing. The community should also have access to dedicated computing resources for both the large scale computations and the data analysis and visualization.
- Astrophysical plasmas are often magnetized. The community has now already developed dedicated devices (MIFEDS – LLE, LULI-HZDR) that are able to generate up to 20 T B-fields. It is very important to plan the development of magnetic devices on LMJ able to deliver up to 20 T.

### 3. High Energy Astrophysics and Interstellar Medium

There are four topics of plasma physics that are currently under intensive investigation in high energy astrophysics community over the world, namely collisionless shocks, particle acceleration, magnetic field generation, small-scale dynamo, and extreme radiation of these plasmas under electromagnetic turbulent state. Nowadays, electrostatic collisionless shocks can be realized with proton beams of a few MeV, which is already interesting. With LMJ-PETAL, higher energies will be achieved and, for the first time, the physics of collisionless shocks will be opened to experimental investigations.

#### 3.1 Short-term goals

##### 3.1.1 Collisionless strong shocks from non-relativistic to sub-relativistic regime

PETAL will produce beams of 10-100 MeV protons (about  $10^{13}$  interacting with a plasma of  $10^{18} \text{ cm}^{-3}$  during 10 ps, corresponding to 10 inertial lengths) and thus will allow the investigation of the physics of some class of astrophysical shocks experimentally. This concerns Super Nova Remnants, Blazar shocks and AGN jets shocks and internal shocks of Gamma Ray Bursts [56]. The investigation can be divided into two aspects, one without external magnetic field and one with an external magnetic field. In the first case, we can explore the transition in the physics of the collisionless shock from the electrostatic regime to the electromagnetic one. The electrostatic regime is governed by the excitation of Two Stream Instability and Buneman instability. Then as the beam energy increases, we can expect the arising of an electromagnetic stage where the shock formation results from the excitation of Weibel filamentation instability [57]. That transition with increasing beam energy would be a first important topic. Now when the energy is large enough to get the electromagnetic regime, the shock precursor will start in the electrostatic regime before becoming electromagnetic. The evolution towards the electromagnetic stage and its characterization would be a second important topic [58]. Then it is expected that electrons continue to be heated during the electromagnetic stage at the expense of the ion stream. The extreme electron heating occurring at that stage is an important issue that would deserve a special investigation; this would be a third point, maybe the most important one.

When an external magnetic field is applied (the second aspect), the physics of the shock is sensitive to two parameters, namely the magnetization ( $w_{ci}^2/w_{pi}^2$ ) and the angle of the field with the shock normal. Even in the non-relativistic regime, some important questions did not receive a clear answer yet from numerical simulations [59]. How does injection of particles in the supra-thermal tail change as a function of the angle?

### 3.1.2 MHD turbulence, dynamo and magnetic reconnection

Turbulence in many astrophysical environments is driven by vorticity generation as shocks sweep up density inhomogeneities [53,54]. While initial work [54] has focused on the generation of the initial seeds of magnetic fields via baroclinic processes (see Figure 6), the values of the predicted fields in cluster of galaxies still remains much smaller than present day observations. The current understanding is that magnetic fields are amplified and reorganized by the twisting and stretching of the fluid elements [55]. Experimental work is strongly complementary to numerical simulations. Simulations have their limitations – to do both with the amount of computing power that can be brought to bear on a problem whose adequate modeling essentially depends on resolving large scale separations and with the fact that in plasmas not dominated by collisions, it remains a nontrivial question what are the correct equations to be solved. Furthermore, we need to determine whether or not coherent magnetic structures on macroscopic scales can emerge out of the initial microscopic ones in the turbulent postshock flow within appropriate timescales. The key breakthrough development we are proposing on LMJ is a laboratory demonstration of the transition from the low- $R_m$  amplification to the high- $R_m$  dynamo regime [60]. In all laboratory plasmas produced at mid-scale laser facilities so far, Ohmic resistivity was dominant, and dynamo is not operative. The picture changes dramatically as the Ohmic resistivity decreases (and  $R_m$  increases). MHD simulations show that above a critical value  $R_{m_c} \sim 100-200$ , small-scale dynamo sets in. This abruptly increases the saturated level of the field to the level where its energy density is comparable to the kinetic energy density of the turbulent motions and independent of the seed/imposed field. Such a large amplification occurs because the field now grows exponentially, at a rate that, for conditions expected at LMJ, we estimate to be comparable to the turnover rate of the viscous-scale motions. Detecting such amplification in the laboratory really is the holy grail of experimental dynamo physics.



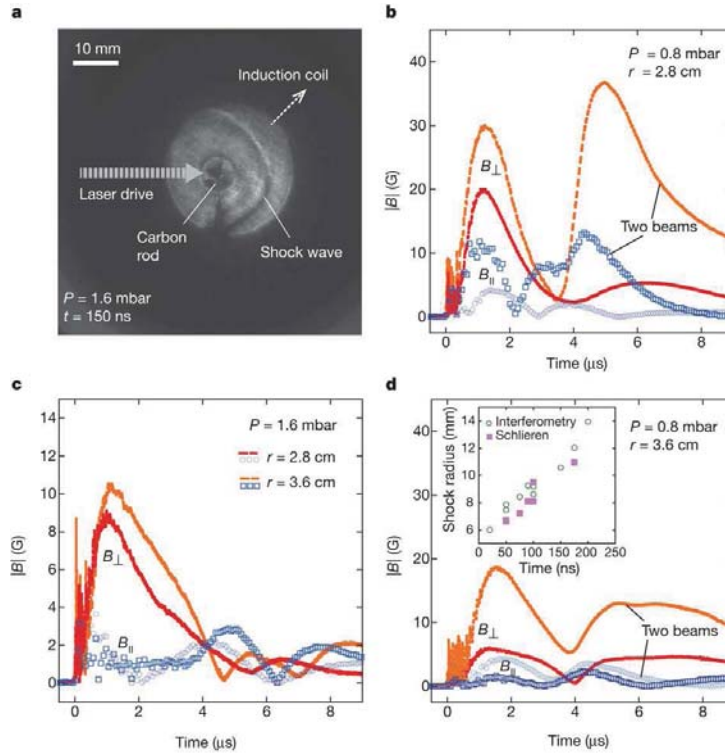


**Figure 6:** *a*, Schlieren image, showing laser and magnetic pick-up coil configuration as well as the shock position. The induction coils were placed at 2.8 cm and 3.6 cm from the carbon rod (that is, the centre of the initial blast) *b*,  $B_{\perp}$  (lines) and  $B_{\parallel}$  (symbols) traces taken at an ambient pressure of  $P=0.8$  mbar. The rise and gradual decay of  $B_{\perp}$  was consistent with the shock front crossing the coil and the subsequent evolution of the shocked material. The second peak at  $t \approx 5 \mu\text{s}$  seen for the case of two beams illumination is probably associated with the ejecta material from the sample arriving at the coil. *c*,  $B_{\perp}$  (lines) and  $B_{\parallel}$  (symbols) traces for the one-beam laser driver at  $P = 1.6$  mbar. *d*, Same as *b* but at  $r = 3.6$  cm. The inset shows the measured shock radius along the laser axis for  $P = 0.8$  mbar and single-beam illumination.

Adapted from ref 54.

### 3.1.3 Facility requirements

- The primary goal of these experiments is to study magnetized plasmas with a magnetic field which is frozen-in the medium. Typically, experiments done so far have relied on external mechanisms (a coil or a magnet) which produces the field, but then it is not clear how such field diffuses into the plasma which is generated by a laser. For these studies to work, we need at least two different laser pulses, where the first one produces the plasma and the second one generates the beams or the shocks in a preformed medium which is already magnetized. Hence, the delay between these two pulses has to be longer than the diffusion time of the magnetic field, and shorter than the hydrodynamic diffusion time of the plasma. This puts constraints on the size of the coils that produces the magnetic field. This implies that time delays have to be of the order of 1-5 ns for spatial scales  $\sim 1$  cm.

- b. All of these experiments must be done inside a pre-filled chamber or gas cell of pressures between a fraction to a few mbars.
- c. In order to investigate magnetic field fluctuations we need to measure the spatial and temporal profiles of the magnetic fields. This can be achieved by a combination of induction coil probes and proton radiography to look at the filaments.
- d. In order to look for particle acceleration and higher energy “cosmic rays” we need particle spectrometers or Thomson parabolas.
- e. Finally, we need global plasma diagnostics for density, temperature and shock/flow hydrodynamics. This could be achieved using Thomson scattering (for local properties) and by optical interferometry/shadowgraphy.

### **3.1.4 Code development**

Although most codes are already well developed, an integrated description of all the physics occurring in the experiments is still missing. In particular, what is needed is:

- For relativistic PIC codes is the appropriate filtering of spurious Cherenkov emission (under development, Gremillet).
- PIC codes should be able to include radiation effects (under development, Tikhonchuk).
- Hybrid codes that could describe the full hydrodynamics prior to the development of instabilities and the transition from microscale to MHD regime.
- MHD with subgrid model for particles.

## **3.2 Mid-term (5-10 years) goals**

### **3.2.1 Relativistic shocks**

When one goes to the relativistic regime, the relevant configuration of the magnetic field is an angle of  $90^\circ$ . The particles reflected at the shock front are responsible for a strong current that produces a Lorentz force that slows down the incoming plasma and changes the nature of the instabilities. This is an important issue for astrophysics. In particular this shock “foot” plays the role of a buffer such that whatever the strength of the shock Lorentz factor, the flow Lorentz factor in the foot is reduced to a same moderate value [61].

At increasing magnetization, the stage of Weibel turbulence disappears; at high magnetization one expects only the formation of the shock through the generation of an intense X-mode with Synchrotron Maser Instability [62]. That coherent wave is accompanied, in a proton plasma, by a wake field that is expected to progressively thermalize electrons, oscillating in relativistic regime, with protons (some authors expect more the generation of a supra-thermal tail also). Between the very low magnetization regime and the high magnetization regime, the physics is not yet clear.

### **3.2.2 Radiation**

Relativistic shocks and relativistic reconnection sites give rise to intense radiation of inverse Compton or synchrotron type, in an unusual regime. At relativistic shocks, supra-thermal electrons

radiate an intense inverse Compton and synchrotron type emission through their interaction with micro-turbulence [63]; this is essentially what is observed in astrophysics. That radiation regime deserves a detailed study, especially in the low frequency side of the radiated spectrum where we could observe a “jitter” radiation. In astrophysics, this emission is the only possible diagnostic of the state of intense micro-turbulence that has been generated at the relativistic shock, and this is actually investigated in the early afterglow of Gamma Ray Bursts.

### **3.2.3 Facility requirements**

In order to reach these goals, positron beams are required for electromagnetic instabilities to develop in the relativistic regime. Currently, copious number of positrons in the 10's of MeV energy could be generated using the PETAL beam, using techniques that have been tested at the Omega laser facility (Rochester, USA).

Another aspect to investigate is the head-on collision between two beams of protons or positrons (in an ambient gas). However, this would require reconfiguration of the PETAL laser into a split-beam operation. Feasibility tests could be performed on smaller scale laser facilities such as LULI (France), Vulcan (UK) or the Orion (UK) lasers.

## **3.2 Long-term goals (>10 years)**

Understanding the processes for the formation and destruction of interstellar dust

This topic was not yet tackled by the European community working in laboratory astrophysics using high energy lasers. However it has been pointed out recently (ref NIF report) as one of the priorities in research directions for the NIF laser in the USA. In Europe there is large community working in this field, on the astrophysics side but the without effective interaction with scientists performing experiments with high energy lasers. Here we would like to highlight the importance of dusty plasmas in astrophysics and in particular its impact on astrochemistry.

Dust particles are produced in the envelope of dying stars and composed of silicates and carbonaceous material. It represents approximately 1% of the total mass of the universe but is important for the radiative transfer in the galaxies since dust absorbs about 30-50% of starlight and re-emit it in the far-infrared wavelength [64]. Dust shapes the form of the galaxies and is the principal ingredient for the formation of planets. Finally, dust plays a key role in the formation of molecules in space [65].

In the diffuse interstellar medium, gas and dust are irradiated by the strong UV field coming from surrounding massive stars (Figure 7). This diffuse medium gets organized in denser filaments, birthplace for stars and planetary systems. In those dense clouds, a complex chemistry can take place to form exotic molecules of many different types, even prebiotic molecules [66]. This chemistry is driven by bimolecular reactions in the gas-phase and reactions at the surface of the grains. Gas-phase species can undergo van der Waals liaisons with the molecules of the grains (physisorption). Once on the surface, the species are diffuse and meet other species, producing chemical reactions. Compared to gas-phase reactions, such processes are more efficient because the probability of

encounter is larger and the surface can act as a stabilizer in the case of the formation of excited complexes. The most simple and abundant molecule,  $H_2$ , is formed at the surface of the grains since all gas-phase formation pathways are inefficient [67]. In star forming regions, complex organic molecules, such as  $CH_3OCH_3$  and  $CH_2NH_2$ , have been observed and are formed through reactions at the surface of the grains [65]. All these processes however depend on the composition and physical properties of interstellar dust. And most of what we know of interstellar dust is based on observations in the interstellar medium. Up to now, no attempt to produce interstellar dust in the laboratory has been convincing.

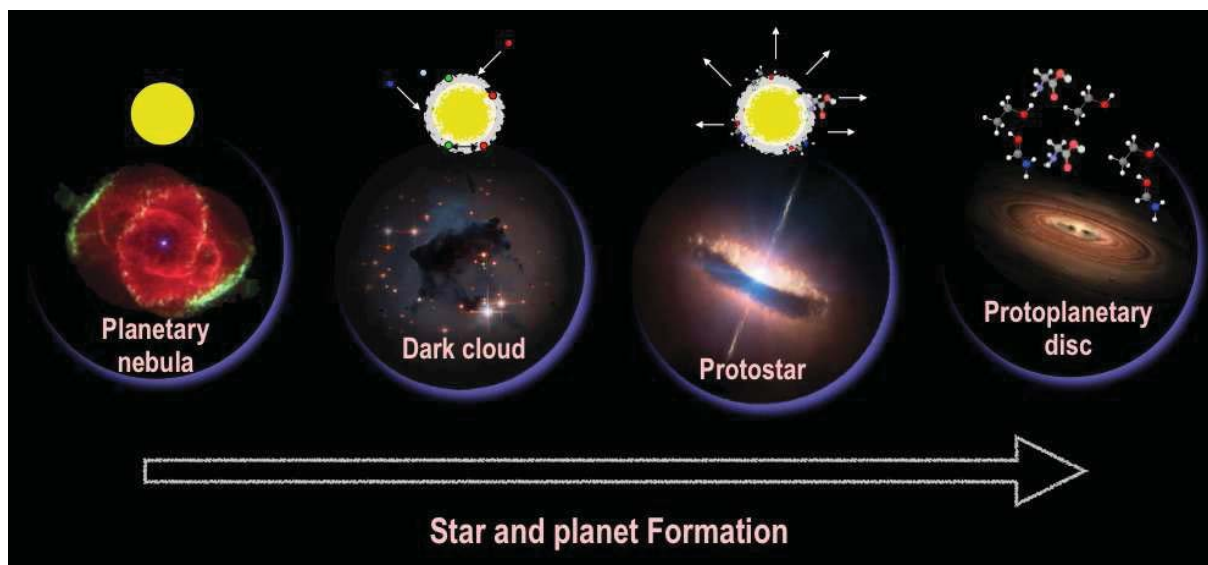


**Figure 7:** Importance of interstellar dust as catalytic surfaces for the formation of complex molecules in dark clouds and protostellar envelopes. The refractory cores of the grains are formed in the envelope of dying stars. Those cores are covered by an icy mantle of simple molecules formed in the gas-phase in dark clouds at low temperature. Those molecules undergo more complex reactions during the collapse of those clouds and are injected in the gas-phase in the warm regions of protostellar envelopes. Those complex organic molecules participate then to the formation of planets.

Understanding the mechanisms of formation and destruction of dust would however be of crucial importance to understand the evolution of the material in galaxies as well. Formation of dust is observed in the atmosphere of red giant stars. There is however inconsistency between the estimated rates of production of dust in these environments and the destruction rate by star formation and interstellar shocks. Taking into account the current estimates of both processes, the rate of formation is smaller or of the same order as the destruction rate ([68] and references therein). Understanding the formation and destruction processes are then of primer importance to understand the budget of dust in the universe.

According to the importance of this field, we think that future strong connections between astrophysicists and experimentalists using high energy lasers will allow to answer some of the main challenges in this field. As mentioned in the NIF report [69], high radiation fluxes and shocks are likely to be produced to study chemistry in interstellar dust. LMJ-PETAL will definitively be the only European facility able to achieve the experimental requirements in this field.

## 4. Diagnostics for laboratory Astrophysics

Diagnostics are needed to measure as large as possible sets of experimental parameters that will constrain modeling or codes; they are therefore essential to laboratory astrophysics. This is the reason why this working group requires much more possibilities of diagnosing the plasmas produced by LMJ-PETAL than the ones planned up to now.

### 4.1 Petal diagnostics

PETAL will be a fantastic tool to produce **very hard and short time** duration x-ray sources [70] to perform x-ray radiograph of a dense plasma [71], x-ray Thomson scattering [72], or absorption spectroscopy [73, 74]. It will also produce large amount of charged particles (electrons, protons, ions) that can be used to diagnose for example electric and magnetic fields [75], or density gradients in a shocked material [76].

### 4.2 LMJ diagnostics

Beside PETAL that will allow the diagnostics mentioned above, LMJ beams or auxiliary laser are needed to complete the big challenges described in this report:

- X-ray Thomson scattering with angular or spectral high resolution.
- X-ray absorption/Emission spectroscopy.
- X-ray radiography (ns).
- X-ray self-emission: DMX and  $\mu$ DMX.
- Optical/UV self-emission.
- Shadowgraphy.
- $4\omega$  Thomson scattering.
- Visar and SOP.

### 4.3 Magnetic field diagnostics

As mentioned widely in this report, magnetic fields play a fundamental role in several astrophysics situations and in laboratory experiments. Therefore it will be absolutely necessary to be able to measure those fields. Several means to measure these fields have been widely used on many different laser facilities with great success and should be installed on the LMJ target chamber: Faraday rotation, B-dots, proton radiography.

The opacity experiments in stellar conditions require a dedicated instrument: a high-resolution photon x-ray spectrometer in the range 400 – 5000 eV, a model of which is given by the OZSPEC-2 spectrometer installed on NIF [77]. The analysing power needed to probe in detail the neighbouring plasma environment of the ions is in the range of 1000.

An XRTS measurement would improve the knowledge of the temperature of the plasma in addition to the DMIX information of the radiative temperature.

The diagnostics for the nuclear physics experiments at LMJ-PETAL are:

- A magnet spectrometer, of the MRS type [78], to determine neutron or charged-particle energy spectra.
- Neutron time-of-flight detectors, e.g. the DEMIN [79].
- Gamma-ray detectors, such as the Gamma Ray History (GHR) diagnostic developed for the NIF
- Nuclear activation detectors [80].

These diagnostics are under consideration or development at CEA. Collaboration between CEA and the academic research community on the design and building of these detectors will be profitable for both the science and the facility since, as mentioned above, these diagnostics will be used for many other scientific goals.

## 5. Recommendations

It is noteworthy that, in parallel to the LMJ-PETAL laser facility itself, the group made three recommendations aimed at improving the probability of success of the experiments to be performed and the return on investment for the co-working communities involved in the present programme.

- First, the development within the academic community of shared numerical tools should be highly encouraged. It concerns first the simulation of unsteady and complex flow in several dimensions of space. In effect, existing hydrocodes meet common needs of the scientific communities of Astrophysics and Inertial Fusion (see topic 2). 3D massively parallel hydrodynamical schemes for real gases, coupled to the transport of radiation and particles with chemical kinetics and non-equilibrium thermodynamics are currently developed by different groups, especially for specific astrophysical needs, but, by their nature, they still lack the specific adaptations for laser laboratory experiment simulations and target design. This concerns also particle in cell (PIC) codes that are now widely developed both to treat ultra high intensity laser interaction with matter but also various astrophysics phenomena.
- New experimental concepts often require the development of new devices (e.g., the production of strong external magnetic fields by cooled coils around the target, or dedicated non existing diagnostics). Such devices, developed by the EU academic community (in collaboration with CEA-DAM teams), should be qualified and then installed while remaining the property of the consortium responsible for its development.



- Finally, the access policy to the LMJ-PETAL should be defined, on a basis similar to that which is already stated by the *'Agreement contract on procedures for experiments under the responsibility of the ILP on the laser facilities of CEA/CESTA'*. In particular, the laboratory astrophysics group recommends that the principal investigator (PI) of proposals belongs to an academic EU institution, in association with at least a French Co-PI.

## References

- 1 H. Takabe, Progress of Theoretical Physics Supplement, 202 (2001).
- 2 J. E. Bailey et al., Physical Review Letters 99, 265002 (2007)
- 3 J. E. Bailey et al., Physics of Plasmas 16, 058101 (2009)
- 4 S. Turck-Chièze, D. Gilles, M. Le Pennec, J.E. Ducret, J. Colgan, D.P. Kilcrease, C.J. Fontes, N. Magee, T. Blenski, F. Thais, F. Gilleron, J.C. Pain, C. Reverdin, V. Silvert, S. Bastiani-Cecotti, G. Loisel, M. Busquet & M. Klapisch, ApJ submitted (2014)
- 5 S. J. Rose, J. of Quantitative Spectroscopy and Radiative Transfer, 71, 635 (2001)
- 6 G. Loisel et al., High Energy Density Physics, 5, 173 (2009)
- 7 T. Blenski et al., Physics Review E, 84, 036407 (2011)
- 8 S. Turck-Chièze et al., High Energy Dense Plasmas, 9, 473 (2013)
- 10 D. J. Hoarty et al., Phys. Rev. Lett., 110, 265003 (2013)
- 11 M. Barbui et al., Physical Review Letters 111, 082502 (2013)
- 12 C. Labaune et al., Nature Comm. 4, 2506 (2013)
- 13 D.T. Casey et al., Physical Review Letters 108, 075002 (2008)
- 14 D.B. Sayre et al., Physical Review Letters 111, 052501 (2013)
- 15 D.T. Casey et al., Physical Review Letters 109, 025003 (2012)
- 16 R. C. Mancini et al, Phys. Plasmas 16, 041001 (2009)
- 17 Tarter, Tucker, Salpeter, ApJ, 156, 943 (1969)
- 18 M. E. Foord et al., Phys. Rev. Lett, 93, 055002 (2004)
- 19 S. Turck-Chièze et al., High Energy Density Physics 5, 132 (2009)
- 20 S. Turck-Chièze & S. Couvidat 2011, Rep Prog. Phys. 74, 086901
- 21 S.Turck-Chièze, Phys. Rev. Lett (2004)
- 23 C. Blancard, P. Cossé, G. Faussurier, ApJ 745, 10 (2012)
- 24 J. C. Pain et al., Proceedings of the 18th APiP, arXiv :1311.7429 (2013)
- 25 J. Colgan et al., High Energy Density Physics 9, 369 (2013)
- 26 S. Turck-Chièze & I. Lopes, Res. Astron. Astroph. 12, 1107 (2012)
- 27 V. Drean et al., Physics of Plasmas, 17, 1227 (2010)
- 28 Y. Xu & S. J. Rose, Proceedings IFSA, 1079 (1999)
- 29 H. Dzitko et al., Astrophysical Journal 447, 428 (1994)
- 30 D. Martinez et al, Abstract UO5.00014, APS Div. Plasma Physics 2013 Annual Meeting, Denver, CO.
- 31 Bailey2001 J. E. Bailey et al JQSRT 71, 157 (2001)
- 32 F. Wang et al Phys. Plasmas 15, 073108 (2008)
- 33 S. Fujioka et al, Nature Physics 5, 821 (2009)
- 34 I. M. Hall et al., Phys. Plasmas, 21, 031203 (2014)
- 35 R. P. Drake, Astrophys. Spac. Sci., 298, 49 (2005)
- 36 S. Bouquet, R. Teyssier & J. P. Chièze, Astrophys. J., 127, 245 (2000)
- 37 C. Michaut et al., Astrophys. Spac. Sci., 322, 77 (2009)
- 38 J. M. Blondin et al., Astrophys. J., 500, 342 (1998)
- 39 M. Hohenberger et al. , Phys. Rev. Letters 105, 205003 (2010)
- 40 C. M. Krauland et al. Astrophys. J., 762, L2 (2013)

- 41 E. Falize et al. High Energy Density Physics, 8, 1 (2012)
- 42 C. Busschaert et al., New J. Phys., 15, 035020 (2013)
- 43 E. Falize, C. Michaut & S. Bouquet, Astrophys. J., 730, 96 (2011)
- 44 M. Cropper, G. Ramsay & K. Wu, Mon. Not. R. Astron. Soc. , 293, 222 (1998)
- 45 Charignon C. & Chièze J. P., A&A 550, A105 (2013)
- 46 P. Clavin and L. Masse, Phys. Plasmas 11, 690 (2004)
- 47 V. Smalyuk *et al.*, Phys. Plasmas 13, 056312 (2006)
- 48 A. Casner et al., Phys. Plasmas 19, 082708 (2012)
- 49 B. Srinivasan, Phys. Plasmas 19, 082703 (2012)
- 50 Pudritz, R. E., M. J. Hardcastle, and D. C. Gabuzda. "Magnetic Fields in Astrophysical Jets: From Launch to Termination." *arXiv:1205.2073 [astro-Ph]*, May 9, 2012.  
<http://arxiv.org/abs/1205.2073>.
- 51 Frank, A., T. P. Ray, S. Cabrit, P. Hartigan, H. G. Arce, F. Bacciotti, J. Bally, et al. "Jets and Outflows From Star to Cloud: Observations Confront Theory." *ArXiv E-Prints* 1402 (February 1, 2014): 3553.
- 52 E. Falize et al., Astrophys. Space Sci. 322, 71 (2009)
- 53 Kulsrud et al., ApJ 480, 481 (1997)
- 54 Gregori et al. Nature 482, 481 (2012)
- 55 Miniati, ApJ 782, 21 (2014)
- 56 Treumann, Annual Rev. Astron. Astrophys. 17, 409 (2009)
- 57 Medvedev & Loeb, ApJ 527, 697 (1999)
- 58 Bret et al., Ann. Geophys. 28, 2127 (2010)
- 59 Bell, MNRAS 353, 550 (2004)
- 60 Schekochihin et al. New J Phys. 9, 300 (2007)
- 61 Lemoine et al., MNRAS in print (2014)
- 62 ironi & Spitkovsky, ApJ 726, 75 (2011)
- 63 Reville and Kirk, ApJ 724, 1283 (2010)
- 64 Draine. Annual Review of Astronomy & Astrophysics, vol. 41, pp.241-289
- 65 Herbst & van Dishoeck 2009 Annual Review of Astronomy & Astrophysics, vol. 47, Issue 1, pp.427-480
- 66 Agundez & Wakelam 2013 Chemical Reviews, Vol. 113, No. 12, p. 8710-8737
- 67 Cazaux & Tielens 2002 ApJ 575, Issue 1, pp. L29-L32
- 68 Draine 2009, Cosmic Dust - Near and Far ASP Conference Series, Vol. 414, proceedings of a conference held 8-12 September 2008 in Heidelberg, Germany. p.453
- 69 Basic Research directions for user Science at the National Ignition Facility, NNSA , Nov 2011
- 70 E. Brambrink et al. Physics of Plasmas **16**, 033101 (2009)
- 71 E. Brambrink et al. Phys. Ref. E 80, 056407 (2009)
- 72 B. Barbrel Phys. Rev. Lett. 102, 165004 (2009)
- 73 G. Loisel et al., High Energy Density Physics, 5, 173 (2009)
- 74 A. Benuzzi-Mounaix et al. PRL 107, 165006 (2011)
- 75 N. Kugland et al. Nature Physics, Volume 8, Issue 11, pp. 809-812 (2012)
- 76 A. Ravasio et al. Physics Review E 82, 016407 \_2010
- 77 R. F. Heeter et al., Review of Scientific Instruments, 79, 10E303 (2008)
- 78 J.A. Frenje et al., Review of Scientific Instruments 72, 854 (2001)
- 79 M. Houry et al., Nucl. Instr. & Methods in Physics Res. A557, 648 (2006)
- 80 O. Landoas et al., Review of Scientific Instruments 82, 073501 (2011)

# DEMONSTRATING DIRECT DRIVE INERTIAL FUSION USING THE LMJ-PETAL LASER SYSTEM

**Contributors:** Stefano Atzeni, Dimitri Batani, Sophie Baton, Catherine Cherfils, Michel Decroisette, Sylvie Depierreux, Roger Evans, Valery Goncharov, Sergei Gus'kov, Javier Honrubia, Christine Labaune, Jiri Limpouch, Hiroaki Nishimura, John Pasley, Piotr Raczka, Christophe Rousseaux, Xavier Rybeire, Joao Santos, Guy Schurtz, Robbie Scott, Vladimir Tikhonchuk, Wolfgang Theobald.

## Introduction

The European project HiPER (*High Power Energy Research*) aims at establishing Inertial Fusion Energy (IFE) as a viable mean for commercial power production. Since its initial launch in 2008, it has provided the framework for scientific and technological developments in Europe with the objective of designing and constructing a demonstration power plant in the next 20-30 years.

IFE relies on the underlying concept of Inertial Confinement Fusion (ICF) where a spherical shell containing a few milligrams of hydrogen isotopes is first compressed then ignited from a hot spot. A major milestone in the HiPER roadmap is the achievement of nuclear gain by means of ICF using existing laser facilities. Different schemes have been proposed for the implosion and ignition of ICF targets. HiPER has down selected direct laser illumination (*direct drive*) for the compression stage and shock or fast ignition to trigger the nuclear burn.

In the Fast Ignition concept (FI), a beam of energetic particles, (low Z ions or relativistic electrons) delivers its energy to the hot spot. These particles are accelerated by means of a short but powerful auxiliary laser pulse. Typical energy is close to 100 kJ, for a 10-20 ps duration. Although the energy-power diagram of Petal falls well below these requirements, the LMJ-PETAL system offers a unique opportunity to optimize the production of the ignition beam and evidence hot spot heating in realistic ICF conditions.

Shock Ignition (SI), as well as the conventional central ignition scheme (CCI), gets ignition from a central hot spot driven to high pressures (500 -1000 Gbar) by hydrodynamic motion. In the conventional scheme, this pressure results from the conversion of the kinetic energy imparted to the imploding shell into internal energy. CCI requires a threshold implosion velocity in the 350-400 km/s range. Conversely, SI targets are driven at sub ignition velocities (250-300 km/s), thus enhancing the hydrodynamic stability and reducing deleterious effects related to laser-plasma interaction. A converging shock wave launched at the end of the implosion raises the central pressure up to ignition. This shock wave is driven by a specific temporal profile of the laser pulse (*ignition spike*). Since the energy of the spike is about 200-300 kJ for a duration of a few hundreds of ps, it can be obtained from lasers having the same technology than the compression lasers, and even from the same beam lines. State-of-the-art numerical simulations predict robust ignition and gain larger than 80 with 400-600 kJ of laser energy and 300 TW of total power. These figures fall within the operating domain of the 1.4 MJ, 400 TW, LMJ laser facility.

The previous arguments form the rationale for the selection of shock ignition as the prior option for HiPER, leaving FI as a second option. This strategy is also consistent with a realistic evaluation of European resources and the necessity to share responsibilities worldwide: US and European defense institutions take the lead on radiation driven ICF, while the Japanese scientists advocate the electron-driven fast ignition approach. SI studies in Europe are conducted in collaboration with the Laboratory for Laser Energetics (U. Rochester, US), enabling access to the Omega and NIF facilities. Meanwhile, a close coordination has been maintained for a long time between Europe, Japan (ILE Osaka) and the USA (U. San Diego, LLE) in the context of FI.

The present programme results from the views of the European scientists involved in ICF research. It complies with the HiPER science roadmap. Its main, long term goal, is nuclear gain by means of shock ignition in the LMJ target chamber. Its success depends on progresses expected in the fields of physics, applied mathematics and technology. The following key elements have been identified:

1. Fuel compression. This issue is shared by all schemes considered here. It will have to deal with the specific, polar arrangement of LMJ beams. Achieving a **polar direct drive (PDD) implosion platform** on LMJ is a major milestone on the path towards ignition.
2. Hot spot heating. This involves **interaction and transport** physics in regimes very different from one another in conventional ignition, SI and FI. Experiments using the early stages of the LMJ-PETAL system are proposed hereafter.
3. Diagnostics and metrology are required in order to control all stages of the process with a resolution sufficient to settle between theoretical assumptions and/or fulfill design requirements.
4. Targetry. This involves the production and characterization of warm or cryogenic shells within given specifications of roughness, sphericity and homogeneity.
5. High performance computing. The hydro code is the essential companion of this programme. Since it capitalizes most of the knowledge we have of ICF, its validation, as well as the demonstration of its predictive capabilities, are central issues. It is interfaced with databases for material properties, post processors for diagnostics and output analysis, and preprocessors for initial and boundary conditions. It must also be linked to codes devoted to detailed physics as plasma kinetics or nuclear combustion. The unification of existing codes and physical packages into a coherent, **high performance computing platform** managed by the community remains a challenge.

## 1. Review of the experimental studies of alternative ICF schemes

This section presents a short review of recent experimental results acquired by European scientists concerning the shock and fast ignition schemes, taking benefit of HiPER slots secured on European facilities as well as international collaborations. Each campaign is in itself a coordinated project which includes the design phase, the manufacture of targets, the development of diagnostics and the acquisition of data, the analysis and interpretation of measurements. This has been made possible by the constitution of integrated teams including engineers, experimentalists, theoretical physicists and computational scientists.

## 1.1 Shock ignition experiments

Since the proposal of SI as an alternative to CCI in 2006, numerous experimental campaigns have been achieved by the ICF community. Implosions of warm and cryogenic shells have been performed on the Omega laser system, demonstrating enhanced areal density and nuclear production from DT and D2 fuel [13], as well as moderate light backscattering and hot electron production with temperature in the 40-60 keV range. Planar experiments have also been achieved in Europe and in the USA in order to investigate the production of very high ablation pressures and the physics of laser plasma coupling in the regime of shock ignition. None of these experiments show any strong backscattered light, with the exception of those reported in 1.1.3 which used short pulses. However, strong discrepancies appear in the estimated shock pressures, which have been explained considering the specific focal spot shapes produced by the different facilities.

### 1.1.1 Shock drive on the LULI facility

The feasibility of SI relies upon the efficiency with which an intense shock can be generated in the long plasma blown off from the imploding target. An experiment related to this essential issue has been performed in 2010 on the LULI laser facility [3]. The principle was to launch a strong shock in a large preformed plasma with the goal to acquire a whole set of relevant parameters such as backscattered energy, hot electrons number and energy, instantaneous velocity of shocks, time history of shocks and coalescence. Two ns-kJ beams were used: the first beam was used to compress the target, this creating a first shock and a large plasma blow-off, and the second beam was used as a spike. During the experiment the two beams were converted at  $2\omega$  ( $0.53 \mu\text{m}$ ).

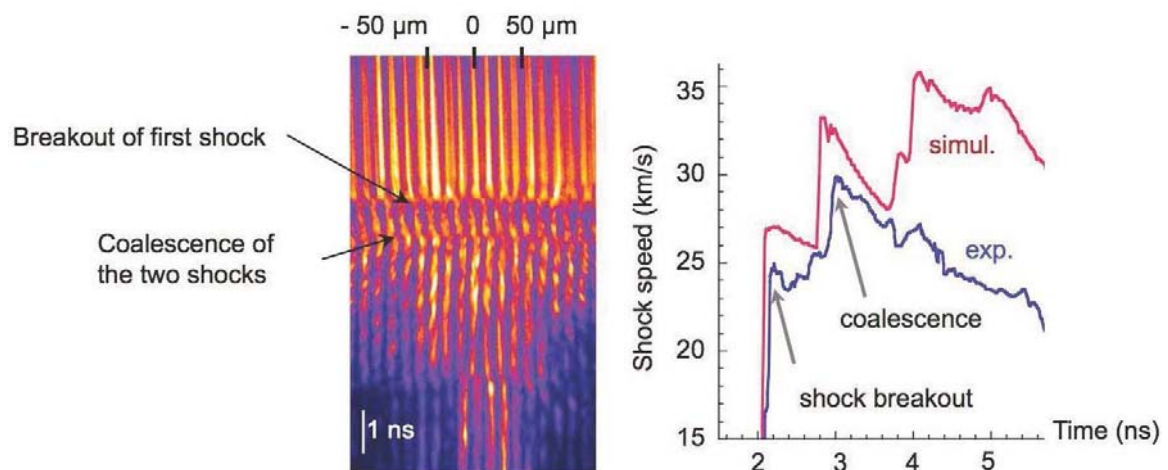


**Figure 1:** a) VISAR image recorded for a delay of 1.7 ns between two laser beams that irradiate the target from the topside of the figure and the time goes down. b) Velocity profiles as the function of time corresponding to panel a) from measured data (blue) and numerical modeling (red).



The numerous diagnostics fielded in this experiment provided a large amount of data that have been analyzed by means of the 2D radiation hydrodynamic codes FCI-2 and CHIC. Backscattered energy due to SBS and SRS has been measured, yielding a moderate reflectivity between 7-11%. According to figure 1b), the measured shock breakout and coalescence times agree with simulations within experimental accuracy, confirming that laser coupling for shock wave generation is appropriately predicted by simulations. The pressure of the shock wave generated in this experiment is 40 Mbar corresponding to the laser intensity of  $10^{15}$  W/cm<sup>2</sup>.

### **1.1.2 Shock drive on the PALS facility**

Planar experiments on strong shock generation were also performed at PALS at intensities larger than those used at LULI, up to  $10^{16}$  W/cm<sup>2</sup>. The goal of the experiment was to characterize the impact of parametric instabilities, the generation of hot electrons and the capability of creating a strong shock. According to the results [2], the level of parametric instabilities was quite low and relatively strong shocks (up to 90 Mbar) were produced. This was however far less than expected, thereby suggesting either a possible change in the scaling law for shock pressure vs. laser intensity, at least in the  $I\lambda^2$  regime used in the experiment, and/or inhibition mechanisms acting on the energy transport from the critical region to the overdense part of the target. According to numerical simulations [7], the hot electron generation is due to the resonance absorption, and magnetic fields, locally generated by the plasma, may explain the inhibition of the energy transport.

### **1.1.3 Laser plasma interaction experiments**

The intensity of the ignition spike considered for SI lies in the range of a few  $10^{15}$  up to  $10^{16}$  W/cm<sup>2</sup>. Most numerical designs of shock ignition targets assume collisional absorption of the ignition spike. However, it is very likely that collective effects as stimulated Raman backscattering (SRS) or stimulated Brillouin backscattering (SBS) occur for these intensities. Cross Beam Energy Transfer may also appear in the multibeam irradiation considered for LMJ.

A series of experiments dedicated to laser plasma interaction under the conditions relevant to the shock ignition have been conducted, with similar principle: multiple laser beams produced a hot and long (few hundred microns scale length) plasma on which an interaction beam which was shot later on.

In all experiments, it was observed that the SBS reflectivity, at high intensity, is always shorter than the interaction pulse duration and that SBS grows at the very beginning of the laser pulse [4]. This means that the average reflectivity measured with laser pulses in the nanosecond range is not meaningful for the shock ignition pulse, which will have a duration of a few hundreds of picoseconds. For a SBS duration of one third of the total laser pulse, reflectivity for the few first hundreds of picoseconds would be 3 times larger than the average reflectivity.

In the case of crossing beams, SBS may be seeded by reflections or shared ion acoustic waves. It is likely that the SBS reflectivity could be very high for the shock ignition pulse conditions. To avoid this problem, all possible beneficial effects that could reduce the SBS emission like beam and plasma smoothing, target composition, aperture of the optics must be considered.

The SRS evolution as a function of the density scale length was studied with foam targets with initial density  $\sim 10 \text{ mg/cm}^3$  at the LIL facility [5]. The scale lengths were deduced from the hydrodynamic CHIC simulations. The SRS reflectivity increases with the foam length varying from 0.5 to 1 mm, and had a longer temporal duration, demonstrating an effect of the expansion of the plasma corona. Although the observed SRS characteristics are in general in agreement with the numerical simulations, premature conclusions on SRS in shock ignition should be avoided because only the lower part of the intensity range has been investigated in this experiment.

Recent experiments at LULI have used a combination of kilojoule and short laser pulses ( $\sim 12 \text{ ps}$  duration) in order to study the laser-plasma coupling at high laser intensities for a large range of electron densities and plasma profiles. It was found again that the backscatter is dominated by SRS while SRS stayed at a limited level [6]. This is in agreement with past experiments using longer pulses but with the laser intensities limited to  $2 \text{ PW/cm}^2$  or short pulses with the intensities up to  $50 \text{ PW/cm}^2$  as well as with 2D PIC simulations.

#### **1.1.4 Shock x-ray diagnostic experiments on the LULI**

Formation of strong shocks in plasma with a corona is one the major goals of the future shock ignition experiments. The diagnostic of such shocks is by itself a challenging problem since the conventional techniques using VISARs are often not usable because of the darkening of the tamper material. X-ray self-emission and x-ray radiography are valuable options under these conditions. The measurements of the shock velocity by using the x-ray radiography of the shock front has been tested in the LULI experiment in October 2013 in planar and hemi-spherical targets to see the influence of the geometry on the shock front. This campaign followed by an experiment on the LIL facility in February 2014 at the energy level of 10 kJ. Preliminary results show ablation pressures exceeding 100 Mbar. A higher shock velocity is measured in hemi-spherical targets thus demonstrating a significant convergence effect.

#### **1.1.5 Planar experiments on the OMEGA facility**

The experiments were aiming at investigating the shock strength and the impact of plasma parametric instabilities on the ablation pressure in conditions of interaction relevant for shock ignition. Planar targets were irradiated with laser pulses comprising a pre-plasma generating foot and a high-intensity spike to launch a strong shock. At a peak intensity of  $1.4 \text{ PW/cm}^2$ , a hot electron temperature of 70 keV was measured with +1.8% of the spike energy being converted to hot electrons, and <10% of the laser energy was scattered. Simulations using the 2-D radiation hydrodynamic codes DRACO and CHIC showed very good agreement with the observed shock propagation. Based on these results, at an intensity of  $1.2 \text{ PW/cm}^2$ , a 70-Mbar shock was generated in the presence of a 350-nm pre-plasma.

Ablation pressures above 200 Mbar have also been reported recently in Omega experiments using Ti-doped CH spheres of reduced radius ( $250 \mu\text{m}$ ). This is the highest pressure reported at SI-relevant conditions, and these experiments constitute an important step toward the experimental validation of the shock-ignition concept [8].

### 1.1.6 Spherical geometry experiments on the OMEGA facility

Scientists at LLE have been performing implosions on the Omega 60 beams facility using the shock ignition technique since year 2007. Warm targets, as well as cryogenic deuterium and deuterium-tritium ice shells produced areal densities close to the 1D prediction and achieved up to 12% of the predicted 1D fusion yield (*Yield over Clean*, or YOC) [13]. Moreover, it was shown that the YOC does not decrease when the implosion convergence increases, as it is the case for conventional implosions. These very encouraging results produced among European teams a strong enticement to propose collaborative shock ignition experiments to LLE.

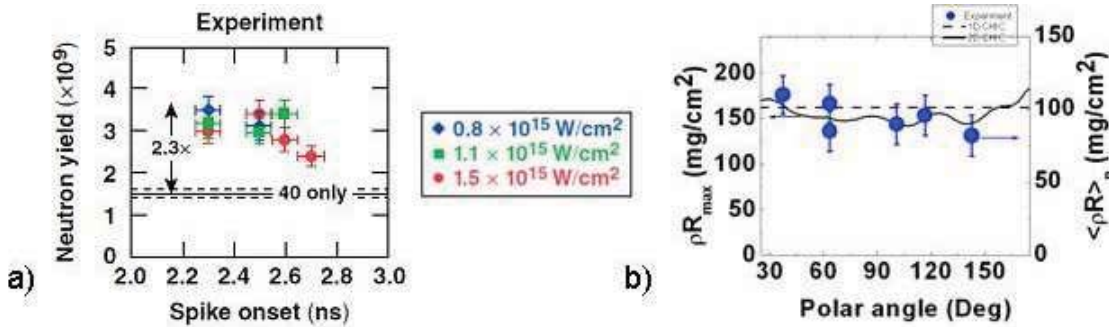


**Figure 2:** a) Measured neutron yields for the 40 + 20 configuration. b) Simulated (curves) and measured (circles) areal density as a function of the polar angle. The dashed line is from a 1D simulation and the solid curve from a 2D simulation.

In the experiment reported hereafter [13], 35  $\mu\text{m}$  thick, 430  $\mu\text{m}$  outer radius deuterated plastic shells filled with  $\text{D}_2$  gas with a pressure of 25 bar were imploded using 40 beams with a low-adiabat shaped 2.7 ns pulse with total energy of 13.6 kJ. The compression beams were repointed to achieve a good illumination uniformity for the implosion. An ignition shock was launched by the remaining 20 beams that were delayed in time and tightly focused to achieve intensities at the critical surface ranging from 0.8 to 8  $\text{PW/cm}^2$ . The 20 beams ( $\sim 4.6$  kJ) had a  $\sim 600$ -ps FWHM square pulse shape without polarization smoothing and no phase plates in most of the shots in order to reach the highest possible spike intensity on target. Up to 35% of the spike beam laser energy is lost at the highest intensities due to backscatter. The hard x-ray signals measured with four channels are consistent with the hot electron temperature of  $\sim 50$  keV. A neutron yield enhancement by a factor of up to 2.3 is measured when the spike beams are added in comparison with a 40 beams reference implosion (Fig. 2a). The neutron yield does not show a significant dependence to spike intensity. Areal densities (Fig. 2b) were inferred from secondary proton spectra.

The two-dimensional hydrodynamic simulations performed with the code CHIC compared to the observations. The areal density modulations result from both the imprint pattern from the 40 drive beams and the dodecahedron imprint pattern of the 20 spike beams. The simulated neutron yield enhancement 3.6 compared with the measured figure of 2.3 indicates that the onset time of the spike strongly affects the neutron production.

### 1.1.7 Previsions for the spherical geometry NIF experiments

The composite configuration in OMEGA experiments reproduces the configurations that could be achieved in the future on the NIF [11,12] and for the LMJ. Figure 3a displays a target designed for integrated shock ignition experiments on NIF. A similar target including a wetted-CH foam ablator [10] is predicted to produce a fusion energy gain between 50 and 100 for the total delivered laser energy less than 1 MJ (Fig. 3b) [11]. Compared to conventional direct-drive, high velocity, hotspot ignition targets, this design is characterized by a stable, low-aspect-ratio thick shell that should be less susceptible to both initial speckle imprint and hot electron preheating.

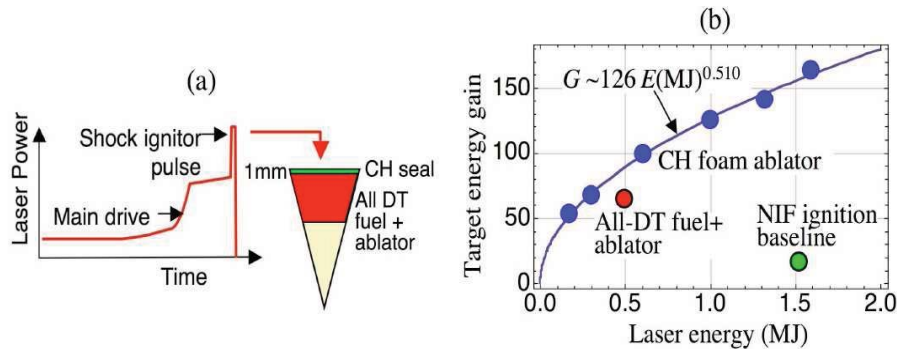


**Figure 3:** (a) Candidate all-DT NIF shock ignition target (~to scale) for nominal gain ~60 (30 MJ yield) at a total drive energy of ~0.5 MJ. (b) Energy gain curve (1D LASNEX) versus laser drive energy for NIF shock ignited targets (wetted foam ablators – blue points) together with corresponding performance for the all-DT fuel+ablator candidate design at ~0.5 MJ (red point).

To obtain these performances the NIF facility needs to be modified. A new cryo-target-positioner must be developed, the Polar Direct Drive (PDD) illumination configuration needs to be tested, and the beam smoothing should be improved [9]. However, the shock ignition scheme demands in energy and power remain well below the actual performance of the NIF facility.

Recent simulations propose a new target design for the shock ignition on NIF [1], which is within the NIF Laser System specifications. Although the target implosion velocity is larger than for standard SI designs, the ignition security factor  $\text{ITF}^1$  1D is increased to 4.1 by using 700 kJ of input laser energy. Hot electrons generated during the spike, if any, are expected to have a positive effect on ignition robustness provided that their temperature remains below 150 keV, and their energy below 20% of the incident spike laser energy. Two-dimensional simulations using either a split-quad or a full-quad beam configuration predict a good shell uniformity and ignition with the gains 40-50. That target design requires only minor modifications to the NIF system. Alternative designs have been proposed for the LMJ facility [71].

<sup>1</sup> The Ignition Threshold Factor (ITF) is a function of the dynamic parameters of the implosion. The probability of ignition is conventionally expressed as  $p_i = \text{ITF}/(\text{ITF}+1)$

## 1.2 Experiments related to the fast ignition scheme

According to present evaluations, the demonstration of fast ignition in scale one would require a  $\sim 100$  kJ, 20 ps laser pulse. This is presently out of reach at the NIF or LMJ, but many analytical or integrated experiments can be conducted on sub-ignition scales in order to evaluate the potential of the electron and ion fast ignition schemes for IFE. The European scientists have been conducting such experiments in a continuous collaboration with American and Japanese scientists.

Despite the large amount of experimental data acquired so far, the results obtained need to be scaled to pulse durations and laser energies relevant to fast ignition. The experimental efforts must be accompanied by a similar effort and progress in simulations providing benchmarking models of fast particle acceleration and transport in fusion plasmas.

Several factors affect the achievement of full-scale fast ignition:

- Assembly of the compressed fuel to densities  $300 \text{ g/cm}^3$  less than  $100 \text{ }\mu\text{m}$  from cone tip.
- Laser to fast electron coupling efficiency.
- Transport of fast electrons from interaction region to the compressed core through the cone tip (if any).
- Energy deposition in the compressed core. In full-scale fast ignition, the large  $10^{14} \text{ A.cm}^{-2}$  electron current density may enhance significantly the dissipation of the electron beam far from the compressed core of nuclear fuel.

Therefore, some of these processes have to be investigated experimentally and benchmarked using state of the art hybrid/PIC codes so that accurate predictions could be made for full-scale fast ignition experiments.

The experiments performed in various laboratories in Europe and the United States in the last ten years were dedicated to:

- The survey of the electron energy loss mechanisms.
- The scaling of these mechanisms in function of the fast electron current density and the target thickness in solid density targets.
- The transition between the solid and warm dense matter states exploring in particular the transient behavior of the material resistivity.
- The magnetically-assisted fast electron beam transport by the dual-collinear laser interaction and the resistivity gradients.
- The use of reduced mass targets to obtain a detailed information on the laser energy transferred into fast electrons.
- The effects of the electron transport barriers.

At the same time, the FIREX project is being carried out in Japan, mainly based on the GekkoXII + LFEX facility in the Osaka University, pursuing the goal of driving the compression of DT-shell targets, with an inserted cone, and heating to temperatures in the range of several keV, by a proper timing between the shell compression and the fast electron beam injection on the cone.

### 1.2.1 Fast electron beam energy transport in solids

The experimental and theoretical results obtained in the last years with metallic solids and in warm-dense targets (representative of the cone material), suggest that the resistive effects related to the return current play a major role compared to the collisions of the incident fast electrons, for beam current densities above  $5 \times 10^{11} \text{ A.cm}^{-2}$  [35]. The time-averaged ohmic stopping power is expected to always saturate at a maximum of a few keV/ $\mu\text{m}$  when the heating time scale of the target up to temperatures above Fermi temperature becomes negligible compared to the fast electron beam duration [30]. This will be the case for the fast ignition conditions, but experimentally such 10 ps, multi-PW electron beam driver regime remains still unexplored.

### 1.2.2 Magnetically-assisted confinement of the electron beam

Electron beam divergence might be a severe limitation of FI, hence the idea to engineer magnetic fields in the target in order to guide the beam. Resistivity gradients induce significant magnetic fields inside the dense plasma region, and may be used for this purpose. In the past years, two approaches for such electron guiding have been tested experimentally:

1. an artificial fabrication of resistivity gradients or
2. using the existing current gradients.

Targets presenting resistivity gradients are relatively easy to manufacture since they can be made of successive layers of different materials having different resistivity. The experiments conducted on the Vulcan and Titan facilities indicated a smaller electron beam in the presence of the Fe core in Al bulk target, thus showing that electrons were magnetically guided inside a more resistive Fe cylinder [22, 29].

The axial compression of cylindrical targets provides such a combination of temperature and density gradients that may guide the fast electrons along the axis over the length of more than 100  $\mu\text{m}$  [26]. Another possibility of electron beam guiding has been experimentally demonstrated recently [32] by using a sequence of two laser pulses, the prepulse is creating a magnetic field structure at the solid target surface, which guides the electron beam created by the second more intense pulse.

### 1.2.3 Fast electron generation efficiency inferred from the reduced mass target experiments

Such targets provide a unique access to the hot dense matter regime and for diagnosing the laser generated fast electron population. Time integrated x-ray  $K\alpha$  emission spectroscopy has been used to infer the efficiency of fast electron acceleration and energy deposition rate. An efficient PW-laser-to-fast-electron conversion is demonstrated but the large electron beam divergence remains the main issue [25]. It is demonstrated in the recent experiments that it is due to the transport barriers at the solid target surface. The laser prepulse has a significant effect on the fast electron beam characteristics and a considerable technical effort has been carried out in the facilities to significantly reduce the laser intensity contrast to levels of  $10^{-10}$ .



### 1.2.3 Hole boring for fast ignition

Hole boring might be the key to fast ignition. Since hole boring does not require a reentrant cone, simple spherical shells could be used, which is a great advantage for IFE. An analytical model and numerical simulations [24, 31] suggest that pulses with intensities exceeding  $10^{22}$  W/cm<sup>2</sup> may penetrate deeply into the overdense plasma as a result of efficient ponderomotive acceleration of ions in the forward direction. The penetration depth as large as hundreds of microns depends on the laser fluence, which has to exceed a few tens of GJ/cm<sup>2</sup>. The fast ions, accelerated at the bottom of the channel with an efficiency larger than 20%, show a high directionality and may heat the precompressed target core to fusion conditions. Hole boring in lower density targets can be achieved at lower laser intensities  $\sim 10^{18-20}$  W/cm<sup>2</sup> which will be achievable on PETAL. It can be diagnosed with the Doppler shift technique as it has recently been demonstrated [28].

### 1.2.5 Fast ion acceleration experiments

Ion fast ignition (IFI) is a viable alternative to the electron fast ignition. Since ions are carrying larger kinetic energy, they are much less affected by the electric and magnetic fields in plasma. Therefore, ballistic focusing can be achieved. The needed proton energy for the efficient energy deposition in the compressed fuel is in the range of 10-20 MeV which is already achieved in many experiments by using the Target Normal Sheath Acceleration (TNSA) mechanism. The work related to the ion fast ignition has recently been reviewed [20]. The weak part of the IFI scheme is a low conversion efficiency of the laser energy to the protons in the needed energy range. However, novel designs employing low density or expanding thin solid targets show increasing conversion efficiency, presently in excess of 6% for carbon ions [23].

### 1.2.6 Integrated fast ignition experiments

Experiments coupling the spherical compression of cone-in-shell targets with fast electron beam generated inside the cone by a PW-level short laser pulse have recently been fielded on the Omega-EP and Gekko XII – LFEX facilities.

In the Omega-EP experiments, the K $\alpha$ -fluorescence imaging revealed, for the first time, the spatial distribution of the energy transport [34]. The observed K $\alpha$  emission size is consistent with the size of the assembled fuel in front of the cone tip, expected from 2D hydrodynamic simulations of the target implosion. These were benchmarked by monochromatic X-ray radiography images of the targets at different times. In shots with high laser intensity contrast, a significant enhancement (up to 60%) in the total K $\alpha$  and neutron yields was measured (compared to those without fast electrons) [17].

### 1.2.7 Magnetized fusion

Magnetized fusion is foreseen as a promising path towards high gain fusion [27], mostly after the successful experimental demonstration of seeded B-field amplification during spherical target implosions driven at the Omega facility (LLE – Univ. Rochester, USA) and the resulting fusion yield enhancement [18,21]. In the particular case of fast ignition, the relativistic electron beam divergence

can be controlled by an axial B-field in the range of a few kT imposed externally to the imploded capsule, according to several numerical studies of integrated particle-in-cell and hydrodynamic modeling of electron transport in the full-scale fast ignition conditions [33]. In particular, the simulations by Strozzi *et al.* indicate that even in the case of near perfect collimation, the laser intensity required for depositing of a sufficient energy within the hot spot within the inertial confinement time corresponds to a too high fast electron temperature, which exceeds the optimal temperature. That observation points on another problem of fast ignition that even if collimation can be achieved the electron stopping in the hot spot may be inefficient.

The capability of generating kT-level magnetic fields by laser has recently been demonstrated in Japan using 1 kJ, 1 ns laser pulses by Fujioka *et al.* [19], and confirmed at LULI in 2013, exploring different target materials and target geometry [16]. A proof-of-principle experimental demonstration of the collimated propagation of a relativistic electron beam in solid targets, by imposing such an external magnetic-field, has been performed at LULI in 2014.

## **2. Theoretical and numerical developments: the actual status and the developments required to achieve the objectives**

The LMJ-PETAL facility opens for the first time a possibility for demonstrating ICF and further address important issues in reactor design. Shock Ignition [45, 37, 44] constitutes one of most promising schemes as it provides a large flexibility in separate tuning of implosion and ignition phases, while keeping the operational parameters within the existing technical limits. Nevertheless, the success of shock ignition on LMJ or NIF is not granted and the study of the fast ignition scheme, including the electron and ion variants, needs being pursued. Several potential causes of failure of SI have been identified so far. Some are related to the characteristics of the LMJ facility, mostly designed for indirect drive implosions. Some are related to unexplored physical aspects in the laser plasma interaction and implosion dynamics.

The work on IFE requires a close coordination between the theoretical developments, numerical modeling, experiments, diagnostic developments and target fabrication. This section describes the needs in the theory and simulations related to IFE.

### **2.1 Challenges of the ICF research**

ICF is built on solid theoretical and experimental backgrounds. The physics of laser plasma interaction and laser induced hydrodynamics are well-developed disciplines that have demonstrated their performance in various domains. Moreover, it was successfully demonstrated in 1950s and 1960s that the fusion reactions can be ignited with nuclear explosions releasing an energy of hundreds of kt, which corresponds to more than  $10^{15}$  J. The challenge is to realize this process on the non-destructive, laboratory scale with the energy release on the level of 1 GJ or even less. The dramatic

reduction of the energy scale implies much smaller temporal and spatial scales, which means that both the theory and the experiments must be much more precise and controllable [41].

This is not the case at present time. The experimental campaign NIC on the NIF facility in 2009-2012 has demonstrated significant limitations in our predictive capacities and in the control of the experimental conditions [38]. The challenge for the theory and for numerical simulations is to develop more precise and robust models that can describe with a sufficient accuracy all steps of the ICF process, to calibrate these models using dedicated experiments, and, finally, to design and to perform the integrated experiments on the LMJ. The issues to be studied are related to the laser plasma interaction, temporal shaping of the implosion beams, the fast electron and fast ion generation, transport and energy deposition, the strong shock wave generation and convergence, the hydrodynamic stability of implosion schemes, the ignition of fusion reactions and propagation of nuclear burn.

Only detailed studies of all these issues, confirmed in partial and integrated experiments may open a way for the design of a new facility dedicated to the demonstration of the technical feasibility of IFE power plant.

## **2.2 State of the art**

The theoretical disciplines related to the ICF process are: hydrodynamics, plasma kinetics, laser plasma interaction, atomic and radiation physics, physics of solid state and phase transitions, nuclear physics, applied mathematics and high performance computing. Significant results have been obtained in last 30-40 years in all directions [36].

The hydrodynamic models successfully describe the shock waves, the target implosions in cylindrical and spherical geometries, the hydrodynamic instabilities and possible ways of their control, the timing of shocks and compression waves needed to create the appropriate conditions for ignition of fusion reactions and fuel burn.

Plasma kinetics and atomic physics describe the processes of plasma ionization, energy transport by electrons and x-ray radiation, formation of the ablation front, heating and cooling the fuel, kinetic processes in the shock fronts, the energy deposition by the fusion reaction products and plasma expansion.

The laser plasma interaction is describing the laser energy coupling to plasma, the competition between plasma heating and electron and ion acceleration, the competition between the diffusive and kinetic energy transport mechanisms, the homogeneity of energy deposition and control of unavoidable nonlinear effects, proposing new methods of plasma and target diagnostics.

Solid-state physics provides a detailed knowledge of the target material properties under extreme pressures and temperatures typical of ICF. The velocities of shocks propagating through the target, the modifications of the material state in the shock, transitions between the fuel and ablator, mixing of materials are of a great importance for the dynamics and the stability of the target performance.

Nuclear physics is the basis of ICF providing the rates for basic fusion reactions, but it is also very important for development of efficient diagnostic methods in integrated experiments where the

extremely high density of the imploded core makes it difficult to use the optical and x-ray diagnostics, which are much better developed.

All physical models mentioned above are realized as numerical codes. Rapid progresses in applied mathematics and computing allowed combining different physical models and making them operate together.

The code used for target design and analysis of experiments is a radiation-hydrodynamics code based on the following assumptions: the plasma forms a single, quasi neutral fluid, where electrons and ions are in Local Thermal Equilibrium (LTE), with different temperatures. Heat conductivities and ion-electron equilibration rates are provided by coulombian transport theory. A specificity of ICF modelling is the use of a tunable limitation of the electron heat flux. The propagation and absorption of the laser light is treated by a ray-tracing method, under the assumption of geometrical optics. Non thermal particles, as photons or burn products are accounted for by means of various models, going from diffusion to full kinetics. All material properties as pressure or plasma emissivity are usually calculated at LTE and tabulated. In recent implementations, a package for computing magnetic fields, and a non-local heat conduction package complement this standard model.

Such codes are developed by the academic community in Europe (DUED, MULTI, CHIC) [36, 43, 70, 46] and in the USA (LILAC, DRACO, CRASH), and tested by comparison with experiments. Moreover, many numerical models of experimental diagnostics have been developed. One observes a rapid progress last 10-15 years in agreement between the experimental data and the results of numerical simulations.

However, in spite of significant improvements, the predictive capabilities of theoretical and numerical models remain questionable. This is related to both the insufficient precision of some semi-empirical models and the incompatibility of physical processes on completely different spatial and temporal scales. The main challenge for the next period is to develop new models describing a micro-physics on the hydrodynamic scale and to reduce the number of empirical parameters. Another issue concerns the robustness and productivity of codes. All above mentioned improvements will require efficient methods of high performance computing in order to enable reliable integrated simulations.

## **2.3 Long-term programme in computational ICF**

The major objective of the theoretical and numerical developments in future 10-15 years is to provide predictive, integrated simulations of ICF experiments from the laser pulse focusing on the target to the energy release and target expansion.

Although some of the physical uncertainties may be circumvented by experimental tuning, some models implemented in the code present a known inability to deal with the situation encountered in ICF. This occurs specifically when kinetic effects appear on the hydrodynamic scale. A classic example is the heat conduction. However, full kinetic simulations of an ICF implosion are completely out of scope and probably of little use, and simplified models must be implemented in the design code, benchmarked against detailed kinetic codes, and validated using analytical experiments.

Having in mind the complexity of the problem and the enormous difference in the scale, one would need a specialized center for the ICF theory and numerical modeling. The main role of this center is to create and to maintain a computer platform that will host the suite of mutually compatible numerical codes. These codes, describing different facets of the physics, should be able to communicate between them, to be accessible to the developers and to the users in an efficient secure and stable environment.

According to the present level of development, one can think of the following constituting elements of such a platform:

- hydrodynamic 1D/2D/3D ALE (Arbitrary Lagrangian-Eulerian) code for target design, stability studies, prevision and interpretation of experiments. The code must include a MHD package and transport of non thermal particles.
- Kinetic code describing the energy transport in plasma by non-thermal and energetic electrons.
- Simplified electromagnetic code describing the laser beams propagation and energy deposition in plasma.
- Electromagnetic code describing the laser beams transport and nonlinear laser plasma coupling.
- Databases and associated codes describing material properties.
- Kinetic code describing the fusion reactions and the energy transport in plasma by the fusion products.
- modules describing the plasma diagnostics (active – radiography, and passive – self-emission) providing the data ready for comparison with experiments.
- codes describing the interaction chamber environments due to the laser target interaction (generation of the electromagnetic pulse and activation of the diagnostics).
- And, more specifically dedicated to FI studies.
- Kinetic code describing the fast electron and ion generation in solid targets.
- Full kinetic code describing the relativistic laser target interaction detailed studies of laser plasma interaction and secondary sources of x-ray radiation and energetic particles.

## **2.4 Near term scientific program**

### **2.4.1 Laser plasma interaction**

In the context of laser interaction with under-dense fusion-relevant plasmas, the understanding of the mechanisms responsible for the nonlinear saturation of parametric instabilities – especially the two scattering instabilities SRS and SBS – is an important goal. Both instabilities involve excitation of longitudinal plasma waves, which can be easily excited to high amplitudes, up to nonlinear saturation, at laser and plasma parameters corresponding to fusion-relevant conditions. In particular, one should be able to predict the absorption efficiency and the repartition of the absorbed energy between the thermal and energetic electrons. The objective is to develop a simplified predictive LPI model that can be incorporated in the hydrodynamic code.

The obliquely propagating beams in the PDD scheme may induce nonlinear processes on a more significant level than the standard beams at normal incidence. The issues of parametric instabilities and cross beam transfer need to be studied. Moreover, the numerical schemes describing the laser plasma interaction need to be developed and coupled to the radiation hydrodynamic codes.

### 2.4.2 Plasma kinetics

In SI, the intensity of the ignition spike varies in the range  $3 \times 10^{15} - 10^{16}$  W/cm<sup>2</sup>, the exact value depending on the target design and the required ITF. At these values, energetic electrons are likely to be produced in the blow off plasma of the target, especially if the highest part of this range must be used. In the traditional central hot spot ignition scheme, hot electrons lead to fuel preheating and lower compression. In shock ignition, hot electrons accelerated during the spike could be beneficial provided their range was smaller than areal density the target has acquired at this time. Based on this observation, several publications suggested electron driven Shock Ignition as an alternative to the classical hydrodynamic approach [40, 69]. These issues need to be described theoretically and numerically and investigated in specially designed experiments.

Magnetic fields become one of important issues in FI both providing more flexibility and control in the energy transport and guiding of electron beams. They could also affect the energy and angular distribution of the beam. Therefore, methods for engineering externally produced and/or self-generated magnetic fields need being investigated. This requires both the inclusion of magnetic fields in simulations and robust diagnostics of magnetic fields in experiments.

Having in mind the possibility of using of energetic ions in the fast ignition scheme, methods for efficient ion acceleration and the control of their angular distribution and energy spectrum need to be developed.

### 2.4.3 Hydrodynamics

Stability of shell implosion [41] is the major preoccupation of all inertial confinement fusion schemes. By imploding thicker targets at lower velocity, shock ignition is naturally less prone to hydro instabilities. However, the growth of target perturbations needs to be appropriately modeled. In particular, the studies of sensitivities of the fusion yield with respect to low modes, high modes non-uniformities, de-centering target need to be undertaken. This includes the analysis and the control of the target perturbations at the outer and inner surfaces, and the control and reduction of the laser intensity fluctuations including the spatial and temporal smoothing and the design of the laser intensity temporal profile. These theoretical and numerical studies need to be compared to the experiments and in the planar and converging geometries. The result will be a set of technical requirements on the target surface roughness (internal, external), target positioning, laser imprint (may be expressed in terms of laser bandwidth), laser pointing, beam to beam imbalance, pulse shape tolerances, etc.

### 2.4.4 Atomic physics

The hydrodynamic simulations of the ICF targets require accurate basic data – equations of state (EOS), plasma emissivity, and transport coefficients [36]. Theoretical models providing these data have to be improved, especially at high density, and validated in well-diagnosed experiments.

Understanding the early stages of inertial fusion also requires a good knowledge of the Warm Dense Matter (WDM) state; experimental evidences have to be collected to validate underlying hypothesis and models currently used in simulations. Laser-accelerated particle (especially proton) sources can



be used to isochorically heat a solid target and thus produce WDM. This will open the route towards accurate measurements of ion stopping powers and the fusion reaction rates in high temperature, high density plasmas and validation of numerical tools.

#### 2.4.5 Code developments

The hydrocode will be the workhorse of the proposed programme. Besides the long term developments detailed in sec. 2.3, significant improvements are required in the next to come years in order to fulfill the requirements of the experimental programme.

- Productivity: parametric studies in 2 dimensions of space require restitution times shorter than a few hours, which is achievable by means of mass parallelization of the code using state of the art computer science.
- Availability: cooperating teams must have access to simulation tools and numerical databases.
- LMJ-Petal relevance. Preprocessors must provide a numerical model of the facility (geometry, focusing, smoothing, bandwidth, pulse shapes). Post processors must contain the detailed description of actual LMJ-Petal diagnostics in order to reconstitute the experimental measurements in convolution mode.
- Robustness and Reliability: Causes for code failure must be reduced. This supposes the development of ALE methods and algorithms for mesh management, as well as indicators for code convergence and consistency of input.
- Predictivity and accuracy. The models for the transport of non thermal or non local electrons presently included in codes will be improved. In particular, effects of electron- electron collisions and low frequency plasma fields must be taken into account more accurately. Such models, operating at the hydrodynamic scale, will be benchmarked against Vlasov-Maxwell-Fokker-Planck calculations.

This latter point is mainly an issue in transport theory and computational physics. Conversely, the four former ones require an important effort in the fields of software engineering and computer science, for which the European ICF community has only limited capabilities. Moreover, considering the constant concern of code validation, the code must be viewed as the receptacle of the knowledge we gain from experiments. This knowledge must be shared within our co-working ICF community and the development efforts coordinated. Simulations using the validated code will in turn enhance the credibility of further proposals for experiments.

These observations form the rationale for the construction of a common, community managed ICF computational platform. The proposal of CEA to use TGC (*Tres Grand Calculateur*) for this purpose offers numerous advantages: huge CPU and storage resources, security of software and databases, scientific and technical support from CEA engineers.

### **3. Experimental goals**

#### **3.1 Shock ignition as the basis of consolidation of ICF research in Europe**

Upon the present status, shock ignition might be one of the solutions that can demonstrate a high gain performance on NIF and on LMJ. These facilities are capable of providing the required laser energy (400 – 600 kJ) and power (200 – 400 TW) with minor facility adjustments. However, at the present moment, neither all aspects of physics behind the shock ignition scheme nor technological issues are fully addressed. Although the final demonstration of ignition and burn can be performed only with LMJ and NIF, the key issues need to be addressed theoretically and demonstrated experimentally also with smaller laser facilities available in Europe, the USA and Japan.

A Shock Ignition programme in which Europe could take the leadership is complementary to the American programme based on the indirect and direct-drive conventional central hot spot schemes and the Japanese programme on the electron fast ignition. These three programmes have many common issues which implies a tight collaboration. That means in particular, that some experiments related to fast ignition may be also fielded to the LMJ-PETAL facility. Thus the programme should provide opportunities for conducting experiments in interest for all alternative schemes, while retaining the priority for the shock ignition.

#### **3.2 Parameter domain for the experimental research**

Shock ignition substantially relaxes the requirement for high implosion velocities (350 - 400 km/s) needed for the central spark/ignition scheme since the roles of drive laser for fuel compression and ignition are separated. A lower implosion velocity allows adopting a lower in-flight-aspect-ratio target, leading to mitigation of hydrodynamic instabilities at the implosion and stagnation phases. Typical designs predict ignition of targets imploded at less than 280 km/s with a spike intensity lower than 4 PW/cm<sup>2</sup>, driving an ablation pressure of 200-300 Mb. Increasing the spike intensity will increase the ITF. This will be probably necessary on LMJ, where the irradiation conditions (arrangement of beams, smoothing, laser stability and contrast) are likely to degrade the implosion performances as compared to 1D, and raise the ignition threshold. Higher spike intensities, up to 10<sup>16</sup> W/cm<sup>2</sup> are considered therefore. In this range of irradiance, the shock ignition scheme is prone to parametric instabilities resulting in laser scattering, filamentation, and hot electron generation.

#### **3.3 Physical issues of the shock ignition scheme**

The physical problems related to the shock ignition scheme can be unfolded into several research directions as follows:

### 3.3.1 Laser plasma interaction physics

The success of shock ignition requires a predictive knowledge of laser-plasma interaction in conditions which have been seldom encountered in past experiments: intensity of several PW/cm<sup>2</sup>, long scale plasmas, durations of a few hundreds of ps.

NIF and LMJ have been constructed to dedicate for the indirect drive scheme where numerous beamlets are bundled in two opposing clusters. To attain the highly uniform drive pressure required for direct drive implosions, these beams need to be adequately adjusted by way of re-direction, re-pointing, smoothing and de-focusing: the polar direct drive (PDD). Obliquely propagating beams in PDD may induce nonlinear processes on a more significant level than what is observed at normal incidence. Because of parametric instabilities, not only hot electrons are likely to be generated but also a significant fraction of incident laser could be reflected, thus affecting uniformity of target illumination via cross beam conversion and filamentation. Issues involved in the laser-plasma interactions will be:

- Investigation of dominant processes over laser plasma interactions.
- Investigation of cross beam transfer.
- Growth and mitigation of filamentation.
- Local magnetic field generation via filamentation.
- Hot electron generation and correlation with laser plasma interactions.

To accomplish these studies, time-resolved spectroscopy of scattered light and calorimetric detection of drive laser will be important. Quantitative x-ray spectroscopy to infer the hot electron distribution will be also needed.

In the conventional central hotspot ignition scheme, hot electrons are of concern due to preheat of the main fuel, resulting in degraded compression. By contrast, in shock ignition, hot electrons are potentially beneficial since they may improve the transport of energy and enhance the shock uniformity. These conjectures need to be clarified theoretically and numerically, and validated in specially designed experiments. Issues involved in the role of hot electrons specifically generated with the spike will be listed, similar to the case of hot electrons in the fast ignition scheme, as:

- Hot electron distribution function and corresponding transfer efficiency from the spike pulse to hot electrons
- Angular spread of hot electron propagation
- Energy coupling efficiency of hot electrons to the compressed fuel and hot spark

To accomplish these studies, time-resolved spectroscopy for x-ray emission from tracers embedded in the compressed fuel and the hot spark will be needed. In addition, x-ray monochromatic imager adjusted to the tracer emission will provide energy coupling process and efficiency.

### 3.3.2 Polar Direct Drive: low mode non-uniformities

Independently of the ignition process, high nuclear gain requires fuel compression to high areal densities. Low mode asymmetries of the drive cause non uniformities of the velocity field which grow with shell convergence, thus endangering the final compression. The classic uniformity requirements of conventional ignition also apply to shock ignition. Despite the non-symmetrical beam arrangement at NIF or LMJ facilities, a nearly uniform irradiation can be achieved by repointing the beams (PDD). Calculations suggest that the PDD arrangement produces sufficient drive uniformity to achieve the required level of compression.

The achievement of a Polar Direct Drive implosion platform on LMJ is an essential milestone on the path to ignition. The tuning of Polar Drive implosions may be achieved using room temperature surrogate targets with measurements of the shell symmetry at successive phases of the implosion. Experimental verification is, however, required before a compelling case can be made for full-scale compression experiments. A series of experiments need to be performed in advance at the existing intermediate scale facilities such as Orion, Omega and Gekko. The issues to be clarified will be:

- Check code predictions with reduced scale implosion where a P2-dominated irradiation pattern produces a prolate/oblate compressed core. Orion may be well suited for this purpose.
- Effects of oblique incidence and beam crossing.
- Influence of target convergence on irradiation uniformity for a static illumination (i.e., time-dependent uniformity).
- Experiments with beam zooming and/or dynamical pointing.

For these experiments, the observation of hydrodynamic motion of spherical target by means of time-resolved 2D x-ray imaging will be a baseline diagnostic method. In addition, x-ray imager for self-emission from tracers or dopants will be useful.

### 3.3.3 High mode non-uniformities

Any small scale imperfection of the target (roughness, inhomogeneities), as well as high frequency structure of focal spots (speckles), seed perturbations that are subject to further amplification under hydrodynamic instabilities. The Rayleigh-Taylor growth may result in shell break-up at time of acceleration and pollution of the hotspot by cold material at final convergence. Different approaches exist that circumvent the consequences of instabilities: by design (larger shell aspect ratio, lower velocity, larger fuel mass), by technology (surface finish, beam smoothing), by mitigation (control of adiabat gradients in the ablator). In the specific case of shock ignition, the presence of cold material in the hot spot requires a higher power in the ignition spike than in the “clean” case. A correct understanding of hydro instabilities is therefore essential in trading off risks and costs of an IFE design, and, in the case of LMJ, in the choice of the optimal operating point in the energy-power diagram of this facility.

Issues involved in the hydrodynamic instabilities are:

- Control of the ablative Rayleigh-Taylor (RT) instability.
- Growth of surface perturbations by Richtmyer-Meshkov (RM) instability.

- Effect of laser imprint and target non-uniformities on RT and RM instabilities.
- Impact of a spike shock on instability growth at deceleration.
- Effect of nonlocal electron and radiative transport on instability growth.
- Laser beam energy exchange in a plasma.
- Role of self-generated magnetic fields generated by hydro-instabilities in the electron energy transport.
- Laser imprint mitigation by means of plasma and radiative smoothing techniques.

Advanced diagnostics for measurements of shell uniformity will be needed. Time-resolved x-ray shadowgraph with an intense, external x-ray source will be needed as a baseline diagnostics method. Time-resolved spectroscopy for x-ray emission from a compressed fuel and a hot spark region will be also needed to derive plasma parameters. In addition, x-ray monochromatic imager adjusted to an x-ray tracer line will provide energy coupling process and efficiency. At peak compression, Compton radiography will enable imaging of the cold fuel.

### 3.3.4 Shock generation and propagation

Ignition occurs at central pressures of a few hundred Gbar. Numerical simulations indicate that the initial shock generated with an ablation pressure exceeding 300 Mbar is needed, and corresponding predictions indicate a possibility of achieving such a high pressure with a spike intensity of  $\sim 4 \cdot 10^{15} - 10^{16} \text{ W/cm}^2$ . However, most experiments ever performed verified the ablation pressures of less than 100 Mbar at lower intensities. Hence, the leading goal of this part of the programme is to **achieve an ablation pressure of 300 Mbar** using lasers.

Issues involved in generating the strong shock will be folded as:

- Experimental verification of ablation pressure exceeding 300 Mbar.
- Scaling of ablation pressure on laser parameters such as the intensity temporal profile and the laser wavelength.
- Validation of a “bipolar” drive of the shock spike.
- Shock propagation behavior through inhomogeneous imploding materials.
- Shock collision and stability of distorted shock fronts.
- Multi-dimensional uniformity of shock waves.
- Side-on observation of shock propagation (1D in space and 1D in time).
- Face-on observation of shock propagation (2D in space and 1D in time).
- Amplification and stability of converging shock in spherical geometry.

Since only planar experiments will be achievable during the first phase of LMJ, a particular attention should be paid to the formation of spatially uniform (i.e., planar) shock for all issues above. Previous experiments indicate that pressure dissipation to the lateral direction may result in deleterious misunderstanding of shock behavior.

### 3.4 Target development and manufacturing

The study of the above mentioned physical issues needs to be supported by the development of a substantial capability in target manufacturing and metrology. Targets of various geometries (planar, conical, cylindrical, spherical) and compositions (including a wide variety of tracer layers, foam layers) are considered in the proposed programme.

The existing chart of conducting the academic experiments on the CEA installations implies that the laser shots will be provided free of charge, on the basis of the peer-review of proposals by the international selection committee. However, the targets and diagnostics are on the charge of the group that is proposing the experiment. Having in mind the increasing complexity of the target fabrication and the cost, it is necessary for the IFE academic community in Europe to develop its own capacities of target fabrication, including the targets for future integrated experiments.

### 3.5 Target geometry

Addressing all such experimental issues requires performing experiments both in planar geometry and in converging geometry. Planar experiment is an indispensable test-bed for understanding the physics issues due to simplicity and full-access for diagnostics. Some issues, however, intrinsically require a converging geometry. Cylindrical experiments may be considered since they address the physics issues while maintaining a privileged axis for access of diagnostics. The “cylindrical” and “cone” implosion platforms could be also developed in order to provide benchmark data for radiation hydrodynamic codes. The planar and spherical targets with low dense foam absorbers, including foams doped by high-Z elements, can be used for laser energy deposition smoothing [48] as well as for inhibiting the development of hydrodynamic instabilities in double ablation fronts [49,50].

In planar geometry:

- Experiments on competition of RM & RT under various imposed modulations; studies of the effect of double ablation fronts on the RT&RM instabilities inhibition in experiments with ablator doped by high-Z elements.
- Studies of laser plasma interaction under the shock ignition conditions such as stimulated Raman and Brillouin scatterings, filamentation and two-plasmon decay.
- Quantitative studies of thermal smoothing by using modulated focal spot with a given wavelength as well as thermal smoothing in a low density foam absorber.
- Quantitative studies of transport coefficients on the different level of laser intensity.
- Effects of de-localized absorption on heat transport ablation pressure.
- Magnetic fields at high intensities in expanding plasma. Proton radiography will be useful to see magnetic field formation.
- Efficiency of fast electron generation and the control of angular divergence and the energy distributions; studies of fast electron contribution to ablation and preheating.
- Fast ion generation in high intensity laser plasma interactions, optimization of the conversion efficiency and the energy distribution.



In spherical geometry:

- Demonstration of code control of Polar Drive implosions.
- Optimization of polar drive implosions of warm targets.
- Measurements of bang time, the first shock and the spike shock pressures.
- Measurements of RT instability growth by means of neutron imaging and/or hard x-ray backlighting.
- Effect of RM instability caused by the shock spike on hot spark formation.
- Impact of parametric instabilities on the laser energy absorption and fast electron generation, and fast electron preheating on shock ignition conditions.
- Effect of shell areal density and spike launching time on hot electron penetration and shock formation.
- Comparison between tight and uniform illuminations for shock formation.
- Evaluation of the feasibility of bipolar illumination for the shock spike.
- Studies of the possibilities to improve the stability of spherical target implosion by using the foam absorber, including the absorbers doped with high-Z elements.

The “keyhole” targets developed on NIF have been extremely useful for many measurements including shock timing, early time drive asymmetry etc. Similar developments will be needed on the LMJ-PETAL facility.

### 3.6 Diagnostics

Experimental IFE program could be efficient only if it is supported by a large number of high performance diagnostics installed in the PETAL LMJ interaction chamber and available on request. Here we present a list of diagnostic instruments needed for the ICF experiments.

**Table 1:** List of diagnostic technology and instruments needed for LMJ-PETAL experiments

	@CEA		detection obj.	range	resolution	purpose	remarks
<b>Particle diagnostics</b>							
<b>Spectrom- eter</b>		Thomson Parabola ion analyzer	ions	0.1-100 keV	$\varepsilon/\delta\varepsilon=10$	ion constituents	
		filtered track detector (CR39, RF)	protons	0.5-100 MeV	$\delta\varepsilon=1$ MeV	energy distribution	
	<b>NA</b>	electron spectrometer	electrons	0.1-10 MeV	$\varepsilon/\delta\varepsilon=10$	energy distribution	multi-angular setting is preferable
	<b>NA</b>	positron spectrometer	positrons	0.1-10 MeV	$\varepsilon/\delta\varepsilon=10$	energy distribution	multi-angular setting is preferable

	@CEA		detection obj.	range	resolution	purpose	remarks
	NA	proton spectrometer (B-diffraction)	protons	0.1-20 MeV	$\varepsilon/\delta\varepsilon=10$	pusher $\rho R$	
	A	$\alpha$ -particle spectrometer	$\alpha$ -particles	0.1-10 MeV	$\varepsilon/\delta\varepsilon=10$	ion temp., $\rho R$	
imager	A	proton track imager (CR-39, radiochromic films)	protons	0.1-100 MeV	$\delta\varepsilon=1$ MeV	proton radiography	
neutron TOF	A	neutron detector (current mode)	neutrons	1-20 MeV	$\varepsilon/\delta\varepsilon=100$	ion temp., $\rho R$	
	A	neutron detector array (single hit mode)	neutrons	1-20 MeV	$\varepsilon/\delta\varepsilon=100$	ion temp., $\rho R$	over 1000ch is preferable
neutron yield	A	Ag counter	neutrons	-	-	absolute n-yield	hard to exclude photo-nuclear n
	A	bubble detector	neutrons	-	-	absolute n-yield	hard to exclude photo-nuclear n
neutron generation	A	dYn/dt measurement	neutrons	dYn/dt>1e4	dt<10 ps	burn history	
neutron imager	A	neutron source image	Nuclear fusion products	-	-	burn region	
<b>X-ray diagnostics</b>							
Spectrom- eter	NA	Laue-type x-ray spectrometer	K $\alpha$ lines	10-100 keV	$\varepsilon/\delta\varepsilon=10-50$	Conversion efficiency for hot electrons	
	A	crystal spectrometer	resonance line, K $\alpha$ line	1-20 keV	$\varepsilon/\delta\varepsilon=100-500$	Te, density	
	A	DANTE-type soft x-ray detectors	x-ray conversion for drive	0.1-3 keV	$\varepsilon/\delta\varepsilon=1$	Tr	
imager	A	monochromatic x-imager	resonance line, K $\alpha$ line	1-20 keV	$\varepsilon/\delta\varepsilon=100$	Hydrodynamics	
	A	monochromatic x-framing imager	resonance line, K $\alpha$ line	1-20 keV	$\varepsilon/\delta\varepsilon=100$ , dt<50ps	Hydrodynamics	
	A	x-ray framing camera (w/ filter)	wide range of x-ray	0.1-10 keV	$\varepsilon/\delta\varepsilon=1$	hydrodynamics	
	A	x-ray streak camera (w/ filter)	wide range of x-ray	0.1-10 keV	$\varepsilon/\delta\varepsilon=1$	Hydrodynamics	
	A	x-ray pinhole camera (w/ filter)	wide range of x-ray	0.1-10 keV	$\varepsilon/\delta\varepsilon=1$	Hydrodynamics	

	@CEA		detection obj.	range	resolution	purpose	remarks
	A	x-ray tele- microscope	wide range of x-ray	0.1-10 keV	$\varepsilon/\delta\varepsilon=10$	Hydrodyna- mics	
<b>Backlight- ting</b>	NA	x-ray source	quasi- mono. source	1-20 keV	$\varepsilon/\delta\varepsilon=100$	Hydrodyna- mics	
<b>Optical diagnostics</b>							
<b>Spectrome- ter</b>	A	time-resolved optical spectrograph	drive laser	0.5-3 eV	$\varepsilon/\delta\varepsilon=1000$	SRS, SBS, interactions	
<b>imager</b>	A	optical interferometer	optical probe			Hydrodyna- mics	
	A	optical shadowgraphy	optical probe			Hydrodyna- mics	
	A	VISAR	temporal evolution of int.			shock breakout	
<b>calorimetric</b>	A	optical calorimeter	drive laser scattering			absorption, scattering	

## 4. Preparatory plans for LMJ-PETAL: work at intermediate scale facilities and numerical modelling development

### 4.1 General purposes of the LMJ-PETAL academic IFE program

In order to effectively exploit the capabilities of LMJ-PETAL within a reasonable time-scale and with available resources a consolidation of all HEDP programmes is necessary. Moreover a large amount of work on small and intermediate scale laser facilities is needed in order to prepare for the experiments at LMJ-PETAL.

Assuming that the polar beam geometry will be available on LMJ, the common point of all academic ICF research will be the development of the PDD irradiation platform. After the successful demonstration of the PDD implosion technique various approaches to the fuel ignition can be studied. The integrated experiments with various ignition schemes will be considered depending on their maturity.

At the initial stage most of the work will be devoted to the development of diagnostics. The general diagnostic requirements for all academic access experiments on LMJ-PETAL are presented in the special section of this document, however, the preparatory work related to implementation of the specific ICF diagnostics is discussed here.

The experimental programme on the LMJ-PETAL should be supported by two complementary programmes: the preparatory experimental programme on small and intermediate scale laser-

facilities and the development of the numerical tools for the experiment modeling and diagnostic simulations. These developments are important from the standpoint of carrying out integrated modeling of relevant experiments and interpretation of the experimental data. Modeling techniques for the implosion phase are quite well developed. However, much less work has been performed in relation to the ignitor shock pulse. Furthermore, the polar-direct drive relies upon the smoothing of the laser energy deposition by the electron conduction and radiation transport that are poorly treated in existing radiation hydrodynamic codes. Therefore, a special attention is necessary for rendering our simulation capabilities adequate to address the expected physical effects, both in terms of code development and code benchmarking on existing and new experiments.

In what follows we consider four axes of experimental activity: i) SI related preparatory experiments, ii) PDD preparatory experiments, iii) code-benchmarking experiments, iv) FI preparatory experiments.

## **4.2 Preparatory shock-ignition studies at small and intermediate scale facilities**

The three major aspects of physics related to SI that will require sub-scale experimental development work are:

- Laser launching of strong shock waves of a strength relevance to the ignitor pulse.
- Generation of suprathermal electrons and their use in supporting the ignitor shock.
- Diagnostics of the shock collision between the rebound shock and the ignitor shock.

### **4.2.1 Laser launching of shock waves of a strength relevant to the ignition**

Only a few experiments have been so far performed that are of direct relevance to the ignitor shock pulse, [67,62]. In order to support the project of SI on LMJ, it will be necessary to perform further experiments, particularly examining the scaling of shock pressure with laser intensity and wavelength at relevant intensities of  $1 - 10 \text{ PW/cm}^2$ . Experiments employing standard shock wave diagnostics such as VISAR and SOP are mandated, however, although these diagnostics are long-time established (and already planned for LMJ-PETAL) performing experiments at such high intensities can introduce new problems, particularly in terms of the preheating encountered ahead of the shock waves and the effect that this can have on the viability of the data [65].

On this basis it is proposed firstly that VISAR experiments should be performed at facilities where relevant shock-wave intensities might be generated (e.g. ILE Osaka and AWE Orion) and that effort is invested to optimize this technique at LMJ scale.

### **4.2.2 Generation of suprathermal electrons and their use in supporting the ignitor shock**

At reactor scale (fuel mass larger than 1. mg) ignition requires spike intensities of a few  $\text{PW/cm}^2$ . At these intensities, suprathermal electrons, if any, are expected to have only second order effects on shock formation. This is the regime of shock-assisted central ignition.

At lower scales, or for degraded implosions, one must consider higher spike intensities and the possibility that a significant part of the laser energy is transferred to hot electrons. From the

observation that hot electrons could be more efficient than thermal transport to form the ablation pressure comes the novel, though speculative, concept of electron driven shock ignition.

Whilst some experiments have been performed in this area [51] they are few in number.

Far more work is required to attain a predictive capability that will enable the proper integration of suprathermal electron production and transport in the driving of SI shocks [55]. Such experiments must principally aim at benchmarking the emerging kinetic and hybrid codes that are being used to tackle this problem [57,58].

In order to have a detailed account of the hot electron component of the shock drive, it is necessary to consider both the initial velocity distribution of the injected electrons as well as their transport in the dense plasma. These are all difficult features to diagnose experimentally and an innovative experimental campaign is mandated to effectively characterize the behavior in sufficient detail that code-development work may be supported effectively.

### 4.2.3 Shock collision

Another unique feature of SI is the reliance on the collision between the inward-going ignitor shock and the rebounding shock to provide the necessary final strength of the ignitor shock wave. Such physics cannot be probed using neither a conventional VISAR/SOP methodology nor the now familiar keyhole technique [65], due to the fact that it occurs after the first shock has rebounded off the center of the capsule.

One possible approach for the investigation of such physics might be to employ streaked x-ray radiography using a backlighting source or radiography based on self-emission, similar to that shown in Fig. 4. This shows the interaction of FIREX with an imploded capsule at GekkoXII, and it is possible to discriminate the emission associated with the short pulse interaction from that caused by the final stagnation of the capsule [59].

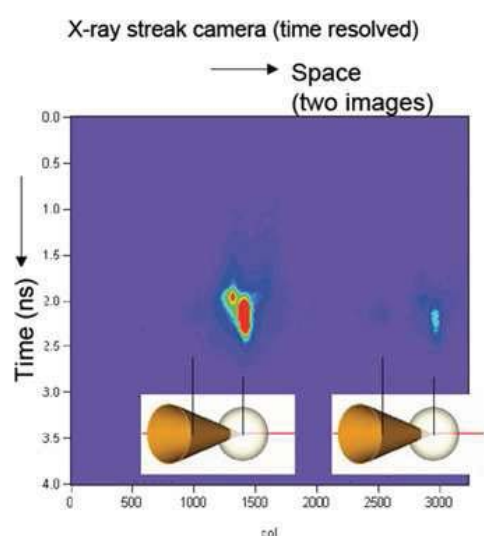


**Figure 4:** Data from two shots on a Fast Ignition preparatory experiment conducted at FIREX; on the left the streaked x-ray emission from a target imploded with the heater beam turned-on is shown. On the right the emission from a similar target imploded without use of the heater beam is shown for comparison [59]

It is certainly worth considering whether a similar diagnostic could be fielded to examine the interaction of the ignitor shock and re-bound shock in SI, possibly in combination with a fluorescent dopant in the shell. Such a diagnostic scheme would test the limits of the x-ray microscopes (XRM) and x-ray streak cameras (XSCs) currently proposed for LMJ-PETAL, and therefore further work should be commissioned to determine whether the existing specification will be sufficient to perform such a diagnostic function.

Another possibility that might offer some potential would be to consider the use of non-spatially resolved x-ray diagnostics (or temporal variation in emission from XSC and XRM that is not sufficiently resolved to pick-out the shock collision in space). These might render the shock-collision apparent by an overall enhancement in emission from the stagnating plasma even if it is not possible to spatially resolve the collision.

Work at small and intermediate-scale facilities should focus upon improving the capability of existing diagnostics of this type to resolve such strong shock collisions. A planar colliding shock experiment might, for instance, provide a suitable test bed for such a diagnostic.

### **4.3 Preparatory fast-ignition studies at small and intermediate scale facilities**

The fundamental studies related to fast ignition (FI) have reached a certain maturity, however, they are so far mostly based on experiments carried out using solid targets and laser beams with energy limited to a few hundred Joules and duration less than a few picoseconds. Only recently sub-PW and PW-class lasers became available for performing integrated experiments of target compression/implosion and relativistic electron beam energy transport. The scalability to full-scale FI conditions of the existent data is an open question.

The experimental strategy for FI feasibility assessment must be twofold: on one hand, performing integrated experiments with progressively rising laser energy and power and with well-defined conditions, and, on the other hand, continuing the smaller scale and simpler experiments that are sufficiently precise and reproducible to benchmark codes and models with a predictive capability for the full-scale conditions.

Some bottleneck questions are still unanswered: the energy transfer from intense laser beams to the deuterium-tritium core must be optimized, in particular by forcing the fast electron collimation over the  $\sim 100\ \mu\text{m}$  stand-off distance between the cone-tip and the dense core. Magnetic beam collimation using either externally imposed or self-generated magnetic fields is a promising approach. Its efficiency has been explored in numerical simulations [68]. It is concluded that the electron beam can be radially confined in an appropriate external longitudinal magnetic field. The employment of an external magnetic field increases also the fusion yield in the FI scheme [66]. The magnetic field shape and amplitude can be optimized to improve the energy gain from the fusion reactions. One must also refer here on a new design of the ICF target with magnetic collimation proposed recently [63]. Some proof-of-principle experiments of such magnetic collimation have been performed for LULI, in a first step, and then at GekkoXII-LFEX facilities.

The integrated experiments with a PW interaction beam will be continued on the OmegaEP facility using pulses with the 10 ps duration required for FI. They constitute a preparatory step for future



experiments on NIF-ARC and LMJ-PETAL. The magnetic field generation can also be further optimized by an appropriate capacitor-coil target design and by using a laser beam of higher energy, that will be available at LMJ.

The inherent fast electron beam generation and transport physics are among the most actively studied and challenging topics currently being investigated within relativistic plasma physics. The intensity of the laser PETAL will be among the highest for lasers capable of delivering energies in the kJ range in the time scale of less than 10 ps. There are exciting possibilities of exploring magnetically-assisted electron beam transport by coupling LMJ, for both target compression and magnetic field generation, to PETAL, for the electron beam injection.

Besides electron transport, the magnetized fusion in general is foreseen as a promising path towards a high gain fusion yield, mostly after the successful experimental demonstration of the magnetic field amplification in spherical target implosions [54].

#### **4.4 Preparatory Polar Direct Drive studies at small and intermediate scale facilities**

Sub-scale PDD studies will concentrate principally upon the following three areas:

- Pressure smoothing and lateral electron conduction.
- Symmetry and mix diagnostics.
- Control of compressed core geometry and verification of code predictions.

##### **4.4.1 Pressure smoothing and lateral electron conduction**

There have been a few integrated polar-direct-drive experiments [60]. Concerning experiments that can provide more specific benchmarks for the lateral electron conduction and pressure smoothing there is little existing data. The development of non-integrated experimental platforms to investigate this issue is vital. Inferring the accuracy of electron and radiation transport modeling at or near the ablation surface using the results of integrated implosion experiments is probably not feasible. Planar experiments to isolate the relevant physics are called for, and this will require a substantial effort on behalf of the community to develop suitable experimental concepts and to field them at the existing smaller facilities.

##### **4.4.2 Symmetry diagnostics**

Symmetry diagnostics concern the fuel mix and the overall implosion uniformity. In the case of PDD and SI, these topics must be considered separately since a poor symmetry is both a greater risk in PDD and a greater threat in SI even where it does not lead to extensive mixing between the adjacent regions of the fuel capsule.

The bulk of the work required in this area on small and intermediate scale facilities pertains to diagnostic development. A suite of diagnostics comparable to that which already exists on NIF would be ideal for the purpose of diagnosing symmetry on LMJ-PETAL. These diagnostics are including in particular, the “key hole” VISAR instrument and the Compton radiography. The expertise for developing such a comprehensive set of diagnostics does not currently exist in Europe. Therefore the

immediate action in this area should be to identify which relevant diagnostics in the current NIF inventory can be replicated on LMJ-PETAL only after preparatory experiments at small and medium-scale facilities have been performed.

#### **4.4.3 Control of predicted core symmetry**

Since numerical simulations predict the success of Polar Drive implosions, it is essential to verify that code predictions are realized in simple implosion experiments. The Orion laser system features a 2 sided beam arrangement which produces a P2-dominated irradiation pattern on a sphere. Repointing Orion beams inwards (resp. outwards) will result in oblate (resp. prolate) cores in low convergence implosions. If available, Orion implosions using various beam repointing and measurements of core shape, will provide an essential tool to demonstrate the capability of codes to tune Polar Drive implosions.

## **5. Proposals for the first phase of LMJ-PETAL experiments**

For the first phase of the LMJ-PETAL operation with two LMJ quads and one PETAL beam the experiments will be performed in the planar geometry. In the context of ICF studies the priorities should be given for the following three experiments:

### **5.1 Strong shock excitation for the conditions relevant to the shock ignition scheme**

*Goal:* by using PETAL as an interaction beam and the LMJ beams for the plasma preparation and radiography perform an experiment on excitation of a strongest possible shock, aiming on the pressures of the order of 1 Gbar. This is of the primary interest for shock ignition but also in a more general sense for HEDP.

*Originality:* the use a high density layer to model a compressed shell, a possibility to attain a record ablation pressure. Preliminary experiments are ongoing on OMEGA in collaboration with the LLE team.

### **5.2 Laser plasma interaction in a long scale length plasma**

*Goal:* study the physics of laser plasma interaction and suprathermal electron generation under the conditions relevant for the shock ignition scheme. The plasma is prepared from a low density foam or aerogel with the LMJ beams (which can also be used for the radiography), and the uncompressed PETAL pulse provides the interaction beam.

*Originality:* assessment of the laser plasma interaction physics for the shock ignition conditions, the use of a special foam target with a prepared density profile. Direct measurement of fast electron characteristics.

### **5.3 Optimization of the ion acceleration for the ion fast ignition scheme**

*Goal:* optimization of the laser-ion energy conversion in the energy range of 10-20 MeV protons or 300-500 MeV carbons in PETAL beam interaction with specially designed targets. By controlling the target design and interaction conditions achieve the conversion efficiency more than 10% and to measure the angular and energy distribution of the fast ions.

*Originality:* use of low density foam or aerogel targets for optimization of the ion acceleration efficiency and the high energy PETAL beam for the efficient laser plasma coupling in the induced transparency regime. In the same experiment but with a denser target the physics of hole-boring can be investigated.

## References

- 1 K. Anderson *et al.*, Phys. Plasmas, **20**, 056312 (2013)
- 2 L. Antonelli *et al.*, Acta Technica **56**, T57 (2011)
- 3 S. D. Baton *et al.*, Phys. Rev. Lett. **108**, 195002 (2012)
- 4 S. Depierreux *et al.*, Phys. Rev. Lett. **102**, 195005 (2009)
- 5 S. Depierreux *et al.*, Phys. Plasmas **19**, 012705 (2012)
- 6 C. Goyon *et al.*, Phys. Rev. Lett. **111**, 235006 (2013)
- 7 S. Gus'kov *et al.*, Laser & Particle Beams, (2014)
- 8 M. Hohenberger and W. Theobald, LLE Review, p. 137, V. 131, April–June 2012, DOE/NA/28302-1064
- 9 J. A. Marozas, *et al.*, Bull. Amer. Physical Soc, **53** (2008)
- 10 L. J. Perkins *et al.*, Phys. Rev. Lett. **103**, 045004 (2009)
- 11 L. J. Perkins *et al.*, "On the Fielding of a High Gain, Shock-Ignited Target on the National Ignition Facility in the Near Term", Lawrence Livermore National Laboratory Technical Report, LLNL-TR-428513 (April 2010), website: <https://library-ext.llnl.gov>
- 12 L. J. Perkins *et al.*, "Development of a Polar Drive Shock Ignition Platform on the National Ignition Facility", LL Technical Report, LLNL-TR-432811 (May 2010), website: <https://library-ext.llnl.gov/>
- 13 W. Theobald *et al.*, Phys. Plasmas **15**, 056306 (2008)
- 14 W. Theobald *et al.*, Plasma Phys. Control. Fusion **51**, 124052 (2009)
- 15 W. Theobald *et al.*, Phys. Plasmas **19**, 102706 (2012)
- 16 M. Bailly-Grandvaux *et al.*, Forum ILP 2014, Orcières, France
- 17 F. Beg *et al.* IFSA 2013, Nara, Japan
- 18 P. Y. Chang *et al.*, Phys. Rev. Lett. **107**, 035006 (2011)
- 19 S. Fujioka *et al.*, Scientific Reports **3**, 1170 (2012)
- 20 B. M. Hegelich *et al.*, Nuclear Fusion **51**, 083011 (2011)
- 21 M. Hohenberger *et al.*, Phys. Plasmas **19**, 056306 (2012)
- 22 S. Kar *et al.*, Phys. Rev. Lett. **102**, 055001 (2009)
- 23 D. Jung *et al.*, New J. Phys. **15**, 023007 (2013)
- 24 N. Naumova *et al.*, Phys. Rev. Lett. **102**, 025002 (2009)
- 25 F. Pérez *et al.*, Phys. Rev. Lett. **104**, 085001 (2010)
- 26 F. Perez *et al.* Phys. Rev. Lett. **107**, 065004 (2011)
- 27 L. J. Perkins *et al.*, Phys. Plasmas **20**, 072708 (2013)
- 28 Y. Ping *et al.* Phys. Rev. Lett. **109**, 145006 (2012)
- 29 B. Ramakrishna *et al.* Phys. Rev. Lett. **105**, 135001 (2010)
- 30 J. J. Santos *et al.*, J. Plasma Phys. **79**, 429 (2013)
- 31 T. Schlegel *et al.*, Phys. Plasmas **16**, 083103 (2009)
- 32 R.H.H. Scott *et al.*, Phys. Rev. Lett. **109**, 015001(2012)
- 33 D. J. Strozzi *et al.*, Phys. Plasmas **19**, 072711 (2012)
- 34 W. Theobald *et al.*, submitted to Phys. Plasmas
- 35 B. Vauzour *et al.*, Phys. Rev. Lett. **109**, 255002 (2012)
- 36 S. Atzeni & J. Meyer-Ter-Vehn, The physics of inertial fusion, Oxford science publication
- 37 R. Betti *et al.*, Phys. Rev. Lett. **98**, 155001 (2007)

- 38 D. S. Clark *et al.*, Phys. Plasmas **20**, 056318 (2007)
- 40 S. Gus'kov *et al.*, Phys. Rev. Lett. **109**, 255004 (2012)
- 41 J. Lindl, Phys. Plasmas **2**, 3933 (2007)
- 42 P. H. Maire *et al.*, SIAM J. Sci. Comput. **29**, 1781 (2007)
- 43 R. Ramis, J. Meyer-ter-Vehn, J. Ramirez, Comp. Phys. Commun. **180**, 977 (2009)
- 44 X. Ribeyre *et al.*, Plasma Phys. Control. Fusion **51**, 015013 (2009)
- 45 V. A. Scherbakov, Sov. J. Plasma Phys. **9**, 240 (1983)
- 46 S.Yu. Gus'kov, N.V. Zmitrenko *et al.*, Plasma Phys. Control. Fusion **51**, 095001 (2009)
- 47 T. Collins *et al.*, Phys. Plasmas **19**, 056308 (2007)
- 48 S.Yu. Gus'kov, V.B. Rozanov, N.V. Zmitrenko, J. Exp. Theor. Phys. **81**, 296 (1995)
- 49 S. Fujioka, A. Sunahara, K. Nishihara, *et al.*, Phys. Rev. Lett. **92**, 195001 (2004)
- 50 C. Yanez, J. Sanz, and M. Olazabal-Loumé, Phys. Plasmas **19**, 062705 (2012)
- 51 S. D. Baton *et al.*, Phys. Rev. Lett. **108**, 195002 (2012)
- 52 A. R. Bell and M. Tzoufras, Plasma Phys. Control. Fusion **53**, 045010, 2011
- 53 D. Cao *et al.*, Bulletin of the American Physical Society **58** [16], 2013
- 54 P. Y. Chang *et al.*, Phys. Rev. Lett. **107**, 035006 (2011)
- 55 S. Gus'kov *et al.*, PRL **109**, 255004 (2012)
- 56 M. Hohenberger *et al.*, Phys. Plasmas **19**, 056306 (2012)
- 57 O. Klimo and V. T. Tikhonchuk, Plasma Phys. Control. Fusion **55**, 095002 (2013)
- 58 O. Klimo *et al.*, Plasma Phys. Control. Fusion, **52**, 055013, 2010
- 59 M. Koga *et al.*, Nucl. Instr. Meth: A **653**, 84, 2011
- 60 J. A. Marozas *et al.*, Phys. Plasmas **13**, 056311, 2006
- 61 A. Marocchino *et al.*, Phys. Plasmas, **20**, 022702, 2013
- 62 D. D. Meyerhofer *et al.*, Nucl. Fusion **51**, 053010 (2011)
- 63 K. Mima, IFSA 2013 talk
- 64 L. J. Perkins *et al.*, Phys. Plasmas **20**, 072708 (2013)
- 65 H. F. Robey *et al.*, Phys. Rev. Lett. **111**, 065003 (2013)
- 66 D. J. Strozzi *et al.*, Phys. Plasmas **19**, 072711 (2012)
- 67 W. Theobald *et al.*, Bulletin Am. Phys. Society, **56** [16] (2011)
- 68 Yang *et al.*, Phys. Plasmas **18**, 093102 (2011)
- 69 A.R. Piriz *et al.*, Phys. Plasmas **19**, 122705 (2012)
- 70 J. Breil *et al.*, SIAM Journal on Scientific Computing **29** (4), 1781-1824, 209, 2007.
- 71 G. Schurtz *et al.*, *De la possibilité de mettre en œuvre l'allumage par choc dans les expériences de fusion inertielle avec le LMJ*. Ed. by ILP.

# HIGH ENERGY PHYSICS

***Contributors:** Hui Chen (LLNL), Emmanuel d'Humieres (U. Bordeaux), Alexander Andreev (Max Born institute, Berlin), Nikolay E. Andreev (JIHT RAS Moscow), Leonida Antonio Gizzi (CNR, Pisa), Erik Lefebvre (CEA, DIF), Tito Mendonca (IST, Lisbon), Gérard Mourou, Brigitte Cros*

## Introduction

The topic named “High Energy Physics” in this document is related to the generation of energetic particles and radiation during the interaction of high power laser beams with matter. The use of LMJ-PETAL is proposed for specific cases taking advantage of the large energy delivered by the PETAL beam in a relatively short duration, in order to investigate:

- the acceleration of **electrons** to ultra-relativistic energies by laser wakefield in one stage, in a regime of low density and long plasmas; alternative methods to accelerate electrons to a few GeV, such as direct laser acceleration in vacuum.
- the generation of intense relativistic **ions** beams in the high intensity and high energy regime and their interaction. These beams have a strong potential for studies on relativistic collisionless shocks for laboratory astrophysics and the exploration of this regime could result in important progresses for applications of such ion beams to inertial confinement fusion and to medicine.
- the relativistic electron-**positron** pair jets and plasmas and the consequent gamma-ray burst due to pair annihilation.
- the generation of **radiation** and its amplification in plasmas.
- the nonlinear and dispersive properties of quantum vacuum in **strong fields**.

Producing energetic particles and intense fields will provide a unique tool for exploring the structure of matter and vacuum relevant to astrophysics. The use of plasmas as amplifying and focusing media may lead to a new laser approach to circumvent the low damage threshold of today's existing optical components.

*N.B.: acronyms, references and authors are listed at the end of section.*

## 1. The big challenges of the topic

Particle accelerators are used to probe and understand the structure of matter. The accelerating gradients of modern accelerators are limited to 20-100 MV/m range, which has led to large devices, culminating in the 27 km circumference, 7 TeV LHC at CERN. These huge accelerators are some of the largest scientific instruments in existence, which are used to answer questions on the structure of matter beyond the standard model, the nature of mass (the Higgs mechanism), supersymmetry etc.



Microwave cavities of conventional accelerators however break down above field gradients of 100 MV/m due to plasma formation, which makes even modest energy linear accelerators long and expensive devices. **One of the big challenges of accelerator development is to design an electron-positron collider at the energy frontier (> TeV) with an affordable cost.** Validating laser wakefield acceleration mechanism for energies of the order of 100 GeV would exceed the current state-of-the-art energy using plasma as an acceleration medium by two orders of magnitude.

Two big challenges are envisioned for **ion acceleration**: the demonstration of the production of intense GeV proton beams for applications in the study of relativistic collisionless shocks for laboratory astrophysics and the control of the characteristics of such relativistic beams (energy spread, divergence, number of energetic ions...). These challenges will also have strong implications for studies on Ion Fast Ignition concept for ICF and on laser hadrontherapy.

**Relativistic electron-positron pair** plasmas and jets are believed to exist in many astrophysical objects and are invoked to explain energetic phenomena related to Gamma Ray Bursts and black holes. [1 – 9].

On earth, positrons from radioactive isotopes or accelerators are used extensively at low energies (sub-MeV) in areas related to surface science positron emission tomography, basic antimatter science such as antihydrogen experiments, Bose-Einstein condensed positronium, and basic plasma physics. Creating dense relativistic electron-positron (antimatter) plasmas has been elusive, due to the difficulties to produce the pairs in high density and their highly relativistic energies. As a result, the experimental platforms capable of producing the high temperature pair plasma and high-flux pair jets required to simulate astrophysical positron conditions have so far been absent. **With the advent of new, much more powerful lasers, we expect to create extreme relativistic plasmas that display conditions never before encountered. Comprehending observed phenomena under those conditions, whether predicted by existing theoretical and computational capabilities or not, will be a challenge.**

## 2. The state of the art

### 2.1 Plasma based electron acceleration

In 1979, Tajima and Dawson [10] proposed harnessing the electric fields of high amplitude plasma density waves driven by intense laser pulses or relativistic charged particle beams. They showed that for nearly 100% density modulation, acceleration gradients of electric fields due to the charge separation can exceed 1 TV/m for plasma densities around  $10^{19} \text{ cm}^{-3}$ . This reduces the accelerator length by more than three orders of magnitude compared with conventional devices. The maximum energy gain favours low density plasma to reach high energies, even though the gradient is smaller than for high densities. Over the last decade, rapid progress has been made in realising useful laser-plasma wakefield accelerators [11, 12]; (LWFAs). The current state-of-the-art quasi-monoenergetic electron beams from LWFAs exceeds 1 GeV and quality of beams produced has improved;

emittances of around  $1 \pi \text{ mm mrad}$  [13], energy spreads of 0.3% for 100-200 MeV beams [14], bunch durations of the order of 1 fs [15] and charge of 1-100's.pC have been produced, realising the first set of applications of the beams such as gamma ray sources [16] and drivers of light sources [17]

The fact that kJ short pulses will become available for particle acceleration is significant. Compared with 1-10 J lasers that are adequate for densities of plasma around  $10^{17} - 10^{18} \text{ cm}^{-3}$  and a single stage energy gain of 1-10 GeV, the 3.5 kJ PETAL laser can drive plasma with a density of the order of  $10^{15} \text{ cm}^{-3}$  and provide a single-stage energy gain of up to a TeV. This has the challenge of guiding the laser intensity over the dephasing length, typically several tens of meters.

Two other different approaches to extend the particle energies are currently being pursued: The BELLA project [18] (LBNL) is developing 10 GeV stages based on a 30-40 J laser with a  $10^{17} \text{ cm}^{-3}$  LWFA to explore staging as a way to reach much higher energies. This has the challenge of matching/aligning many stages to reach high energies. The other project, FACET [19], is developing a beam driven plasma wakefield to produce beams in excess of 100 GeV, in several km.

A central part of the project proposed with PETAL will be to validate a LWFA for energies of  $\sim 100 \text{ GeV}$  in one long stage driven by a laser plasma injector. This would exceed the current state-of-the-art energy using plasma as an acceleration medium by two orders of magnitude. By demonstrating 100 GeV level acceleration and investigating the characteristics of the accelerator, we will be able to determine (and control) the required parameters for use in high energy physics experiments and other applications.

The IZEST PI and their groups gathers an important part of the scientific community interested in electron acceleration; it covers a range of complementary cross-disciplinary expertise in laser, plasma, accelerator and high field physics. This is augmented by a team of scientists from other institutes who will may provide some of the effort and facilities to undertake the programme of research.

## **2.2. Plasma-based proton and ion accelerators**

Laser-driven acceleration of protons and ions from thin solid state targets produces ion beams with unique properties such as low transverse emittance  $\sim 2.5 \mu\text{m mrad}$ , high current  $\sim \text{kA}$ , ultra-short bunch duration and high particle number per bunch  $\sim 10^{11}-10^{13}$ , which distinguishes them from conventional sources. Laser acceleration experiments so far have not produced ions with energy beyond 100 MeV, which is far from relativistic. This is because the accelerating sheath breaks very quickly at the solid surface [20]. Beyond existing sheath acceleration, two other mechanisms, shock acceleration [21, 22, 23] and radiation pressure acceleration (RPA) [24, 25, 26.], have been shown theoretically to lead to higher energies and to be more efficient.

To achieve high ion energies (possibly  $> \text{GeV/u}$ ), as for the electrons, we will take advantage of the kJ short laser pulses that will be made available by the PETAL laser system to the academic community. By properly compressing and focusing with high contrast kJ-level laser pulses, we could be in a position to deliver to the target an intensity  $> 10^{23} \text{ W/cm}^2$ . This could directly accelerate ions to relativistic energies appropriate for their injection into fast accelerating waves such as LWFA [27]. If this is achieved, we could then accelerate ions to very high energies (such as TeV) over a cm distance.

### 2.3 Plasma based relativistic electron-positron pair creation

In the past few years, groundbreaking steps have been made using high-energy ultra-short laser pulses to make large numbers of positrons in a small volume [28, 29, 30, 31]. It was found that laser-produced positrons have several characteristics that may prove essential for making a relativistic pair plasma. The first is that intense lasers can make a very large number of positrons ( $10^{10}$  to  $10^{12}$  per shot) in a short time (10 – 100 ps) [32]. This feature, in combination with the small volume ( $\sim \text{mm}^3$ ) these positrons occupy, leads to a high density of positrons, even though only for a very short time. The second characteristic is that the target sheath field can accelerate these positrons to 10s of MeV, enabling positrons to be made and accelerated to the relativistic regime in one integrated process. The third characteristic is that MeV electrons and positrons produced from the laser-target interaction form overlapping jets behind the target, allowing much higher pair density to be achieved than it would be if the pairs were distributed isotropically.

Following these initial experiments that produced the high-flux jets of positrons with temperatures of MeV, we performed a new set of experiments focusing on understanding the physics of positron production, beam emittance of the jets, scaling with laser parameters and collimation. The new results show that the emittance of laser-produced positrons is 100 – 500 mm-mrad, comparable to that obtained at the Stanford Linear Collider [33]. The laser contrast was found to have a large effect on the positron yield [34]. The nonlinear scaling of positrons as a function of laser energy is evident when the laser energy is greater than 1000 J [35]. With plasma collimation, we hope to eventually use the multi-kilojoule, short-pulse laser systems worldwide, in combination with more advanced target designs, to create the first relativistic high-density pair plasmas in the laboratory - a completely novel system enabling detailed study of some of the most exotic and energetic systems in the universe [36 to 48].

### 2.4 Investigate the nonlinear and dispersive properties of the quantum vacuum in strong laser fields

How polarisation of the virtual electron-positron pairs of the vacuum can influence a probe laser beam's ellipticity (birefringence) and plane of polarisation (dichroism), is believed to be well-understood theoretically since it is a long-standing prediction of strong-field QED that dates back to the 1930s [49]. Probing such effect, beyond the fundamental interest of doing so, would also be that if any deviation were to occur from QED, it could well be due to several hypothesised particles that are central to many active areas of theoretical physics e.g. mini-charged particles in string theory or axions in QCD. A measurement of the effect would therefore instructively guide beyond-the-standard-model (BSM) physics by constraining the couplings of such postulated phenomena. Therefore, a serious attempt to measure the effect would undoubtedly influence many areas of research.

### 3. The long-term program

#### 3.1 Laser-plasma electron acceleration

High power laser and plasma physics centres<sup>2</sup> will work together with accelerator institutes<sup>3</sup> in a staged programme of research using both theoretical and experimental methods, to (I) produce the highest energy, laser-accelerated, particle beams ever with existing lasers, and (II) to demonstrate a radically new approach to generate higher power lasers, the Cascaded Compression Conversion (C3) approach [50], which would pave the way to even higher energy particle beams, i.e. towards TeV and PeV. Since the C3 approach promises to push the frontier of ultra-intense, ultra-energetic laser pulses, we will (III) scrutinize strong field QED, due to its fundamental importance for the C3 approach itself, and also due to the interest in probing vacuum nonlinearities in strong fields that may prove central to many active areas of theoretical physics.

The first goal will benefit from an exceptional contribution from the CEA-CESTA who will make available the world's largest available laser PETAL<sup>4</sup> hosted at the Laser MegaJoule (LMJ)<sup>5</sup>. They will allow demonstrating acceleration of electrons to 100 GeV using a laser-plasma accelerator and to fully characterise these to determine a strategy for applying this next generation accelerator in experiments in the low luminosity paradigm. Advancing towards a HEP collider is strenuous, long and expensive due to the high luminosity requirement. By relaxing this condition, even though some of the cardinal particle physics may not be pursued, there are extremely valuable new physics that could be explored without high luminosity on much shorter timeline. The introduction of laser energy in this respect is particularly attractive, as it resorts to the prime strength of laser and avoids its weakness. [51].

If successful, this would be a route to acceleration to much higher energies, beyond TeV and towards PeV energies, using either the full energy from the Megajoule Laser or the C3 method detailed below. Our particle acceleration programme will also include proof-of-principle ion acceleration to relativistic velocities (i.e. GeV), which would then allow to apply further “fast wave” acceleration methods, as for electrons, in order to reach 100 GeV - TeV energies, opening the door to compact and ultrafast sources of muons and neutrinos.

#### 3.2 Cascaded Compression Conversion (C3)

In parallel, encouraged by recent experimental [52, 53] and theoretical [54, 55] investigations of plasma as an optically active medium able to amplify and focus intense light pulses, we will

---

<sup>2</sup> CEA-CESTA, Strathclyde, IZEST, GSI, ALLS-INRS, UHI100-Saclay, Dusseldorf.

<sup>3</sup> John Adams Institute, KEK, CERN High Energy Physics, University of BERN, Institut de Physique Nucléaire of Lyon.

<sup>4</sup> <http://petal.aquitaine.fr/>

<sup>5</sup> <http://www-lmj.cea.fr/>

demonstrate the new C3 approach to achieve extremely high intensity and ultra-short laser pulses that will circumvent the low damage threshold problem of conventional optical components, which is the main limitation to higher power amplification. In a staged approach, we will first push the demonstration of C3 to high laser energy on mid-scale laser facilities.

The use of the CEA lasers will then represent the pinnacle of our efforts: by implementing C3 on PETAL, we will have access to 100 PW level femtosecond pulses that can be used to increase the energy of accelerated particles, carry out nonlinear vacuum physics, and to combine particle and high field physics in unique ways. This will open a door to the production of peak power beyond an Exawatt using MJ-scale facilities.

Finally, by implementing C3 on PETAL, the physics community will be placed in a position to, for the first time, investigate a variety of theoretically predicted effects related to the quantum nature of vacuum, e.g. the nonlinear structure of the quantum vacuum in the presence of extreme fields, breakdown of the quantum vacuum by pair production, QED cascades, etc. Furthermore, by combining the extreme light fields produced by C3 with high-energy particles we will couple particle physics with extreme fields, thus allowing the study of e.g. nonlinear Compton scattering, Breit-Wheeler pair production etc.

### **3.3 Plasma based relativistic electron-positron pair creation**

Laboratory created relativistic pair plasma will be used to understand the relativistic collisionless shocks and their roles in astrophysical phenomena as stated above (in “Big Challenge” section). These shock waves propagating in relativistic pair plasmas are responsible for the bulk of nonthermal high-energy emission seen from jets in Active Galactic Nuclei (AGN), Gamma-ray Bursts (GRBs) and Pulsar Wind Nebulae (PWN). The main mechanism for particle acceleration is thought to be the Fermi process, in which some particles can scatter in the magnetic turbulence and repeatedly cross the shock front, gaining energy from the effective convergence of the pre- and post-shock flow at the jump. Although relativistic collisionless shocks can be produced by interactions between two relativistic plasma flows, they have not been made in the laboratory. The laser created pair jet interaction seems to be well suited to make collisionless shocks which may provide the answers to many questions remain about the physics of collisionless shocks and their effect on astrophysics.

### **3.4 Laser-plasma ion acceleration to GeV**

In a first stage, exploration of laser ion acceleration using alternative schemes in the high intensity, high energy regime will be conducted within the initially specified PETAL performances. The particular promising directions are: Break out afterburner (BOA), shock acceleration and low density targets.

The second stage of this task will take advantage of a possible compression, to  $\sim 100$  fs, of the PETAL 0.5 ps 3.5 kJ pulse by using chirped mirrors. This scheme is expected to yield  $\sim 2$  kJ pulses, to be focused into a focal spot of a few microns using a plasma mirror. This will yield laser pulses  $\sim 10^{22}$

$Wcm^{-2}$ , i.e. well within the predicted range to produce ion beams in the GeV/u energy range [56 to 59] with a narrow energy spread. If the laser pulse contrast will not be sufficiently high, we will explore the dual acceleration scheme that has the advantage of using simple and inexpensive targets [60]. We will also need the laser pulse with improved temporal contrast to exploit the pure RPA acceleration mechanism. This can be achieved by frequency-conversion or the use of plasma switches, either in reflection (plasma mirror) or transmission geometries [61].

The third stage will rely on the progress that will be obtained with the C3 technique to compress the high-energy, moderately short PETAL laser pulses to ultra-short ones ( $\sim 10$  fs). Using focusing plasma optics, we expect to be able to increase the focused laser intensity by at least a factor 10 achieving an intensity  $>10^{23}W/cm^2$ . This will ensure, as illustrated by the simulations shown in Figure 1, the production of higher energy ions with a higher efficiency.

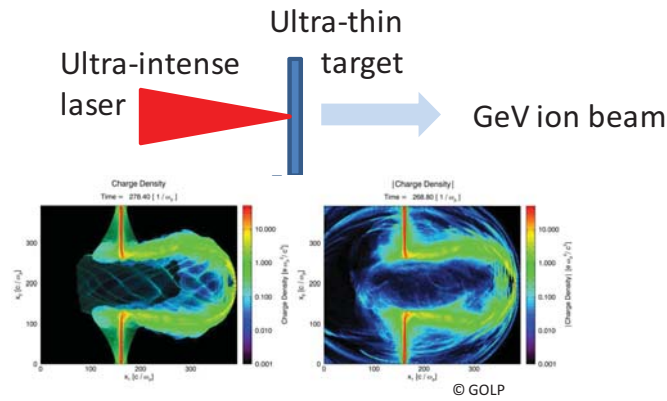


**Figure 1:** Schematic and 2D numerical simulation of GeV proton accelerated by a  $10^{23} Wcm^{-2}$ , 20 fs laser pulse.

Beyond this, we pursue post-acceleration of GeV-class ions (produced by the above methods) using wakefield structure of the laser pulse in underdense plasma, closely coupled with the ion injector. Trapping by high amplitude electrostatic fields moving at relativistic speeds has already been observed to allow trapping of the pre-accelerated protons and their acceleration to tens of GeV [62]. If this is achieved, we could then accelerate ions to very high energies (such as TeV) over a cm.

### 3.5 Control of the characteristics of laser-accelerated relativistic ion beams

For some applications, the controls of the characteristics of the accelerated ion beam are crucial (energy spread, divergence, number of energetic ions...). Specific experiments on the control of these characteristics for high energy ion beams in the high energy, high intensity regime will be proposed.



### 3.6 Application to the study of relativistic collisionless shocks

Collisionless shock experiments by colliding the high energy proton beams produced with gas jets, or a foil exploded by a LMJ beam will allow to investigate for the first time in the laboratory the development of relativistic collisionless shocks. These shocks, which are a very efficient source of high energy particles and radiation, constitute one of the main ingredient of the most recent models of gamma-ray bursts and cosmic rays. The experiments proposed in collaboration with the WG3 (laboratory astrophysics) will aim on the definition of the appropriate interaction geometry and scaling of the astrophysical events to the available interaction conditions.

### 3.7 Alternative acceleration schemes

Direct laser acceleration in vacuum could be an interesting alternative to consider for future CILEX and LMJ-PETAL experiments in the range of multi-GeV electron energies. Various configurations were proposed theoretically in the past, which include the self-trapping acceleration [63], super-ponderomotive acceleration [64], and the photon mirror scheme [65, 66].

We propose to concentrate on photon-mirror acceleration, which is potentially more promising in terms of the final electron energies. In this scheme, a low energy electron beam counter-propagates with an intense laser pulse, and is reflected by the ponderomotive pulse potential. Its final gamma-factor is given by  $\gamma_1 \sim 4 \gamma_0 \gamma_g^2$ , where  $\gamma_0$  characterizes the initial electron state, and  $\gamma_g$  is the laser pulse gamma-factor. Electron reflection can occur when  $\gamma_0 < a_0$ , the normalized laser field amplitude.

We can see that the double Doppler energy shift of the reflected electron beam is similar to the frequency shift of photons reflected by a relativistic mirror. The acceleration process can therefore lead to very high electron energies. For instance, for incident electrons with 5 MeV, interacting with a laser pulse with amplitude  $a_0$  between 10 and 30, and laser pulse gamma factor between 100 and 300, we could in principle attain final electron energies in the range of 200 GeV to 2 TeV.

This is however purely speculative, and still has to be proved, first using PIC code simulations, and then using different stages of preliminary experiments. The main problems to be addressed in the simulations are, the acceleration distance, the radiation losses, side-scattering losses and the laser front group velocity. In plasmas, the laser pulse velocity is mainly determined by corrosion of the laser front due to ionization losses, but in vacuum it will be simply determined by the laser waist. Comparison between near field and far field efficiency should also be tested. Preliminary PIC code simulations are being performed in collaboration with J. Vieira at GoLP/IST. In the future, parameters relevant to CILEX and LMJ-PETAL would be used.

### 3.8 Radiation processes

Betatron radiation is the dominant process for laser wakefield acceleration. We could also add transition radiation as a secondary emission process, due to electron bunch interaction with foils.

In contrast, direct laser acceleration based on the photon-mirror scheme could provide interesting studies on radiation reaction. Strong emission of radiation due to electron reflection would eventually reduce the acceleration efficiency. Two types of radiation should be expected. One is bremsstrahlung associated with nearly one-dimensional deceleration and acceleration, which takes place on the acceleration time scale. The other is nearly instantaneous synchrotron radiation associated with oblique incidence. These two radiation processes will be studied on a further stage of the PIC simulation campaign planned for the photon-mirror scheme.

## **4. Science on a shorter time-line**

On the experimental point of view, the objective will be to bridge the gap between demonstrations of principle feasibility of acceleration and of test of QED into the practical world where essential parameters of the experiment, such as luminosity, efficiency, backgrounds, beam quality, and many other factors need to be carefully considered. A theoretical effort will be necessary to develop the theoretical and numerical tools required to guide further exploration of the structure of matter and vacuum.

### **4.1 Laser-plasma electron acceleration to 100 GeV**

We stress here that we will use PETAL as it will be made available, i.e. without needing to rely on the C3 development that will be pursued in parallel, and that would yield even higher electron energies.

The method to be employed to achieve 100 GeV will be based on experience and methods developed at JAI, Strathclyde and the FACET project. Following a series of staged experiments at the 200-300 TW lasers (e.g. at Strathclyde), 200-300 J lasers (e.g. at GSI) to investigate injection and staging methods at lower energies, we will undertake the 100 GeV experiment using the kJ PETAL laser beam in the LMJ target area. The general outline of the facility and of the experiment is shown in figure 2.

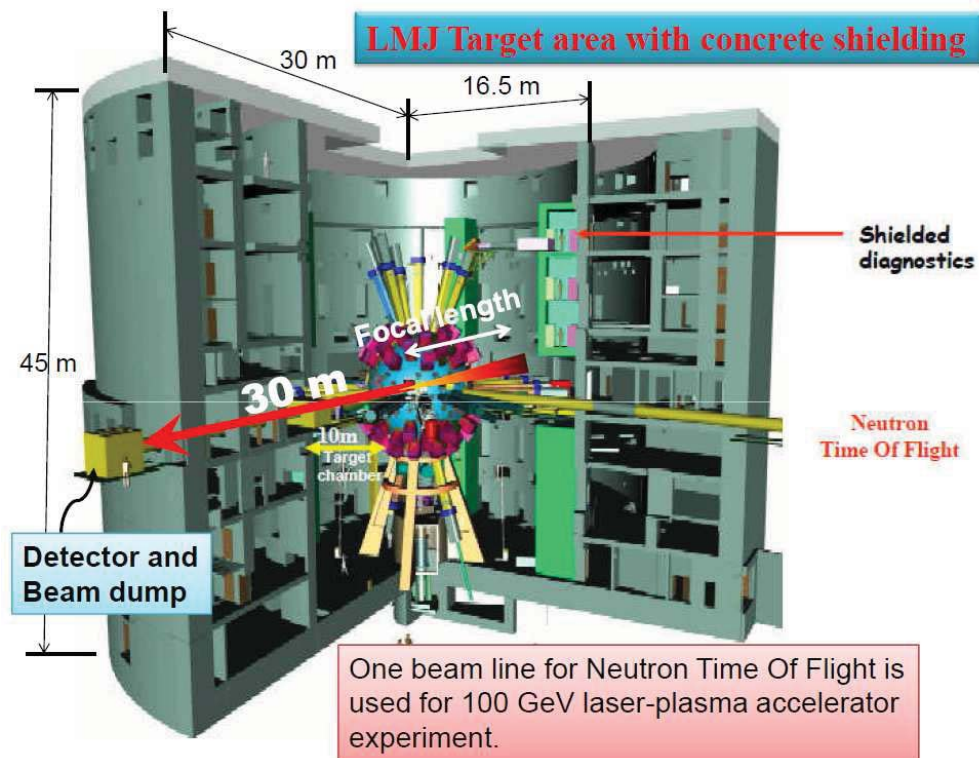


**Figure 2:** An equatorial view of the LMJ area. The 100 GeV plasma acceleration beamline, shown in yellow on the left hand side, is connected to the main vacuum of the target chamber, and ends with a beam dump and the experimental area.

The centre of the target chamber coincides with the laser focus of PETAL (see Figure 3.a). The plasma channel, which forms the acceleration medium, will be located in a 30 m channel built for neutron beamlines. The PETAL laser will be focused into the injection chamber which contains higher density plasma (see Figure 3.b), to produce a 1 GeV electron beam that will be accelerated in the following lower density plasma sections.

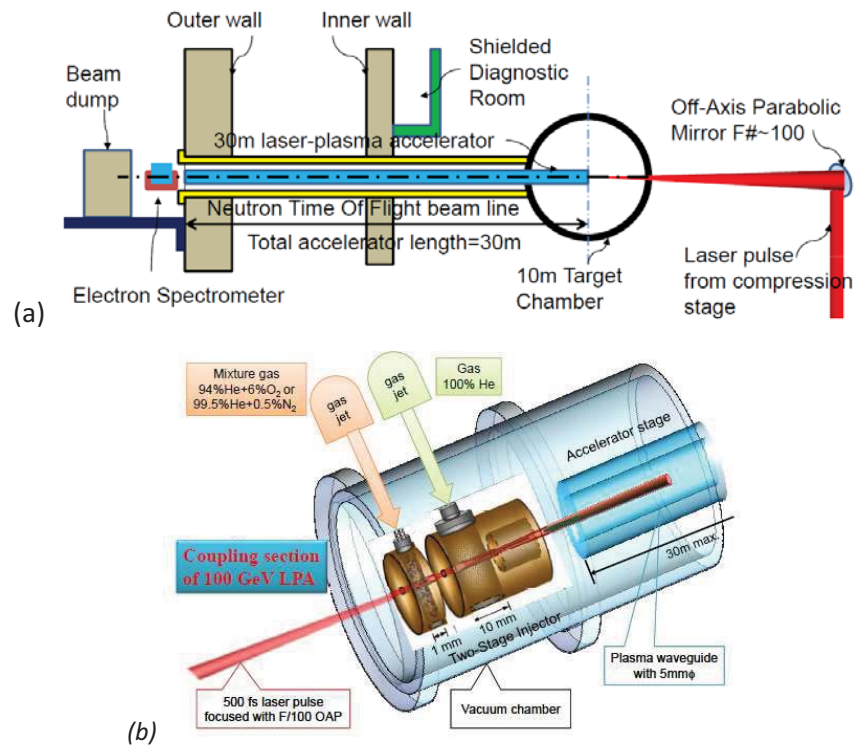


**Figure 3:** (a) Detail schematic of the 100 GeV beamline, where the final focus laser optics, the plasma channel, and location of the electron spectrometer and instrumented beam dump are shown. (b) Laser-plasma injector and front end of the main plasma accelerator stage.

The main parameters of the 100 GeV accelerator are shown in Table 1, including details of the injector and final stages.

Parameter	Injector	Final Stage	Parameter	Injector	Final stage
Energy gain per stage [GeV]	~1	~100	Charge [pC]	160	160
Injection beam energy [GeV]	ionisation	~1	Matched beam radius [ $\mu\text{m}$ ]		90
Plasma density [ $\text{cm}^{-3}$ ]	$2 \times 10^{18}$	$3.5 \times 10^{15}$	Laser wavelength [ $\mu\text{m}$ ]	1.053	1.053
Plasma wavelength [ $\mu\text{m}$ ]	23.6	564	Normalised vector potential $a_0$	3.2	1.5
Accelerating field [GV/m]	193	3.3	Laser pulse duration [fs]	500	500
Focussing constant [ $K/k_p$ ]	0.71	0.35	Laser spot radius [ $\mu\text{m}$ ]	126	273
Stage length [m]	0.006	30	Laser peak power [PW]	3.1	3.1
Plasma channel depth [ $\Delta n_c/n_p$ ]	0	0.44	Laser energy per stage [J]	1.5	1.5

**Table 1:** Laser plasma parameters

## 4.2 Laser-plasma ion acceleration to progress towards GeV energies and to study collisionless shocks

The exploration of laser ion acceleration using alternative schemes in the high intensity, high energy regime will be conducted within the existing PETAL specifications. The BOA mechanism will be studied with ultra-thin solid targets. However, it will require an improvement the PETAL performance by installing a plasma mirror to increase the pulse contrast. The exploration of this regime will allow to refine the strategies envisioned to reach GeV ion energies and could result in important progresses for applications of such ion beams to inertial confinement fusion and to medicine.

The study of shock acceleration in low density targets (underdense or near-critical) will be pursued with existing PETAL characteristics as this acceleration regime has been proven to be very efficient in the high intensity and high laser energy domain [67] and does not require a too high contrast. Ion energies of several hundred MeV are predicted using 2D Particle-In-Cell simulations while the regime has not been completely optimized (see Figure 4 below). Using low density targets allows to decrease the stringent requirements on laser contrast and allows high repetition rates experiments in the preparation phase for the PETAL shots.

Collisionless shock can also start in this period. They will be performed by colliding the high energy proton beams generated with PETAL with plasmas produced from gas jets or thin foils exploded and heated by the LMJ beams.

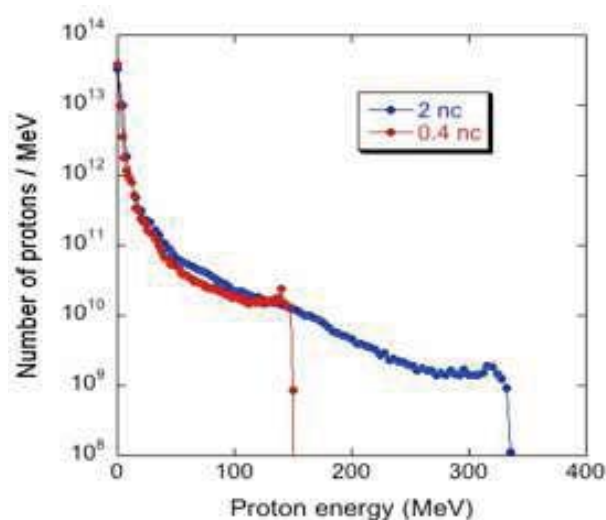


**Figure 4:** proton energy spectra obtained for a 1021 W/cm<sup>2</sup>, 500 fs, 30  $\mu$ m FWHM pulse interacting on a hydrogen plasma (two densities are investigated). Interaction conditions are not optimized.

For some applications, the control of the characteristics of the accelerated ion beam are crucial (energy spread, divergence, number of energetic ions...). Specific experiments dedicated to the

metrology of high energy ion beams in the high energy, high intensity regime will be proposed. These experiments could also result in important progresses for applications of such ion beams to inertial confinement fusion and to medicine

### 4.3 Electron positron pair creation

In the shorter time (let's say 5 years starting from 2017), we could take advantage of LMJ/PETAL configuration to study the pair plasma physics and carry out the experiments to: (1) produce dense relativistic electron positron pair jets in the laboratory, (2) perform experiments and simulations to study the physics of relativistic collisionless shocks using laser-produced pair jets, and (3) understand the interactions of positrons to hot electrons, X-rays and ions.

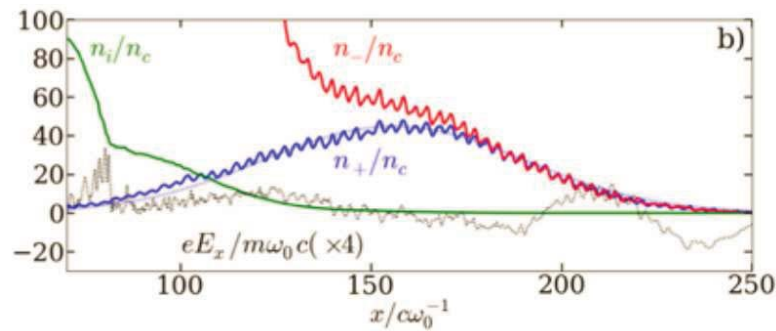


**Figure 5:** *y*-averaged ion density  $n_i/n_c$ , positron density  $n_+$ , electron density  $n_-$  and the electric field  $E_x$  at time  $555\omega_0^{-1}$

For example, 2D Particle-In-Cell simulations including pair creation through the multiphoton Breit-Wheeler process predict the generation of quasi-neutralized positrons beams with a density of around 40 nc (M. Lobet et al. submitted) with a short (60 fs) ultra-intense laser pulse ( $a_0=800$ ) interacting on a thin solid target (see Figure 5). This process could be investigated on PETAL with the C3 technique. Very promising applications in laboratory astrophysics are envisioned (e-/e+ collisionless shocks...).

#### 4.4 Plasma-based high power optics (the C3 technique)

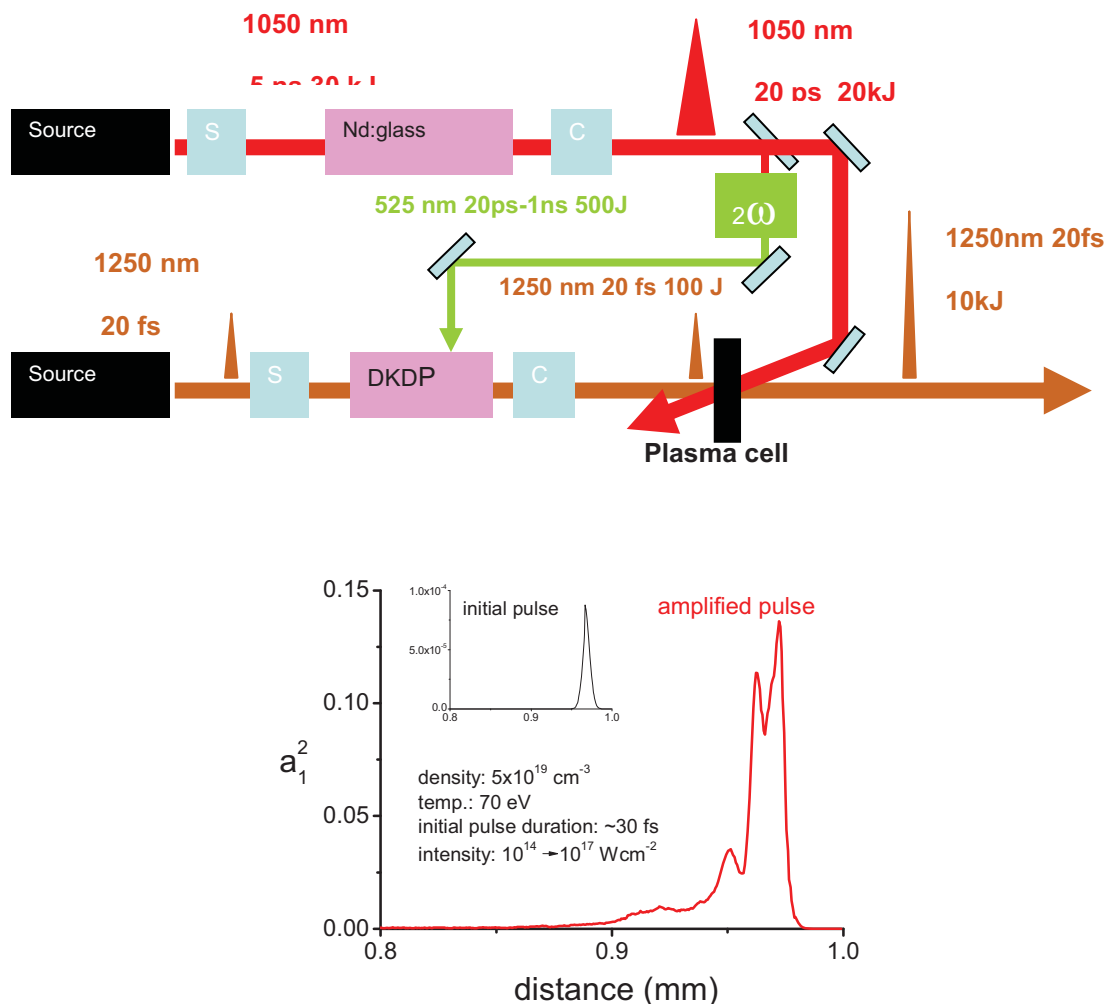


**Figure 6:** The C3 concept: (top) schematic, (bottom) 1-D simulation showing the normalised intensity of amplified pulse showing Burnham Chao ringing (simulations using a hybrid PIC code).

The C3 generic concept description is presented in Figure 6 (top). This scheme is immediately transposable to PETAL, which provides a compressed pump pulse from 0.5 ps to 10 ps with several kJ. Our simulations Figure 6 (bottom) indicate that a 2 ps, 4 kJ/cm<sup>2</sup> pump pulse should lead to a compressed pulse of 1 kJ, 20 fs pulse or 50 PW.

To progressively optimize the use of this technique, we plan to proceed in a step-wise manner, demonstrating amplification at energy levels of J, 10s of J, using 100 TW-scale lasers, and then to move on higher energy levels with PHELIX and finally PETAL. The project will investigate several issues: i) how to optimize the plasma-based amplification processes, ii) understand detrimental effects and how to control them (filamentation, wave breaking etc.), iii) consider the relative merits



of Raman, Compton and Brillouin methods, iv) envisage a possible combination of the two approaches by employing a multi-stage amplification configuration where the CPA-created pulse is first compressed by Brillouin and the resulting pulse further compressed by Raman or Compton processes. This will be pursued combining experiments and modeling. We will benchmark the simulation effort with the experiments to develop insight into plasma-based amplification processes.

The final step of C3 will be to produce intensities of  $10^{24}$  -  $10^{25}$  W/cm<sup>2</sup> by sharply focussing the C3 pulse using, precision, disposable, centimetre size f#1 plasma mirror optics (Figure 7). The fluence on a 1-3 cm diameter glass substrate paraboloid, AR coated mirror is of the order of 1-5 kJ/cm<sup>2</sup> for a 5 kJ beam, which results in an intensity sufficient to create a plasma mirror. Small size high precision optics could be mass-produced and replaced after each shot.

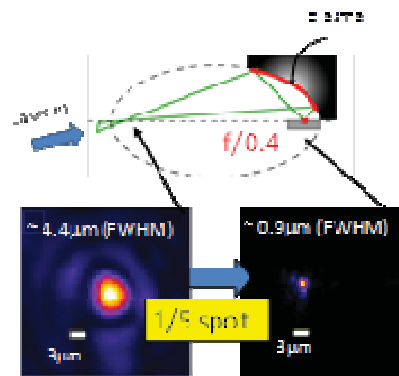


**Figure 7:** Method of focusing of extremely intense light using a disposable plasma mirror demonstrated by M. Nakatsutsumi et al. [68]

#### 4.5 Strong field QED

The set-ups for such experiments have been discussed extensively [69, 70, 71]. We will here employ a focused C3 laser beam to excite vacuum birefringence probe it with an auxiliary probe beam. Ultra-intense fields might also lead to spontaneous electron-positron pair production from the quantum vacuum [72]. Electrons and positrons generated in the focus of an ultra-intense laser pulse by spontaneous vacuum decay might produce secondary electrons, positrons, and photons leading to a rapidly growing cascade of electrons, positrons, and photons. We will here capitalize on the fact that the process is efficient for fields well below the Schwinger critical field for appropriate laser field configurations as they are present in strongly focused laser pulses. Those questions will not only be tackled experimentally, but we will also pursue theoretical work. We will implement nonlinear field solvers to account for vacuum nonlinearities based on Heisenberg-Euler in strong laser fields. Nonlinear field solver will enable us to predict nonlinear self-interactions of high-intensity laser pulses in vacuum such as vacuum self-focussing or solitonic wave behavior. The simulations will also support new particle-physics models as have been recently discussed [73] by determining the range of validity of the four-wave mixing assumption.

## 5. The needed steps to go

The experimental effort proposed has three main objectives:

- Acceleration of electrons to 100 GeV, and of protons possibly to the GeV level.
- Develop the C3 technique to push toward extreme laser intensities.
- Investigating strong field QED.

In 2013-2015, we will validate the concept of high energy particle acceleration at GSI and also prototype the accelerating structures on PETAL. In parallel, the C3 concept validation will progress with the aim on implementation on PETAL in the final two years to the 500J-20fs level pulse, in view of a major push on particle acceleration.

### 5.1 Simulating electron acceleration to TeV and the focusing of laser pulses to extreme intensities

#### 5.1.1 Acceleration of electrons to 100 GeV

We will investigate the acceleration of electrons in wakefields to a few hundred GeV numerically. First, the simulation approach will not be self-consistent but rather parametric since self-consistent numerical simulations of acceleration to a few hundred GeV have yet not been carried out to the best of our knowledge. However, we plan to make progress with full simulations with the help of adaptive mesh refinement in an appropriate boost frame co-moving with the fast electrons and we will take radiative properties of the accelerated electrons into account.

#### 5.1.2 Principle intensity limits

A question that is related the C3 experimental campaign in its final stage concerns the possibility of principle limitations on the intensity achievable in a laser focus. The problem arises due to the possibility of spontaneous vacuum breakdown, vacuum nonlinearities, and strong cascading. The problem can only be investigated numerically by solving a set of extended Vlasov equations with the Particle-In-Cell method. Those simulations are very complex and expensive and require adaptive simulation methodologies. We will address the problem with a systematic numerical campaign.

### 5.2 Theoretical and numerical steps required to achieve ion acceleration to GeV

The CELIA group at the Univ. of Bordeaux will provide access to a complete set of state-of-the-art simulation tools and will perform the simulations needed for preparation and interpretation of experiments: hydrodynamical simulations to obtain the high intensity interaction target conditions,

2D and 3D Particle-In-Cell simulations (in collaboration with the team of Yasuhiko Sentoku at the University of Nevada, Reno) to model the high intensity interaction and obtain the electron and proton sources characteristics [74]. New 3D Particle-In-Cell simulations of the interaction of dense relativistic plasma jets with a secondary low density plasma will be performed for preparing the experiments on the collisionless shocks. The possibility to manipulate the obtained proton beams will also be studied numerically for specific experiments (focusing, energy selection...).

Large scale Particle-In-Cell simulations of the interaction of dense relativistic plasma jets with a secondary low density plasma will be of great importance to prepare the choice of diagnostics in the LMJ-PETAL experiments dedicated to the study of collisionless shocks and to understand in detail the complex physics of the development of the shock [75]. The numerical diagnostic tools will be developed for modeling the experimentally observed interaction characteristics.

To conduct these simulations, which will require millions of CPU-hours, dedicated proposals will be submitted on the largest European super-computers (through PRACE and GENCI for instance).

### **5.3 Diagnostic development for electron acceleration to 100 GeV**

We will undertake a detailed design of electron beam transport optics, electron beam manipulation, compression, focusing, beam dump and radiation shielding, and diagnostic system to control the beam parameters. The present electron spectrometer for HEDP experiments could be used, increasing magnetic field and length.

Alternative techniques will be studied, such as those relying on subnuclear physics processes with known energy threshold and specific signature, looking for the the appropriate ones for the expected energy.

### **5.4 Diagnostics for ion acceleration and positrons generation**

We will need the availability of the particle diagnostics developed in the framework of PETAL+.

### **5.5 Target preparation for electron acceleration to 100 GeV**

We will investigate two approaches for the main plasma medium sections – one based on an ablative plasma discharge (Figure 8: left) and a second based on RF plasma discharges (Figure 8: right). The plasma sections will be created from one meter long independent sections, which will be installed with minimal gap to allow seamless transition between sections and to allow for adiabatic increase of the plasma density, adjustment of the length of the plasma section, convenient assembly and alignment etc.

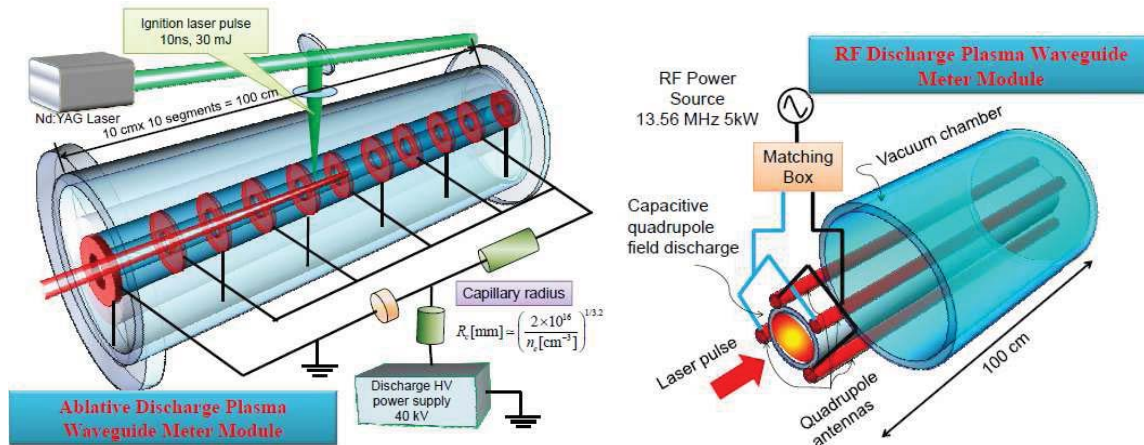


**Figure 8:** Schematic of plasma media; (Left) Ablative plasma, (right) RF plasma waveguide.

The implementation of the 100 GeV acceleration will include several steps. In the first step a detail physics design and an engineering design will be developed. An engineering installation plan, as well as development of auxiliary systems (control system, cable plant, safety system and shielding) will be developed in collaboration with CEA engineers.

## 5.6 Target preparation for ion acceleration

We will need the possibility to use ultra thin targets (~100 nm) and near-critical targets. Ultra-thin targets experiments will require the use of a plasma mirror. Near-critical targets of interest for laser ion acceleration can be produced using recently developed gas nozzles [76]. The implementation of these nozzles in the LMJ-PETAL interaction chamber needs to be considered.

For positron experiments, simple disc targets are used, no development is required.

Experiments at Titan (180J) are already underway to study laser ion acceleration with low density targets (2012 and 2014 experiments). Experiments on the PHELIX laser system at GSI will also be proposed. Intermediate experiments can be achieved on Omega EP or FIREX at laser systems in the USA and in Japan, respectively.

Experiments on positrons are underway on Omega EP and Osaka LFEX.

## Conclusion

In the frame of the proposed program, we first plan to demonstrate that state-of-the-art laser facilities could offer the possibility of producing electrons above 100 GeV, and ions to GeV level. In a broader context, producing energetic particles and intense fields will provide a unique toolbox for exploring the structure of matter and vacuum relevant to astrophysics. We in parallel plan, encouraged by recent developments in using plasmas as amplifying and focusing media, to develop a new laser approach that will circumvent the low damage threshold of today's optical components. This transformational approach will be developed in a staged manner to be finally implemented on PETAL. If successful it will be the prelude to energies beyond the TeV level. This experimental effort will be accompanied by a necessary theory and simulation effort

Experiments on PETAL on laser ion acceleration will allow to tackle two of the main challenges that are envisioned for this topic: the demonstration of the production of intense GeV proton beams for applications in the study of relativistic collisionless shocks for laboratory astrophysics and the control the characteristics of such relativistic beams (energy spread, divergence, number of energetic ions...). These challenges also have strong implications for the studies of Ion Fast Ignition concept for ICF and of laser hadrontherapy. The team that will be dedicated to these studies has the theoretical and experimental expertise to succeed.

One of the objectives of this program is to explore some of novel, yet critical, aspects of pair plasma jets produced by intense lasers. The proposed study will address the optimization and confinement of a relativistic pair plasma through experiments using LMJ-PETAL. Given the limitation of computer simulations, these are the only viable solutions to build up a platform for a range of applications and astrophysics related experiments using pair jets and pair plasmas. We will continue developing cutting edge diagnostic technique and capabilities. We are confident that this work will produce important information to the understanding of the basic science underlying this unique and important, but relatively unexplored, plasma conditions and enable future experimental analogues of some of the most fascinating astrophysical phenomena.

## Sigles

AGN	Active Galactic Nuclei
AR	Anti-Reflection
BELLA	Berkeley Lab Laser Accelerator
BOA	Break out afterburner
BSM	Beyond-the-Standard-Model
C3	Cascaded Compression Conversion
CERN	Conseil Européen pour la Recherche Nucléaire
CILEX	Centre Interdisciplinaire de la Lumière Extrême
CPU	Central Processing Unit
FACET	Facility for Advanced Accelerator Experimental Tests
GENCI	Grand Equipement National de Calcul Intensif
GeV	Giga electron volts
GoLP/IST	Grupo de Lasers e Plasmas / Instituto Superior tecnico
GRB	Gamma-ray Burst
HEP	High Energy Physics
IFC	Inertial Confinement Fusion
IZEST	International Center for Zetta- Exawatt Science and Technology
JAI	John Adams Institute
LBNL	Lawrence Berkeley National Lab
LFEX	Laser for Fast Ignition Experiment
LHC	Large Hadron Collisioner
LWFA	Laser Wakefield Acceleration
MeV	Mega electron volts
PHELIX	Petawatt High-Energy Laser for Heavy Ion EXperiments
PRACE	Partnership for Advanced Computing in Europe
PWN	Pulsar Wind Nebulae
QCD	Quantum ChromoDynamics
QED	Quantum electrodynamics
RPA	Radiation Pressure Acceleration
TeV	Tera electron volts

## References

- 1 E. Fermi, Phys. Rev. **75**, 1169 (1949).
- 2 A. R. Bell, Monthly Notices of the Royal Astronomical Society, 182, 147 (1978).
- 3 R. Blandford, and J. Ostriker, Astrophysics. J, 221, L29 (1978); R. Blandford and D. Eichler, Phys. Rep. **154**, 1 (1987).
- 4 P. Meszaros, Annal Review of Astronomy and Astrophysics **40**, 137 (2002).
- 5 F. Mirabel and L. F. Rodriguez, Review of Astronomy and Astrophysics **37**, 409-43 (1999).
- 6 A. Spitkovsky, ApJ Lett., 673, L39 (2008); A. Spitkovsky, AIP Conf. Proc., 801, 345 (2005); L. Sironi and A. Spitkovsky, ApJ, 698, 1523 (2009); L. Sironi and A. Spitkovsky, ApJ, **726**, 75 (2011).
- 7 J. Wardle, et al., Nature **395**, 457 (1998)
- 8 G. Weidenspointner, et al, Nature **451**, 159 (2008).
- 9 L. O. Silva, R. A. Fonseca, J. W. Tonge, J. M. Dawson, W. B. Mori, and M. V. Medvedev, Astrophysics.J, **596**, L121 (2003).
- 10 Tajima and Dawson, *Laser Electron Accelerator*, Phys. Rev. Lett. **43**, 267 (1979)
- 11 [SPD Mangles et al., Monoenergetic beams of relativistic electrons from intense laser– plasma interactions, Nature **431**, 535 (2004)
- 12 W. P. Leemans, et al., GeV electron beams from a centimetre-scale accelerator, Nature Physics **2**, 696 (2006)
- 13 E Brunetti, et al., *Low emittance, high brilliance relativistic electron beams from a LWFA*, Phys. Rev. Lett. **105**, 215007 (2010).
- 14 SM Wiggins, et al., *High quality electron beams from a laser wakefield accelerator*, Plasma Phys. Control. Fusion **52**, 124032 (2010).
- 15 O. Lundh, et al., *Few femtosecond, few kiloampere electron bunch produced by a laser-plasma accelerator*, Nature Physics **7**, 219 (2011)
- 16 S Cipiccia, et al., *A harmonically resonant betatron plasma wakefield gamma-ray source*, Nature Phys. **7**, 867 (2011)
- 17 H-P Schlenvoigt et al., *A compact synchrotron radiation source driven by a laser plasma wakefield accelerator*, Nature Phys. **4**, 130 (2008).
- 18 <http://www.lbl.gov/Community/BELLA/index.html>
- 19 M J Hogan et al *Plasma wakefield acceleration experiments at FACET* New J. Phys. **12**, 055030 (2010)
- 20 T Tajima, D Habs, and XQ Yan, *Laser acceleration of ions for radiation therapy*, Rev. Accel. Sci. Tech. **2**, 201 (2009).
- 21 LO Silva et al., Phys. Rev. Lett. **92**, 015002 (2004)
- 22 **C PALMER ET AL.**, *Monoenergetic Proton Beams Accelerated by a Radiation Pressure Driven Shock*, Phys. Rev. Lett. **106**, 014801 (2011)
- 23 E. d’Humières et al. *J. Phys.: Conf. Ser.* **244** 042023 (2010)
- 24 A Henig et al., *Radiation-Pressure Acceleration of Ion Beams Driven by Circularly Polarized Laser Pulses*, Phys. Rev. Lett. **103**, 245003 (2009)
- 25 D Jung et al., *Monoenergetic Ion Beam Generation by Driving Ion Solitary Waves with Circularly Polarized Laser Light*, Phys. Rev. Lett. **107**, 115002 (2011)



- 26 A Macchi et al., *Laser Acceleration of Ion Bunches at the Front Surface of Overdense Plasmas*, Phys. Rev. Lett. **94**, 165003 (2005)
- 27 FL Zheng, et al., *TeV quasi-monoenergetic proton beam generation by an ultra-relativistically intense laser in the snowplow regime*, submitted to Phys. Plasmas (2011): arXiv: 1101.2350v2 [plasma.phys.ph] (2011)
- 28 Hui Chen, et al., Phys. Rev. Lett. **102**, 105001 (2009)
- 29 Hui Chen, et al., Phys. Plasmas **16**, 122702 (2009)
- 30 Hui Chen et al., Phys. Rev. Lett. **105**, 015003 (2010);
- 31 Hui Chen, et al., High Energy Density Physics, **7**, 225 (2011)
- 32 Hui Chen, et al., Phys. Rev. Lett. **102**, 105001 (2009)
- 33 Hui Chen, et al. Phys. Plasmas **20**, 012507 (2013)
- 34 Hui Chen, M. Nakai, Y. Sentoku, Y. Arikawa, H. Azechi, S. Fujioka, C. Keane, S. Kojima, W. Goldstein, B. R. Maddox, N. Miyanaga, T. Morita, T. Nagai, H. Nishimura, T. Ozaki, J. Park, Y. Sakawa, H. Takabe, G. Williams, Z. Zhang, New J. Phys. **15** (2013) 065010
- 35 Hui Chen, D. D. Meyerhofer, Y. Sentoku, *et al.*, in preparation.
- 36 E. Fermi, Phys. Rev. **75**, 1169 (1949)
- 37 A. R. Bell, Monthly Notices of the Royal Astronomical Society, **182**, 147 (1978)
- 38 R. Blandford, and J. Ostriker, Astrophysics. J, **221**, L29 (1978)
- 39 R. Blandford and D. Eichler, Phys. Rep. **154**, 1 (1987)
- 40 P. Meszaros, Annal Review of Astronomy and Astrophysics **40**, 137 (2002)
- 41 F. Mirabel and L. F. Rodriguez, Review of Astronomy and Astrophysics **37**, 409-43 (1999)
- 42 A. Spitkovsky, ApJ Lett., **673**, L39 (2008)
- 43 A. Spitkovsky, AIP Conf. Proc., **801**, 345 (2005)
- 44 L. Sironi and A. Spitkovsky, ApJ, **698**, 1523 (2009)
- 45 L. Sironi and A. Spitkovsky, ApJ, **726**, 75 (2011)
- 46 J. Wardle, *et al.*, Nature **395**, 457 (1998)
- 47 G. Weidenspointner, et al, Nature **451**, 159 (2008)
- 48 L. O. Silva, R. A. Fonseca, J. W. Tonge, J. M. Dawson, W. B. Mori, and M. V. Medvedev, Astrophysics. J, **596**, L121 (2003)
- 49 W. Heisenberg and H. Euler, *Folgerungen aus der Diracschen Theorie des Positrons*, Z. Phys. **98**, 714 (1936)
- 50 G. Mourou et al., Exawatt-Zettawatt pulse generation and applications, Optics Communications **285**, 720 (2012)
- 51 T Tajima, M Kando, & M Teshima, *Feeling the Texture of Vacuum - Laser Acceleration toward PeV*, Prog. Theor. Phys. **125**, 617 (2011)
- 52 J Ren et al., A new method for generating ultraintense and ultrashort laser pulses, Nature Physics **3**, 732 (2007)
- 53 L. Lancia et al., Experimental Evidence of Short Light Pulse Amplification Using Strong-Coupling Stimulated Brillouin Scattering in the Pump Depletion Regime, Phys. Rev Lett. **104**, 025001 (2010)
- 54 AA Andreev et al., Short light pulse amplification and compression by stimulated Brillouin scattering in plasmas in the strong coupling regime, Phys. Plasmas **13**, 053110 (2006)
- 55 RMGM Trines et al., Simulations of efficient Raman amplification into the multipetawatt regime, Nature Physics **7**, 87 (2011)
- 56 M. Chen et al., *Enhanced Collimated GeV Monoenergetic Ion Acceleration from a Shaped Foil Target Irradiated by a Circularly Polarized Laser Pulse*, Phys. Rev. Lett. **103**, 024801 (2009)

- 57 B. Qiao et al., *Stable GeV Ion-Beam Acceleration from Thin Foils by Circularly Polarized Laser Pulse*, Phys. Rev. Lett. **102**, 145002 (2009)
- 58 X.Q. Yan et al., *Self-Organizing GeV, Nanocoulomb, Collimated Proton Beam from Laser Foil Interaction at  $7 \times 10^{21}$  W/cm<sup>2</sup>*, Phys. Rev. Lett. **103**, 135001 (2009)
- 59 Z.M. Zhang et al., *High-density highly collimated monoenergetic GeV ions from interaction of ultraintense short laser pulse with foil in plasma*, Phys. Plasmas **17**, 043110 (2010)
- 60 H.B. Zhuo et al., *Quasimonoenergetic Proton Bunch Generation by Dual-Peaked Electrostatic-Field Acceleration in Foils Irradiated by an Intense Linearly Polarized Laser*, Phys. Rev. Lett. **105**, 065003 (2010)
- 61 H.Y. Wang et al., *Laser Shaping of a Relativistic Intense, Short Gaussian Pulse by a Plasma Lens*, Phys. Rev. Lett. **107**, 265002 (2011)
- 62 L.L. Yu et al., *Generation of tens of GeV quasi-monoenergetic proton beams from a moving double layer formed by ultraintense lasers at intensity  $10^{21}$ – $10^{23}$  W cm<sup>-2</sup>*, New J. of Phys. **12**, 045021(2010)
- 63 J. Pang et al, *Phys. Rev. E*, **66**, 066501 (2002)
- 64 A.V. Arefiev et al. *Phys. Rev. Lett.*, **108**, 145004 (2012)
- 65 E.A. Startsev and C.J. McKinstrie, *Phys. Plasmas*, **10**, 2552 (2003)
- 66 J.T. Mendonça, L.O. Silva and R. Bingham, *J. Plasma Phys.*, **73**, 627 (2007)
- 67 E. d’Humières et al., *PPCF* **55**, 124025 (2013)
- 68 M. Nakatsutsumi et al., *Fast focusing of short-pulse lasers by innovative plasma optics toward extreme intensity*, Optics Letters **35**, 2314-2316 (2010)
- 69 T. Heinzl, et al., *On the observation of vacuum birefringence*, Opt. Commun. **267**, 318 (2006)
- 70 B. King, AD Piazza, and CH Keitel, *A matterless double slit*, Nature Photon. **4**, 92 (2010)
- 71 *Double-slit vacuum polarization effects in ultra-intense laser fields*, Phys. Rev. A **82**, 032114 (2010)
- 72 H. Gies, *Strong laser fields as a probe for fundamental physics*, The European Physical Journal D **55**, 311 (2009)
- 73 K. Homma, D. Habs, and T. Tajima, *Probing the semi-macroscopic vacuum by higher harmonic generation under focused intense laser fields*, Appl. Phys. B **104**, (2011)
- 74 D. Batani, S. Hulin, J.E. Ducret, E. d’Humières et al. *Development of the PETAL Laser Facility and its Diagnostic Tools*, Acta Polytechnica **53**, 103 (2013)
- 75 S Davis et al., *J. Phys.: Conf. Ser.* **244** 042006 (2010).

